



UNIVERSITY OF NAIROBI

**SEQUESTERING OF SELECTED HEAVY METAL IONS IN WASTEWATER FROM
INDUSTRIAL AREA IN NAIROBI USING WATER HYACINTH AS A LOW COST
ADSORBENT**

BY

MWANIKI JOSEPH MUNENE

I56/87601/2016

**A Thesis Submitted in Partial Fulfillment of the Requirements for the Degree of Master of
Science in Industrial Chemistry of the University of Nairobi**

2019

DECLARATION

I declare that this thesis is my original work and has not been submitted elsewhere for examination, award of degree or publication. Where other people's work or my own work has been used, this has properly been acknowledged and referenced in accordance with the University of Nairobi's requirements.

SignatureDate.....

Mwaniki Joseph Munene

I56/87601/2016

This thesis has been submitted with our approval as research supervisors.

Signature

Date.....

Dr. John Onam Onyatta

Department of Chemistry

University of Nairobi

Signature.....

Date.....

Prof. Amir Okeyo Yusuf

Department of Chemistry

University of Nairobi

DEDICATION

This project is dedicated to my late mother, Mary Muthoni and my late father, Peterson Mwaniki who instilled in me the value of hard work. To my elder sister, Harriet Mwaniki, my aunt Asnath Nguru and all my relatives for without their support, prayers, patience and understanding the completion of this work would not have been possible.

ACKNOWLEDGEMENT

First of all, I am indebted to the all powerful God for being gracious to provide all that I needed during my studies and kept me in good health all through. All the favor from God was crowned by provision of wonderful supervisors. I am, deeply obliged to my supervisors.

Dr. John Onam Onyatta and Prof. Amir O. Yusuf for the invaluable comments, suggestions, corrections, patience and constructive criticisms that went along way to refine this work. Without whose help; this project would not have been a success. Thank you very much for making sure I kept the focus.

Further, I take this opportunity to express my deep gratitude to my loving family. Special thanks to my sister for the financial and psychological support. Special thanks to my aunt Asnath Nguru for ensuring my tuition fee was cleared in time. I want to appreciate all friends who are a constant source of motivation and for their never ending support and encouragement during this project.

Finally it has been exciting and instructive study in the University of Nairobi. I feel privileged to have had the opportunity to carry out this study as a demonstration of knowledge gained during the period I studied for my master's degree.

ABSTRACT

The adsorption of heavy metals from wastewater and aqueous solution by water hyacinth powder was investigated under batch experiments. The factors such as pH, contact time, particle size and adsorbent dose that influence adsorption efficiency were evaluated. The water hyacinth plant was collected from a point on Lake Victoria, Kisumu County. The stems were washed to remove any dirt and air dried until sufficiently dry and then dried in an oven at 110 °C overnight to remove all the moisture. The dried stems were ground using pestle and mortar and sieved through standardized sieves of 300-2800µm to obtain the powder for the adsorption studies. The heavy metals in the wastewater samples were determined using Atomic Absorption Spectrophotometer (Model AA-6300 Shimadzu AAS). The levels of heavy metals in wastewater were in the range of: 1.2-75.3 ppm for lead, 0.4-87.6 ppm for chromium, 0.1-63.5 ppm for nickel, 0.5-95.5 ppm for zinc and 0.8-52.7 ppm for cadmium. The levels of zinc, lead and cadmium were above the limits set by the National Environment Management Authority (NEMA) for discharge into the environment (0.01 ppm for cadmium and lead, 0.5 ppm for zinc). The study showed that the adsorption efficiency of water hyacinth powder was higher in aqueous solution than in wastewater while at low metal concentrations (0.1-3.2 ppm), the adsorption efficiency was 100% in both wastewater and aqueous solution. The effect of particle size on adsorption showed that adsorption efficiency increased with decrease in particle size and followed the order: >425<2800, >300<425 and <300 µm for each of the concentrations. The adsorption also increased with pH however the optimum adsorption varied with the metal. The pH range for adsorption of Pb, Cr and Cd was 2-5 and 2-6 for Ni and Zn after which a plateau was reached and then the adsorption efficiency dropped. The adsorption also increased with contact time until a steady state was attained however the optimum adsorption time varied with the metal. The study revealed that optimum time for adsorption of Pb was 30 minutes, 40 minutes for Cr, 80 minutes for Ni and 60 minutes for both Cd and Zn. The adsorbent dosage increased until an optimum adsorption was obtained and it was observed that adsorbent dosage for Pb and Zn was 2.5g; Cd was 3.0g; Cr was 4.0g and 4.5g for Ni. The adsorption isotherm according to Langmuir model fitted well the adsorption of Zn²⁺, Cd²⁺, Ni²⁺ and Pb²⁺ in aqueous solution while the adsorption of Cr³⁺ fitted well the Freundlich model. Assessment of kinetics studies showed that the removal of Cd²⁺, Ni²⁺, Pb²⁺, Zn²⁺ and Cr³⁺ followed pseudo first order rate equations according to R² values. The characterization of water hyacinth powder by Fourier Transform Infrared Spectroscopy (FTIR) showed that the adsorption of heavy metals could be attributed to the existence of functional groups such as carboxyl, hydroxyl and carbonyl in the water hyacinth fibre. The study showed that water hyacinth powder is a low cost adsorbent which could be used to remove heavy metals from wastewater and aqueous solution.

TABLE OF CONTENTS

DECLARATION.....	ii
DEDICATION.....	iii
ACKNOWLEDGEMENT.....	iv
ABSTRACT.....	v
LIST OF TABLES	xiv
LIST OF FIGURES	xvi
LIST OF ABBREVIATIONS, ACRONYMS AND SYMBOLS.....	xix
CHAPTER ONE	1
INTRODUCTION.....	1
1.1 Background	1
1.2 Statement of the problem	2
1.3 Objectives.....	3
1.3.1 General objective.....	3
1.3.2 Specific objectives.....	3
1.4 Justification and significance of the study	3
CHAPTER TWO	5
LITERATURE REVIEW	5
2.1 Heavy metals in the environment.....	5
2.2 Water hyacinth in aquatic system.....	5

2.3 Heavy metal contamination in the environment	6
2.3.1 Heavy metal contamination in soils	6
2.3.2 Contamination of water by heavy metals	7
2.3.3 Heavy metals in industrial air.....	8
2.3.4 Heavy metals in wastewater	8
2.4 Health effects of heavy metals	9
2.4.1 Cadmium	10
2.4.2 Lead	10
2.4.3 Nickel	11
2.4.4 Zinc.....	11
2.4.5 Chromium.....	12
2.5 Removal of heavy metals by adsorption on adsorbents	12
2.6 Types of adsorbents.....	13
2.6.1 Activated carbon.....	13
2.6.2 Silica gel	13
2.6.3 Zeolites	13
2.6.4 Clay minerals and oxides	13
2.6.5 Nanomaterial	14
2.6.6 Agricultural by-products and biological waste	14
2.6.7 Ion exchange resins	14

2.6.8 Water hyacinth	15
2.7 Low cost adsorbents	15
2.8 Heavy metal analysis using Atomic Absorption Spectrometer (AAS).....	15
2.8.1 Theory of atomic absorption spectrometry	15
2.9 Components of atomic absorption spectrometer.....	18
2.9.1 Hollow cathode lamps	18
2.9.2 Flames	20
2.9.3 Burners	20
2.9.4 Monochromator	22
2.9.5 Detector	22
2.10 Kinetic models for heavy metal adsorption.....	23
2.11 Characterization of the adsorbent using Fourier-Transform Infrared	23
2.12 Components of Fourier Transform Infrared Spectrometer	24
CHAPTER THREE	26
MATERIALS AND METHODS	26
3.1 Study site	26
3.2 Collection of the samples	27
3.3 Adsorbent collection and preparation	28
3.4 Apparatus and reagents	30
3.4.1 Apparatus.....	30

3.4.2 Reagents	31
3.5 Experimental procedure	31
3.5.1 Digestion of wastewater samples	31
3.5.2 Sample analysis using AAS	32
3.5.4 Working solutions	33
3.5.5 Removal of heavy metals from wastewater	34
3.5.6 Calculation of adsorption efficiency and the adsorption capacity	34
3.6 Removal of heavy metals from aqueous solution using water hyacinth	35
3.7 The effect of selected parameters on heavy metal adsorption	36
3.7.1 The effect of particle size on heavy metal removal.....	36
3.7.2 Effect of pH on heavy metal adsorption on water hyacinth	36
3.7.3 Effect of contact time on heavy metal removal.....	37
3.7.4 The effect of amount of water hyacinth on heavy metal removal.....	37
3.8 Adsorption equilibrium experiments.....	38
3.8.1 Batch experiments and Kinetic models of heavy metal adsorption on water hyacinth....	40
3.9 Fourier Transform Infrared Spectroscopic analysis of powdered water hyacinth before and after heavy metal adsorption.	41
3.9.1 FTIR analysis of raw water hyacinth powder	41
3.9.2 FTIR analysis of metal loaded water hyacinth powder	41
CHAPTER FOUR.....	42

RESULTS AND DICUSSION	42
4.1 Concentration of Heavy metals in wastewater	42
4.2 Adsorption efficiency and adsorption capacity of water hyacinth powder	43
4.3 Factors influencing the adsorption of heavy metals	45
4.3.1 Effect of particle size on adsorption of zinc ions on water hyacinth	45
4.3.2 Effect of pH on adsorption of zinc ions	46
4.3.3 Effect of contact time on adsorption of zinc ions.....	47
4.3.4 Effect of adsorbent dosage on adsorption of zinc ions.....	48
4.4 Adsorption isotherms	49
4.4.1 Adsorption isotherms for the adsorption of zinc ions	49
4.4.2 Adsorption isotherms for the adsorption of lead ions	51
4.4.3 Adsorption isotherms for the adsorption of nickel ions	53
4.4.4 Adsorption isotherms for the adsorption of cadmium ions	54
4.4.4 Adsorption isotherms for the adsorption of chromium ions.....	56
4.5 Kinetic studies	57
4.5.1 Kinetic studies for the adsorption of zinc ions	57
4.6 FTIR analysis for heavy metal adsorption on water hyacinth powder.....	60
4.6.1 FTIR Spectra of water hyacinth powder	60
CHAPTER FIVE	68
CONCLUSIONS AND RECOMMENDATIONS.....	68

5.1	Conclusions	68
5.2	Recommendations	69
	REFERENCES.....	70
	APPENDICES.....	84
	Appendix I: Calibration curves	84
	Appendix Ia: Calibration curve for Cadmium.....	84
	Appendix Ib: Calibration curve for Lead	84
	Appendix Ic: Calibration curve for Chromium	84
	Appendix Id: Calibration curve for Nickel.....	85
	Appendix Ie: Calibration curve for Zinc	85
	Appendix If: Absorbance for the waste-water samples.....	85
	Calculation of sample concentration	86
	Appendix II: Adsorption efficiency (%) vs particle size (μm) for Zn, Pb, Ni, Cd and Cr.....	87
	Appendix II a: Effect of particle size on adsorption of lead ions.....	88
	Appendix II b: Effect of particle size on adsorption of nickel ions	88
	Appendix II c: Effect of particle size on adsorption of chromium ions	89
	Appendix II d: Effect of particle size on adsorption of cadmium ions	89
	Appendix III: Adsorption efficiency (%) vs pH for Zn, Pb, Ni, Cd and Cr.....	90
	Appendix IIIa: Effect of pH on adsorption of lead ions.....	92
	Appendix IIIb: Effect of pH on adsorption of nickel ions	92

Appendix IIIc: Effect of pH on adsorption of chromium ions	93
Appendix IIId: Effect of pH on adsorption of cadmium ions	93
Appendix IV: Adsorption efficiency (%) vs contact time (min) or Zn, Pb, Ni, Cd and Cr	94
Appendix IVa : Effect of contact time on adsorption of lead ions.....	97
Appendix IVb : Effect of contact time on adsorption of nickel ions	97
Appendix IVc : Effect of contact time on adsorption of chromium ions	98
Appendix IVd : Effect of contact time on adsorption of cadmium ions	98
Appendix V: Adsorption efficiency (%) vs adsorbent dosage (g) for Ni, Cd, Cr, Zn and Pb ..	99
Appendix Va: Effect of adsorbent dosage on adsorption of lead ions	101
Appendix Vc: Effect of adsorbent dosage on adsorption of chromium ions	102
Appendix Vd: Effect of adsorbent dosage on adsorption of cadmium ions.....	102
Appendix VI: Equilibrium data for Pb^{2+} , Cd^{2+} , Cr^{3+} , Zn^{2+} and Ni^{2+}	103
Appendix VII: Kinetic graphs for Equilibrium data for Pb^{2+} , Cd^{2+} , Cr^{3+} , Zn^{2+} and Ni^{2+}	106
Appendix VIIa: Pseudo-first-order graphs for the adsorption of lead ions on ground water hyacinth.	106
Appendix VIIb: Pseudo-first-order graphs for the adsorption of nickel ions on ground water hyacinth.	106
Appendix VIIc: Pseudo-first-order graphs for the adsorption of chromium ions on groundwater hyacinth.	107
Appendix VIId: Pseudo-first-order graphs for the adsorption of cadmium ions on ground water hyacinth.	107

Appendix VIIe: Pseudo-second-order graphs for the adsorption of lead ions on ground water hyacinth.	108
Appendix VIIf: Pseudo-second-order graphs for the adsorption of nickel ions on ground water hyacinth.	108
Appendix VIIg: Pseudo-second-order graphs for the adsorption of chromium ions on ground water hyacinth.	109
Appendix VIIh: Pseudo-second-order graphs for the adsorption of cadmium ions on ground water hyacinth.	109
Appendix VIIk: Kinetic data for Kinetic graphs for Equilibrium data for Pb^{2+} , Cd^{2+} , Cr^{3+} , Zn^{2+} and Ni^{2+}	110

LIST OF TABLES

Table 2.1: Heavy metal limits (mg/L) in water according to different national and international organizations.....	8
Table 2.2: Heavy metal limits (mg/L) in wastewater according to different national and international organizations.....	9
Table 3.1 Quantity and purity of the reagents used in the study.....	31
Table 3.2: Amount of salts weighed (g) to make aqueous solution whose concentration was 1000 ppm.....	33
Table 3.3 Conditions set in the investigation of the pH effects on adsorption of heavy metals using water hyacinth	37
Table 4.1 Heavy metal concentrations (ppm) in wastewater.....	42
Table 4.2 Adsorption efficiency and adsorption capacity of water hyacinth powder from wastewater and aqueous solution	44
Table 4.3: Parameters for Langmuir and Freundlich isotherms for adsorption of Zn^{2+} from aqueous solution	50
Table 4.4: Langmuir and Freundlich isotherms parameters for adsorption of Pb^{2+} from aqueous solution.....	52
Table 4.5: Parameters for Langmuir and Freundlich isotherms for adsorption of Ni^{2+} from aqueous.....	54
Table 4.6: Langmuir and Freundlich isotherms parameters for adsorption of Cd^{2+} from aqueous solution.....	55
Table 4.7: Parameters for Langmuir and Freundlich isotherms for the adsorption of Cr^{3+} ions on water hyacinth powder.....	57
Table 4.8: The Pseudo first-order and Pseudo second-order kinetic parameters of adsorption of zinc, lead, cadmium, chromium and nickel ions on powdered water hyacinth.....	59

Table 4.9 Effects of heavy metal adsorption on the water hyacinth spectra.....67

LIST OF FIGURES

Figure 2.1-Water hyacinth on Lake Victoria.....	6
Figure 2.2: The fundamental parts of the atomic absorption spectrometer.....	16
Figure 2.3 Dual beam AAS.....	18
Figure 2.4 -Hollow cathode lamp.....	19
Figure 2.5- The excitation mechanism of a typical multi-element lamp.....	20
Figure 2.6-Total consumption burner.....	21
Figure 2.7- Design diagram of premix burner.....	22
Figure 2.8: Components of FTIR.....	24
Figure 3.1 The map of Nairobi	27
Figure 3.2 A map of sampling points in industrial area, Nairobi Kenya.....	28
Figure 3.3 Collection of water hyacinth from a point on Lake Vitoria.....	29
Figure 3.4: Graded water hyacinth.....	30
Figure 4.1: Effect of particle size on adsorption of Zn^{2+} from aqueous solution.....	45
Figure 4.2: Effect of pH on adsorption of Zn^{2+} on from aqueous solution.....	46
Figure 4.3: Effect of contact time on adsorption of Zn^{2+} from aqueous solution	47
Figure 4.4: Effect of adsorbent dosage on adsorption of Zn^{2+}	48
Figure 4.5: Linearized Freundlich plot for the adsorption of Zn^{2+} ions onto water hyacinth powder	49
Figure 4.6: Linearized Langmuir plot for the adsorption of Zn^{2+} ions onto water hyacinth powder.....	50

Figure 4.7: Linearized Freundlich plot for the adsorption of Pb^{2+} ions onto water hyacinth powder.....	51
Figure 4.8: Linearized Langmuir plot for the adsorption of Pb^{2+} ions onto water hyacinth powder	52
Figure 4.9: Linearized Freundlich plot for the adsorption of Ni^{2+} ions onto water hyacinth powder	53
Figure 4.10: Linearized Langmuir plot for the adsorption of Ni^{2+} ions onto water hyacinth powder.....	53
Figure 4.11: Linearized Freundlich plot for the adsorption of Cd^{2+} ions onto water hyacinth powder	54
Figure 4.12: Linearized Langmuir plot for the adsorption of Cd^{2+} ions onto water hyacinth powder	55
Figure 4.13: Linearized Freundlich plot for the adsorption of Cr^{3+} ions onto water hyacinth powder.....	56
Figure 4.14: Linearized Langmuir plot for the adsorption of Cr^{3+} ions onto water hyacinth powder.....	56
Figure 4.15: Pseudo-first-order for the adsorption of 95.5 ppm Zn^{2+} ions onto water hyacinth powder	58
Figure 4.16: Pseudo-second-order for the adsorption of 95.5 ppm Zn^{2+} ions onto water hyacinth powder	58
Figure 4.17 The FTIR spectra of the water hyacinth powder before and after adsorption of Pb^{2+} ions	61
Figure 4.18 The FTIR spectra of the water hyacinth powder before and after adsorption of Cd^{2+} ions.....	63

Figure 4.19 The FTIR spectra of the water hyacinth powder before and after adsorption of Ni²⁺ ions64

Figure 4.20 The FTIR spectra of the water hyacinth powder before and after adsorption of Cr³⁺ ions65

Figure 4.21 The FTIR spectra of the water hyacinth powder before and after adsorption of Zn²⁺ ions66

LIST OF ABBREVIATIONS, ACRONYMS AND SYMBOLS

AAS	Atomic Absorption Spectrometry
CBS	Central Bureau of Statistics
EU	European Union
FTIR	Fourier-transform infrared spectroscopy
IQ	Intelligence Quotient
NEMA	National Environment Management Authority
KNBS	Kenya National Bureau of Statistics
NA	Not available
UNEP	United Nations Environment Programme
US FDA	United States Food and Drug Administration
USEPA	United States Environmental Protection Agency
WHO	World Health Organization

CHAPTER ONE

INTRODUCTION

1.1 Background

Environmental pollution has been on the rise since industrialization began. Over the past decade the number of industries worldwide has increased remarkably (Tchounwou *et al.*, 2012). These industries have a lot of benefits but along with them is the destruction of ecosystem. Wastewater released from the industries is contaminated by toxic substances such as heavy metals (Barakat, 2011). They get into the surrounding through ejection from industrial practices since they are in dissolved form. Such processes involve the manufacture of agricultural products such as pesticides, phosphates fertilizers and herbicides, petrochemical and oil refining, mining and smelting, manufacture of paints and dye stuffs just to name a few (Kanwal *et al.*, 2012). Emissions from automobiles and untreated domestic waste into aquatic environment also add to the content of heavy metals (Dipak, 2017). According to Abdullar, (2015) heavy transport and increased industrialization in many cities have increased discharge of wastes that contain heavy metals which pollute the environment upon their accumulation.

Heavy metals in dissolved or undissolved form are carried away by water or deposited in the soils (Ojedokun and Olugbenga, 2016; Kumar *et al.*, 2010). Heavy metals ions include nickel (Ni), chromium (Cr), platinum (Pt), mercury (Hg), Tin (Pt), bismuth (Bi) etc. They are persistent, fairly soluble in water and consequently, easily absorbed into living cells (Singh *et al.*, 2011). Elemental mercury is absorbed directly into the body through skin contact (Park and Zheng 2012). Vegetables, fish, cereal crops and rice which are consumed in high amount, have the capacity to accumulate toxic substances such as arsenic (Daping *et al.*, 2015).

Heavy metal pollution poses health problems that require to be addressed (Jaishankar *et al.*, 2014). These metals have dangerous effects on human body especially when their absorption exceeds the acceptable limits. They can cause perilous effects such as liver damage, kidney damage, dermatitis, damage on the circulatory and nervous system, insomnia, tumor formation, rheumatoid arthritis and respiratory cancer (Arif *et al.*, 2015). Due to these and many more

adverse implications, not only to humanity but also to the environment there is a need for protection and rehabilitation of the surroundings through the elimination of heavy metals.

According to Parmar and Thankur (2013), several techniques have been applied to get rid of heavy metals. These methods include use of membranes such as in reverse osmosis, electrochemical techniques such as electrolytic extraction and electro dialysis, ion exchange, and chemical precipitation. Although these methods are effective, they are costly in terms of the infrastructure, control systems and energy (Hegazi, 2013). According to Singh and Susan (2016) there are cheaper methods of eliminating heavy metals which are contained in the wastewater. Adsorption has become a regular technique of eliminating heavy metals contained in the wastewater (Singh and Susan, 2016). This method is relatively less costly, energy efficient, environment friendly and inexpensive (Gunatilake, 2015). Another key advantage of adsorption is the ease of designing, and operating (Gisi *et al.*, 2016). Adsorption of heavy metals is very effective with as low concentration as 1 mg/L (Tripathi and Manju, 2015).

Lately scientists have intensified research in wastewater purification from heavy metals using inexpensive sorbent material. Biological methods such as use of agricultural waste have been put into test and have proved useful (Agarwal and Vaishali, 2017). Rice husks, cow dung, sugarcane bagasse, sawdust, soybean hull and cotton hull have all successfully been utilized. The objective of the study was to assess the adsorption efficiency of water hyacinth as an economical adsorbent in the removal of selected heavy metal ions from industrial wastewater.

1.2 Statement of the problem

Industrial area in Nairobi is the hub to many industries in the County. These industries are involved in manufacturing of paint and dyes, vulcanization of rubber and plastics, manufacture of pesticides, fungicides, welding to produce brass sheet, vehicles repairs, galvanization etc. The existence of these and many other industries are of great economic importance.

However, these industries could be releasing toxic substances in to the surroundings through wastewater. The released heavy metals could reach the food chain since many of the informal urban residents use wastewater for agricultural activities, thereby posing danger to their health (Abdel *et al.*, 2011; Hegazi, 2013).

1.3 Objectives

1.3.1 General objective

The general objective of this study was to assess the adsorption efficiency of water hyacinth as a low cost adsorbent in the removal of selected heavy metal ions from industrial wastewater.

1.3.2 Specific objectives

The specific objectives of this study were:

- i) To determine the concentration of the selected heavy metal ions in the industrial wastewater from industrial area in Nairobi.
- ii) To determine the percentage of the adsorbed heavy metal on water hyacinth as influenced by:
 - pH of the medium
 - contact time
 - particle size and
 - amount of the adsorbent used
- iii) To determine the adsorption efficiency of water hyacinth in the removal of selected heavy metal ions.
- iv) To determine the kinetics of heavy metal adsorption on adsorbent
- v) To characterize water hyacinth powder for the presence of functional groups accountable for adsorption using Fourier Transform Infrared (FTIR)

1.4 Justification and significance of the study

Adsorption method has been widely utilized in the elimination of heavy metals contained in both drinking water and wastewater by utilizing activated carbon. Nonetheless, this method is costly. There is need therefore to devise a cheap method that uses inexpensive adsorbent. Industrial wastewater that is discharged to the environment through various output points could contaminate the surroundings due the occurrence of toxic heavy metals. This is because they are non-thermo degradable and over time they accumulate to lethal levels in living organisms (Kayastha, 2014).

The wastewater released from industrial activities such as manufacturing of paint and dyes, vulcanization of rubber and plastics, manufacture of pesticides, fungicides and welding. The

heavy metal contamination of land and water in Nairobi dam, dumpsites and its environs have been reported (Ndeda and Manohar, 2014; Mulamu, 2014; Njagi *et al.*, 2016; Onyatta *et al.*, 2009). Water hyacinth (*Eichornia crassipes*) is a menace in many dams and lakes in Kenya. Therefore its use as an inexpensive adsorbent to eliminate heavy metals from the wastewater from industrial area in Nairobi, Kenya would be one way to put it into use. The study was of significance since it provided information on the use of water hyacinth as a low cost adsorbent in the removal of heavy metal ions from the wastewater and aqueous solutions. It will also provide information on baseline content of the heavy metals in the wastewater. Therefore there is need to develop a cheap method. The adsorption efficiency of water hyacinth would provide a remediation strategy to control heavy metal ejection into the surroundings.

CHAPTER TWO

LITERATURE REVIEW

2.1 Heavy metals in the environment

Heavy metals are poisonous and destructive contaminants that are released into the environment from industrial activities (Kamar *et al.*, 2014). Their density is usually higher (4-5 times) than that of water (Chibuike and Obiora, 2014; Tchounwou *et al.*, 2012). They can penetrate into human body via contact, breathing and food consumption (Monachese *et al.*, 2012). Heavy metals pile up in the soils, water as well as bio-accumulate in living organism without being broken down (Govind and Madhuri, 2014; Schalow *et al.*, 2007). Bioaccumulation refers to the chemical increase in an organism in comparison to the surrounding over time (Kandziora-Ciupa *et al.*, 2017).

Heavy metals affect human beings and animals because they are non-biodegradable. Heavy metal accumulation causes various diseases and disorders (Achparaki *et al.*, 2012). Heavy metals also form bonds with sulphur groups in the enzymes hence interrupting enzymatic functions and can cause various diseases and disorders (Ojedokun and Olugbenga, 2016; Oves *et al.*, 2016).

Heavy metals form part of the earth's crust where they contribute to the balance of the planet (Vodyanitskii, 2016). According to Rehman *et al.*, (2018) natural activities (weathering and volcanicity) and anthropogenic activities (mining) could be responsible for bringing heavy metals to the earth's surface from deep earth's crust hence exposing living organism to contamination. Once on the earth's surface they can occur in the soils, air, rock and aqueous ecosystems (Shaban *et al.*, 2016).

2.2 Water hyacinth in aquatic system

Water hyacinth is a hydrophyte that thrives in water and contaminates the water. Figure 2.1 shows water hyacinth thriving on Lake Victoria.



Figure 2.1- water hyacinth cover on the lake-shore of Lake Victoria (Source: UNEP, 2013)

The invasion of water hyacinth in the ecological systems reduces aquatic biodiversity, reduces fishing ground and clogs water ways and forms excellent mosquito breeding site (Anzeze *et al.*, 2014; Villamagna and Murphy, 2010).

2.3 Heavy metal contamination in the environment

The heavy metal contamination in selected environments is described below.

2.3.1 Heavy metal contamination in soils

High level heavy metal contamination of soils is of concern because the metals are able to build up in the food chain thereby causing health risks to human beings. Soil is an important asset to mankind. However, some of the anthropogenic activities have been responsible for the soil contamination (Garbuio *et al.*, 2012; Akbari *et al.*, 2017). They exist as free ions or organic or inorganic metal ligands that can either be taken up by plants thereby increasing their chances of entering the food chain. According to Jaishankar *et al.*, (2014) these toxic substances can remain on the rocks or beneath organic matter or they can be transported through the soil to ground water. The application of phosphate fertilizers has been shown to enhance cadmium release from soils (Onyatta and Huang, 2005) while the use of sewage sludge and bio-solids as manure are known to increase heavy metal concentration in soils (Echem, 2014).

Their toxicity, mobility and solubility can be altered by microorganisms common in the soils (Baran and Tarnawski, 2015). The microorganisms facilitate mechanisms such as methylation, dimethylation and oxidation-reduction processes that transform the toxic substances (Fashola *et al.*, 2016). The Organic (methylated) form of Hg is more poisonous than the inorganic form (Zimmermann *et al.*, 2013). Methylation by microorganisms is highly preferred in soils of low pH (Frohne *et al.*, 2012). Soil contamination in most cases occurs near roads, industrial areas and areas where intensive agricultural activities are carried out (Jiao *et al.*, 2015). They have the ability to move in the soils. Their movement depends on bonding, metal properties and soil properties (Wauna and Okieimen, 2011; Arshadi *et al.*, 2014).

2.3.2 Contamination of water by heavy metals

Pollution of water sources is mainly attributed to urbanization, industrialization, agriculture, municipal effluents and increase in population (Waseem *et al.*, 2014; Abbas *et al.*, 2017). Contaminated water is unsuitable for consumption, recreational activities, wildlife, industrial use and agriculture (Dipak, 2017). In the aquatic environment, heavy metals occur as colloids, complexes and dissolved ions (Angelovicova and Fazekasova, 2014; Ahenda *et al.*, 2019). Water pollution can be in the form of foul smell, dissolved chemicals, colloidal suspensions and high temperatures (Kant, 2012).

Heavy metals get into aquatic environment either through natural occurrences such as chemical weathering and soil leaching or through human activities (Ogunkule *et al.*, 2016). Once they are in the environment, the metals can undergo complexation, chelation and hydrolysis which alter their distribution and availability (Tchounwou *et al.*, 2012). The accumulative and toxic nature of metals influences the water species as well as disrupting the ecosystem (Govind and Madhuri, 2014; Garba *et al.*, 2016). Use of water containing heavy metals for consumption, irrigation puts human kind at risk of developing heavy metal related diseases and disorders (Balkhair and Ashraf, 2015).

Water is an essential commodity to human being hence there is need to develop efficient techniques for assessment and purification of water (Clark *et al.*, 2012). The standard limits in drinking water according to the national and international organizations are provided in Table 2.1.

Table 2.1 Limits for selected heavy metals (mg/L) in drinking water according to different National and International Organizations

Parameters	Maximum permissible levels in mg/L			
	NEMA	WHO	EU	USEPA
Cadmium	0.0100	0.0050	0.0050	0.0050
Lead	0.0500	0.0100	0.0100	0.0100
Nickel	NA	0.0200	0.0200	0.1000
Chromium	NA	0.0500	0.0500	0.1000
Zinc	1.5000	5.0000	NA	5.0000

Source: Mebrahtu and Zerabruk (2011)

NA: Not available

2.3.3 Heavy metals in industrial air

Heavy metals get into atmosphere mainly through combustion, mining and smoking where they occur in the form of gases, vapor and dust particles. Smoking of nickel and cadmium containing cigarettes (one cigar has 1-2 microgram of Cd and Ni) contributes to the presence of cadmium and nickel in air since the smoke contains cadmium and nickel particles (Balkhair and Ashraf, 2015). Lead gets into the atmosphere through the use of leaded paints, smelting of lead and burning of leaded waste such as old batteries (Wani *et al.*, 2015). Chromium is released into the atmosphere by industries involved in chrome plating, steel manufacturing and leather tanning (Sun *et al.*, 2015). Chromium is also released into air after coal burning especially by plants that burn coal to produce electricity (Sun *et al.*, 2015; Mousavi *et al.*, 2009). Zinc gets in the air from tyre wear while cadmium and lead pollute air when they are emitted from industrial activities (Abdullar, 2015).

2.3.4 Heavy metals in wastewater

Industrialization is the major contributor of heavy metals in the industrial wastewaters. These pollutants in wastewaters come from anthropogenic industrial activities (Mbui *et al.*, 2014). The major source in wastewater include industries dealing with steel production, welding, paint

manufacturing, manufacturing of hydrogenated vegetable oils etc (Ngugi, 2014). The pollutants can be grouped into the following: organic matter such as sludge, inorganic particles such as minerals and biological particles such as fungi spores (Azimi *et al.*, 2017). The continued release of wastewaters to the surroundings, the concentration of heavy metals has been on the rise (Abdullar, 2015). The standard limits of heavy metals in industrial waste-water according to the National and International Organizations are provided in Table 2.2.

Table 2.2 Limits for selected heavy metals (mg/L) in industrial wastewater according to different National and International Organizations

Parameters	Maximum permissible levels in mg/L			
	NEMA	WHO	EU	USEPA
Cadmium	0.01	0.10	0.01	0.01
Lead	0.01	0.10	0.05	0.05
Nickel	NA	0.02	0.01	0.01
Chromium	NA	0.10	0.05	0.05
Zinc	0.50	2.00	2.00	0.50

Source: NEMA (2006)

NA-Not available

2.4 Health effects of heavy metals

Human exposure to heavy metal contamination has mainly been propelled by Industrial activities such as metal processing, nuclear power generation, petroleum combustion, coal burning, paper processing, military testing of ballistic missiles and vehicular emissions (Guan *et al.*, 2014; Mahurpawar, 2015). The heavy metals effects on human being, depends on the type of heavy metal that one is exposed to and whether the duration of exposure was short or long (Ahenda *et al.*, 2019;Nghah and Hanafiah, 2008a). Copper, chromium, manganese, zinc, magnesium and nickel are essential for various biochemical functions such as phosphorylation and glycolysis hence inadequate supply of these heavy metals results to diseases and disorders (Tchounwou *et al.*, 2012).

In the hydrological cycle, heavy metals are carried by sediments (Chiba *et al.*, 2011). The sediments are consumed by benthic organisms such as crabs enhancing the potential of heavy metal entry into the food chain (Chiba *et al.*, 2011). The following metals have adverse health effects on human:

2.4.1 Cadmium

Its atomic number is 48 hence it belongs to period 5 and group 12. It is silver-white, hexagonal crystal whose preferred oxidation state is +2 (Lane *et al.*, 2015). Cadmium is a chemical element whose chemical symbol is Cd. Cadmium is a d-block element with a density of 8.64 g/cm³. The melting point and boiling point of Cd is 321 °C and 766 °C respectively. Cadmium mostly occurs as a mineral called greenockite (CdS) (Murithi *et al.*, (2014).

Exposure to cadmium has varied hazardous effects. Cadmium causes kidney poisoning, nausea and respiratory problems (Johri *et al.*, 2010). It also causes the destruction of mucus producing membranes, liver dysfunction, cadmium induced pneumonitis (lung tissue inflammation) and prostate cancer (Benhoft, 2013). It is teratogenic (Velazquez *et al.*, 2013). Teratogen is any substance that alters the normal growth and development of embryo and can cause birth defects in a child (Gernand *et al.*, 2016).

2.4.2 Lead

It occurs naturally as PbSO₄, PbS, PbCO₃ (Wauna and Okieimen, 2011). It is silvery metal that is very toxic and can affect all body parts (Jaishankar *et al.*, 2014). It has face-centered crystalline structure. Lead has a melting point and boiling point of 327 °C and 1749 °C respectively (Jaishankar *et al.*, 2014). Lead is mostly found in storage batteries, soldering materials, paints, cable cladding and ammunition such as lead bullets.

Exposure to lead is known to cause lead poisoning characterized by symptoms such as nausea, brain damage, headache, death, abdominal pain and swelling of optic nerve (Jaishankar *et al.*, 2014). In children it lowers the IQ, causes convulsions while in adults it causes memory loss, damages reproductive organs, nephropathy (damage of kidney), insomnia (inability to sleep),

anorexia (lack of food appetite), abdominal pain and high blood pressure (Wauna and Okieimen, 2011).

2.4.3 Nickel

Nickel has atomic number 28 with chemical symbol Ni. It is found in group 10 and period 4. Nickel is a d-block element with a density of 8.90 g/cm^3 . The metal melts and boils at $1455 \text{ }^\circ\text{C}$ and $2913 \text{ }^\circ\text{C}$ respectively. It has a slight golden tinge. Nickel occurs in small quantities on the earth's surface especially in ultramafic rocks (Michaela *et al.*, 2016). Mostly Nickel occurs in nickel iron meteorites.

Nickel is an important catalyst in the manufacture of hydrogenated vegetable oil (Babae *et al.*, 2007). It is used in medical equipment, making of jewelry, manufacture of stainless steel, batteries and coin manufacture (Tasker *et al.*, 2014). One of the ways nickel gets in the body is inhalation of smoke from tobacco containing nickel (Cameron *et al.*, 2011). Other ways in which nickel gets in the body are consumption of food and drinking of water (Tasker *et al.*, 2014). Once in the body nickel mostly moves through the blood stream into the kidney (Babae *et al.*, 2007). Exposure to nickel has varied effects which include nickel poisoning characterized by headache, fever, abdominal pain, nausea, skin irritation, rapid cough, dizziness, sweating etc. (Michaela *et al.*, 2016). Nickel causes lung cancer, asthma and heart attack (Mahurpawar, 2015).

2.4.4 Zinc

Zinc has atomic number 30 with chemical symbol Zn. It belongs to period 4 and group 12. It is a d-block metal whose density of 7.15 g/cm^3 .

The metal melts and boils at $419 \text{ }^\circ\text{C}$ and $907 \text{ }^\circ\text{C}$ respectively. Zinc occurs as a mineral in nature. It is a bluish-white shiny diamagnetic metal whose concentration has been on the rise due to coal burning, steel production and processing. Zinc ions are important in regulating the immune system function by activating the T-cells (they attack the affected body cells and regulate the immune responses) in the body (Deshpande *et al.*, 2012). Zinc is vital for good health as it helps cells to divide and repair (Gower *et al.*, 2013). It is very vital in the treatment of diarrhea (WHO, 2011). Rehydration being the first step in treatment of diarrhea, involves the use of oral rehydration solution (water that contains glucose, salt and zinc supplements) that help reduce the severity of diarrhea especially in children (Henry *et al.*, 2014). Zinc is also crucial in hormonal

balance and acts as an antioxidant in the body, therefore, small deficiency of zinc in our bodies can cause diseases such as diabetes and infertility, hair loss, poor concentration and memory loss (Guo and Katta, 2017).

Excess zinc concentration in our bodies can result in heavy metal poisoning, nausea and vomiting, headaches, loss of appetite stomach upsets, dizziness and lowered immune function (Plum *et al.*, 2010). Excess ingestion of the metal causes kidney stones (accumulation of minerals in kidney) resulting in severe pain and can block ureter (Tang *et al.*, 2010).

2.4.5 Chromium

Chromium has atomic number 24 with chemical symbol Cr. Chromium is soft and malleable d-block element with a density of 7.19 g/cm³. It occurs on the earth's crust as a chromite (FeCr₂O₄). Chromium has a melting point and boiling point of 1907 °C and 2671 °C respectively. Chromium (VI) is used in several industrial processes which include: skin tanning, manufacture of stainless steel, electroplating of metals to prevent corrosion, production of pigments, metal alloys, etc. Improper discharge of waste from such processes results to pollution of natural water resources (Sarin and Pant, 2006). Cr (VI) is toxic, can cause genetic change and induce cancer when inhaled (Mamybaev *et al.*, 2015). Its presence in the environment is of public health concern as it poses danger to aquatic life.

2.5 Removal of heavy metals by adsorption on adsorbents

This is an economic, environmental friendly method of removing heavy metals from wastewater. It involves movement of substance from liquid phase to solid phase. The transferred substance is bound by chemical or physical interactions (Tripathi and Manju, 2015). Adsorption mainly is used in purification of gases or liquid. The adsorbing material is known as adsorbent. The material being adsorbed is called adsorbate (Gisi *et al.*, 2016). In chemical adsorption the adsorbate and adsorbent react (Hegazi, 2014; (Addagalla *et al.*, 2009). The interaction between the two is characterized by strong covalent or ionic bond. The chemical adsorption is also called chemisorption while physical adsorption is also called physisorption (Gisi *et al.*, 2016).

2.6 Types of adsorbents

These include activated carbon, silica gel, zeolites, clay, nanoparticles, biological wastes, exchange resins and water hyacinth.

2.6.1 Activated carbon

It is an organic material that forms a porous medium for adsorption. The structure of this medium is composite. The building blocks in this structure are carbon atoms. Activated carbon can remove substances such as dyes and pesticides as well as in the purification of waste-water (Kilpimaa *et al.*, 2014). This is because it is extremely effective in cadmium, lead and zinc removal. The removal of pollutants such as chlorinated hydrocarbons, purification of helium, removal of phenols, removal of gas odors and removal of nitrogen from air have all utilized activated carbon (Addagalla *et al.*, (2009).

2.6.2 Silica gel

This is a porous form of silica. It's mainly used to control moisture because of its high ability to absorb water vapor (Astrini *et al.*, 2015). Silica gel is also used to control moisture in shoes boxes and removal of moisture from transformer oils and gases. Silica gel is widely used since it is cheap and can be regenerated (Hameed *et al.*, 2009).

2.6.3 Zeolites

It occurs naturally in the form of crystalline alumina that can be used in the adsorption of organic molecules from a gaseous phase. Zeolites have high water uptake since it has an extensive surface area. Zeolite is used in industries to purify hydrogen gas.

It's also used to recover carbon dioxide. In petroleum manufacturing normal paraffin is separated from branched paraffin by the use of Zeolites through adsorption. Clinoptilolite and bentonite which is a form of Zeolite has been reported as an proficient adsorbent in the purification since it adsorbs the heavy metals (Terdkiatburana *et al.*, 2009; Mbui *et al.*, 2014).

2.6.4 Clay minerals and oxides

They are available in nature and widely used because of their ability to adsorb all types of species. They adsorb cations such Cu^{2+} , anions such as N^{2+} and neutral metallic species. Clay can be categorized into three; mica, smectite, kaolinite and montmorillonite. Although they are

readily available, they are less efficient in the adsorption of heavy metals when compared with Zeolites.

2.6.5 Nanomaterial

Nanomaterial is porous material whose pore diameter is less than 200 nm. These materials pose special properties such as distinctive surface, structure properties such as crystallinity and defect. Nano materials are used in processes such as ion exchange, catalysis and separation. Nanomaterials are efficient in adsorption although it is expensive (Kragovic *et al.*, 2013). Most of the nanomaterials that have been used as an adsorbent include carbon nano-tube, activated carbon and graphene.

2.6.6 Agricultural by-products and biological waste

Agricultural by-products and biological wastes have been utilized in adsorption of heavy metals. They are readily available, requires modest processing, economical, selective adsorption and easy to generate. Agricultural by-products such as pecan shell, coconut shell, rice husks, cow dung and maize cob have all been used effectively (Barakat, 2011).

2.6.7 Ion exchange resins

These are organic materials (polymer) that have the ability to substitute ions within them with ions in a solution. This occurs when a solution containing ions is passed through the polymer. Resins can either be anionic or cationic. Anionic resins are negatively charged. As the solution passes through the resin, the positively charged ions in the solution are trapped since the resin is negatively charged (Bai and Bartkiewicz, 2009). Anionic resins are either a weak or a strong acid. Cationic resins are positively charged. They trap the negatively charged ions in the solution. The ion exchange resin is used in water softening to substitute Mg^{2+} and Ca^{2+} with Na^+ converting hard water to soft water (Fil *et al.*, 2012). In this case the resin is regenerated by rinsing it with a solution whose concentration of sodium ions is high. Resins are also used to purify water. In such a case the poisonous heavy metal ions are replaced with ions such as potassium. Water containing no mineral content is purified using a resin that contains H^+ and OH^- in order to replace anions and cations.

2.6.8 Water hyacinth

The plant can be planted in the contaminated soils to absorb the heavy metal ions (Lissy and Madhu, 2011). The plant can also be harvested, dried and ground into powder before dispensing it in water that is contaminated by the heavy metal. Water hyacinth powder should be allowed time in the contaminated water for adsorption to occur, before the water can be used. The constituents of water hyacinth is cellulose (30-50%), hemicelluloses (20-40%) and lignin (15-30%) (Murithi *et al.*, 2014) The cellulose contains functional groups such as O-H, which are involved in adsorption through deprotonation (Anah and Astrini, 2018)

2.7 Low cost adsorbents

These types of adsorbents provide cheap and readily available material to use as adsorbents. The adsorbents that have been used successfully include sawdust, rice husks, banana peels, cashew nut shell, sugarcane bagasse, clay, zeolites, orange peel coconut shell etc. These adsorbents are cleaned and ground to the desired particle sizes before being used for adsorption while others are modified using modification techniques to improve the active sites (Gisi *et al.*, 2016). Adsorption has several advantages such as metal recovery, metal selectivity, regeneration of the adsorbent material and its effectiveness (Tripathi and Manju, 2015).

Comparative study on efficiency of water hyacinth, water lettuce and vetiver grass showed that the three plants have different abilities to eliminate water contaminants and the ability of each plant is influenced by factors such as climate, temperature, etc. (Gupta *et al.*, 2012).

2.8 Heavy metal analysis using Atomic Absorption Spectrometer (AAS)

AAS is an important analytical instrument which is used to quantify a chemical species by measuring the absorbed radiation. The working principle of the AAS is based on the following theory.

2.8.1 Theory of atomic absorption spectrometry

Atomic absorption occurs when an atom in ground state absorbs radiation of a specific wavelength elevating the atom to excited state. The determination of the quantity of an element in the sample requires one to determine the basis for comparison using standards of known concentration. This is done by making a calibration curve.

Atomic absorption involves the use of a flame. One of the processes that occurs in the flame is atomization. This step involves conversion of the metal ions present in the sample into metal atoms (Pereira-Filho, 2002). When a flame cell containing sodium chloride solution is set in the flame, evaporation of the solvent occurs, leaving behind a crystalline solid of sodium chloride. Upon evaporation, the sodium chloride crystals are dissociated into ground state atoms (Donati *et al.*, 2006). This process is called atomization. Consequently, it's the atoms that are present in the flame and not the ions. Because most of these atoms are in their ground state, they take in enough energy from the flame hence they are promoted to excited state (Peng *et al.*, 2012). Therefore there are many atoms present in the flame to be promoted to excited state by other means such as the use of ray of light. AAS uses a beam of light to promote the ground state atoms in the flame into excited state (Gaspar, *et al.*, 2000). The amount of light absorbed (as the ground state atoms are promoted to excited state) is measured.

The amount of light absorbed and concentration are then related (Aleixo *et al.*, 2004). The key elements of the AAS are shown in the Figure 2.2 below.

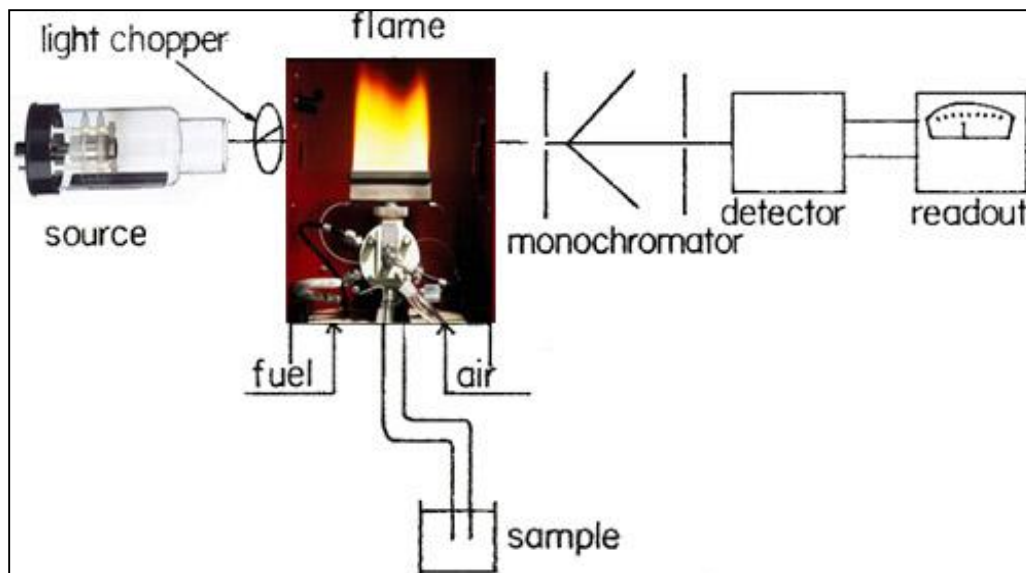


Figure 2.2: The fundamental parts of the atomic absorption spectrometer (Source: García and Baez, 2012)

The light source in AAS is known as the hollow cathode lamp. It is a lamp designed to give out exactly the wavelength needed for analysis. Light emitted is directed at the centre of the flame where the sample is placed. The sample is aspirated in a technique analogous to flame photometry. The flame is wide enough to give a long path length. This allows detection of little concentrations of the metal atoms in the flame.

The beam of light past the flame enters the monochromator. The monochromator is then set to the same wavelength as the one absorbed by the sample. Light intensity is then measured by the detector, upon adjusting for the blank. Measured light intensity is output of the readout.

This absorption follows the Beer-Lamberts law where the unknown concentrations are determined. Beer-Lambert's law is expressed as in Equation 2.1.

$$A = a l c \quad (2.1)$$

where, A-absorbance, a-absorptivity of the atomic species, l- lightpath and c- concentration of absorbing species.

The beam of light originating from the source passes through mechanical choppers (rotating half mirrors). The detector perceives interchanging light intensities. At one instance, the light intensity of the flame is detected and read. At that moment the beam from the source has been stopped by the rotating half mirrors. At another instance the intensity of the flame emission and that of the beam from the source are detected and read. At such instance the half rotating mirrors allows the beam from the source to pass. The detector is designed such that it measures the difference between the total signal and the transmitted signal. This difference which is measured is called transmittance, T. The readout, however, displays absorbance, A.

In AAS there is also the use of double beam instruments. In this case the mechanical choppers split the beam from the source into two. The beam directed through the flame is called sample beam while the beam that by-passes the flame is called reference beam. In double beam AAS the reference beam is meant to monitor the energy of the lamp while the sample beam shows absorption by the sample. The absorbance measured in this case is the ratio of the intensity of reference beam and sample beam. The double beam AAS design eliminates variations due to fluctuations in the light intensity at the source. Figure 2.3 shows a binary beam AAS

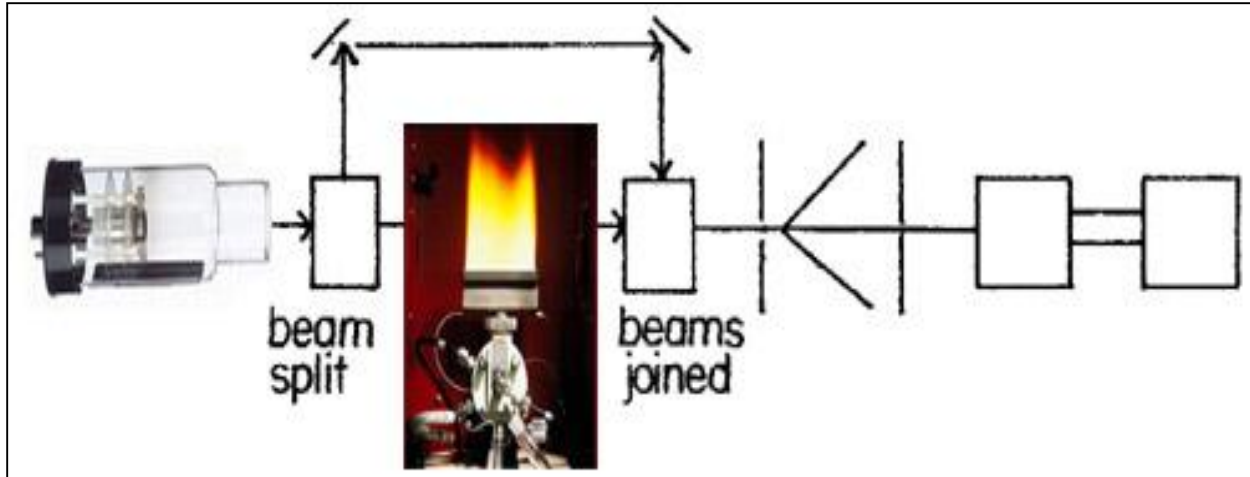


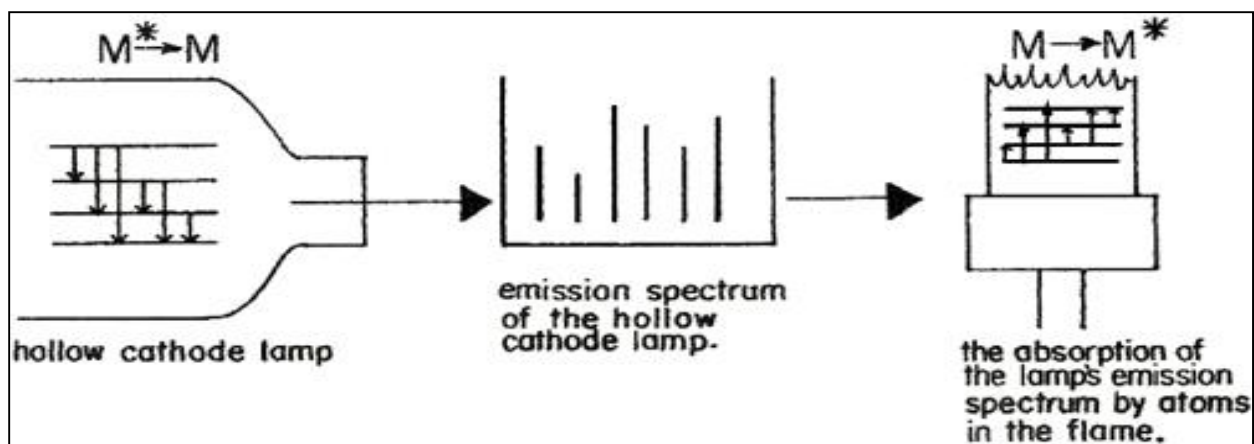
Figure 2.3: Dual beam AAS (Source: García and Baez, 2012)

2.9 Components of atomic absorption spectrometer

The components include cathode lamp, flame, burner, monochromator and detector

2.9.1 Hollow cathode lamps

It is the source of light. It is a lamp designed to give out precisely the light needed for analysis. This is done by making sure that the lamp being used is of the same metal as the one being analyzed in the sample. This ensures that the lamp has similar atoms to the ones being tested in the sample. The atoms within the lamp absorb sufficient energy when the lamp is switched on. The energy promotes the atoms in ground state to excited state. The atoms then return from excited state to their ground state emitting energy. The metal atoms in the sample absorb the wavelength from the hollow cathode lamp since the energy gap is the same. Figure 2.4 shows how the hollow cathode lamp works.



The Figure 2.4 Absorption of the wavelength emitted from the hollow cathode lamp (Source: García and Baez, 2012)

The lamp to be used for analysis must have the same element as the one contained in the sample. A classical AAS laboratory has diverse lamps stored such that they can be interchanged based on the metal to be analyzed. In some cases there are multi-elemental lamps. These kinds of lamps contain different but specific atoms that are excited once the lamp has been switched on. Light in the form of spectral lines is emitted when the atoms go back to ground state. In such a case interference does not occur provided that the beam for any metal can be established and clearly alienated from the other lines by the monochromator.

The lamp is covered with a glass envelope that is full with an inert gas such as neon. When the lamp is switched on, the gas atoms get ionized as shown in Figure 2.5. Upon ionization the gas ions hit the cathode while the electrons move to the anode. The bombardment of the electron causes the metal atoms to be excited and driven out from the cathode.

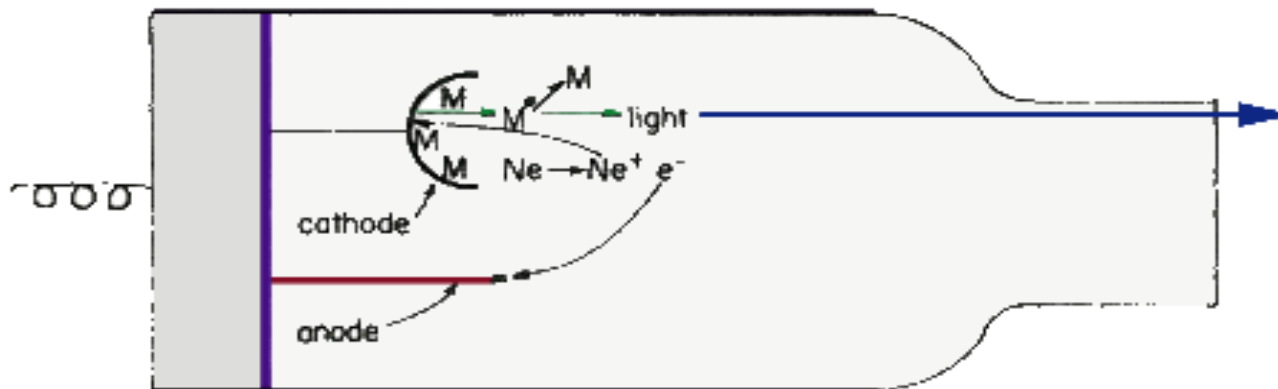


Figure 2.5. The excitation mechanism of a typical multi-element lamp (Source: Nicolas *et al*, 2013)

Upon their return from excited state to their ground state, a typical line spectrum is released by those atoms. The spectrum released is then directed to the centre of the flame. In the flame, all the atoms in the ground state, belonging to the same element are excited upon absorption of the radiation. The measured absorbance is then related to concentration.

2.9.2 Flames

Flames in AAS are facilitated by an oxidant and fuel. In AAS, acetylene is used as a fuel while air is the oxidant. A temperature of about 2300 K is attainable when using the air-acetylene flame. Oxygen-acetylene flame can also be used since it has a temperature of about 3100 K, but such a flame burn very fast hindering complete atomization, therefore affecting sensitivity of AAS. Another oxidant that is used reasonably is dinitrogen oxide, N_2O . The N_2O -acetylene flame burns slowly at about 2900 K.

The flame to be used in AAS for analysis is determined by the velocity at which the flame burns and the temperature produced by the flame. The most generally used type of flame is air-acetylene.

2.9.3 Burners

The burners that are mostly used in flame atomization are of two types. The first type of burner is called total consumption burner. The sample meets the fuel and oxidants at the bottom of the

flame in this type of burner. The three are then pressurized to the flame. The fuel gas combined with oxidant is then passed through the burner head at a high velocity that forms a vacuum in the capillary tube. The sample rises through the sample line into the flame due to pressure difference. Total consumption burner is never used in AAS but it is widely used in flame photometry. The flame produced by this burner is unstable and non-homogenous making it ineffective in AAS (Figure 2.6.).

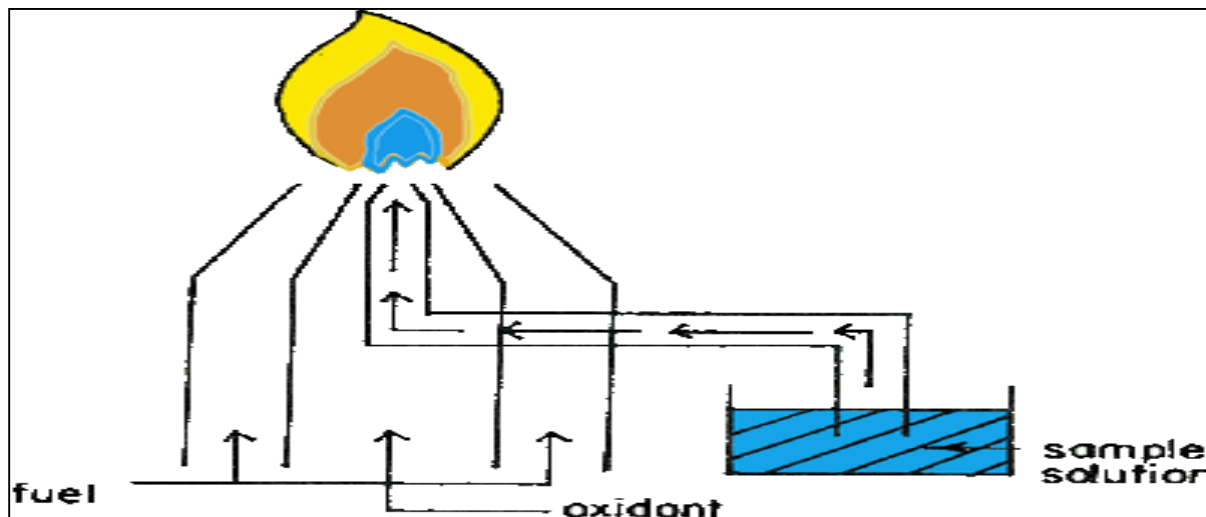


Figure 2.6 Total consumption burner (Source: Nicolas *et al*, 2013)

The other type of burner that is used in AAS is called premix burner. In this burner, a mixture of the sample oxidant and the fuel gas is made. A sequence of baffles is then used to introduce the mixture into the flame.

A mixture of fuel gas and oxidant is passed through the burner head at a high velocity that forms a vacuum in the capillary tube. The sample rises through the sample line into the flame due to pressure difference. Premix burner has a drain line that is used to remove the droplets of the sample solution that do not get to the flame (Figure 2.7).

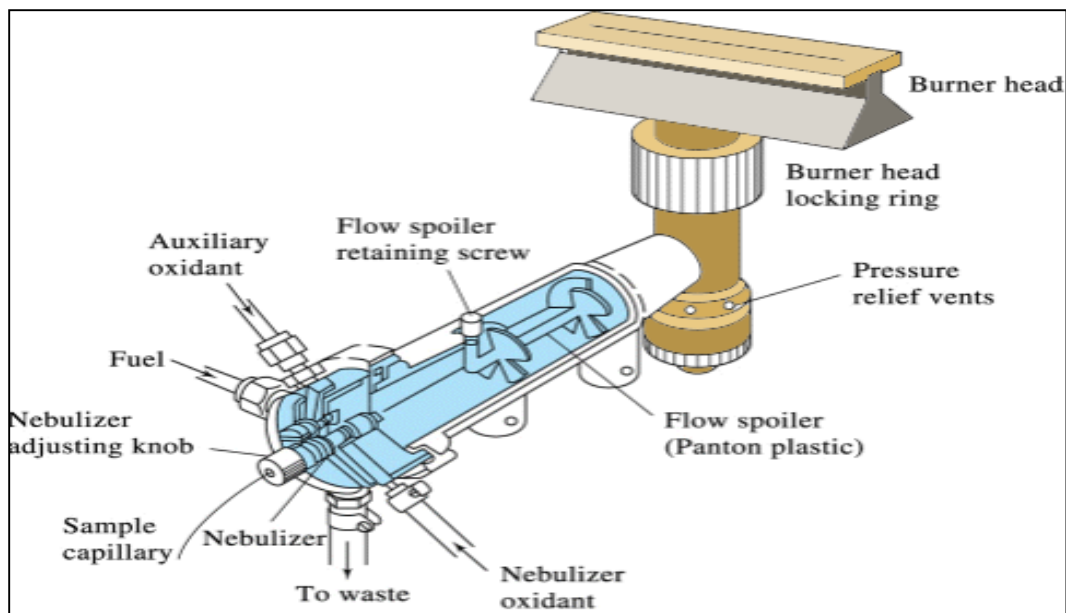


Figure 2.7: Design diagram of premix burner (Source: Nicolas *et al*, 2013)

AAS are designed in a way that allows the user to have several burner heads depending on combination of velocity and temperatures of the flame. A mixture that burns quickly would call for a burner head designed with a smaller slot to avoid explosion.

2.9.4 Monochromator

This disperses the incident beam of light and allows a narrow band of wavelength of light to reach the detector.

2.9.5 Detector

The detector generates signals proportional to the amount of light received hence determining the intensity of the photons received. It measures transmittance and absorbance.

Absorbance is the amount of light absorbed by the sample while transmittance refers to remaining amount of light which goes to the detector from the sample.

2.10 Kinetic models for heavy metal adsorption

Kinetics of heavy metal adsorption on the water hyacinth biomass in aqueous solution was assessed so that one may understand how adsorption took place. The heavy metal adsorption or release in an aqueous solution could be represented as follows:



where S_f represents the different adsorption sites on the adsorbent where the metal, Me can be retained. The adsorption of the metal on the sites could be enhanced by both physical and chemical characteristics of the medium (Mbui *et al.*, 2014). Langmuir and Freundlich isotherms have been applied on heavy metal adsorption studies. The Langmuir isotherm assumes that the adsorbing material has a definite number of active spots which are evenly distributed (Jeppu and Clement, 2012). Langmuir model assumes that adsorption is a reversible process while the Freundlich isotherm describes the multilayer adsorption (Nimibofa *et al.*, 2017)

2.11 Characterization of the adsorbent using Fourier-Transform Infrared

The infrared light, which is part of electromagnetic spectrum, is used to scan test samples and observe chemical properties. The basis of FTIR is that molecules have different chemical bonds which vibrate at specific frequencies (Griffiths and de Hasseth, 2007). These frequencies occur between 4000 cm^{-1} - 200 cm^{-1} in the infrared region. When infrared radiation is directed to a sample it is either absorbed or transmitted. The frequencies at which the radiations are absorbed by the sample correspond to the molecular vibrational frequencies (Griffiths and Holmes, 2002).

A plot of the energy absorbed by the sample vs frequency is referred to as infrared spectrum. Different materials have different infrared spectra. This makes the identification of different substances easier. The frequency of absorptions is important in determining the presence or absence of a chemical group. FTIR saves time in comparison to dispersive instrument. This is because the scanning process of a sample in FTIR uses an interferometer. The signal which is produced by the interferometer contains every infrared frequency, hence all infrared frequencies can be scanned simultaneously (Alben, 1996). Therefore the time aspect in FTIR is reduced.

The dispersive instrument scans one infrared at a time hence it is time consuming. The interferometer uses a beam splitter that partitions the radiation into two. One beam is reflected by a mirror in motion while the other is reflected a mirror in a fixed place. The beam splitter then recombines the two beams. The path length of one beam is varying while the path length of the other beam is constant hence the signal (interferogram) exiting the interferometer is as a result of two beams obstructing one another (Goormaaghtigh *et al.*, 2006). The interferogram is unique since every data point has information pertaining every infrared from the source (Khurana and Fink, 2000). This further means that as the signal is measured; all the infrared frequencies are measured concurrently (Chen *et al.*, 2010). The measured signal is then decoded by a computer through a mathematical technique called Fourier transformation. The results of transformation are spectra which can be interpreted.

2.12 Components of Fourier Transform Infrared Spectrometer

The components of FTIR which are shown in Figure 2.8 include: infrared source, interferometer, sample, detector and Computer

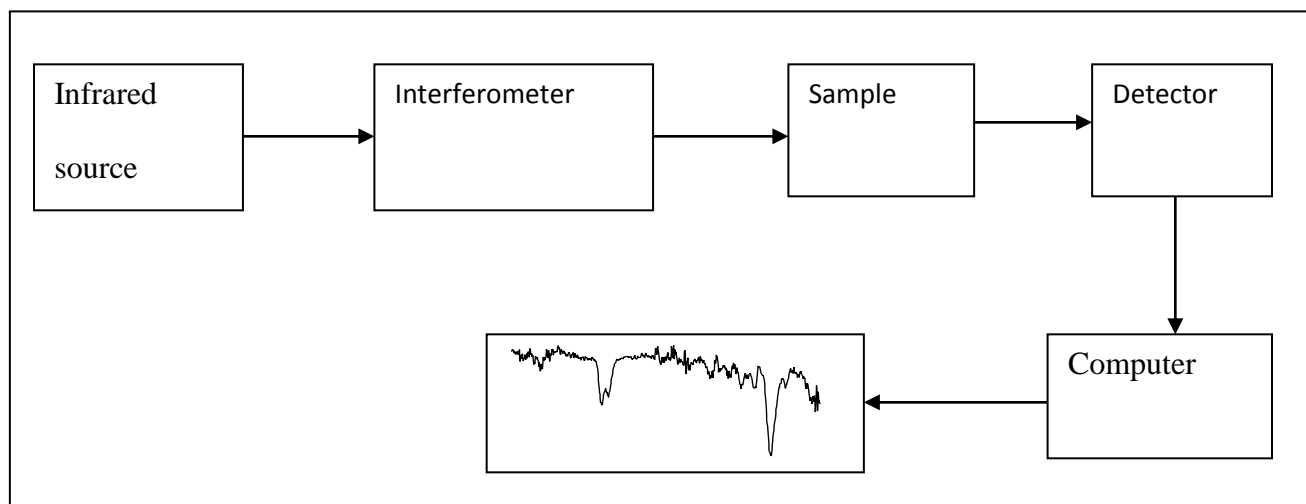


Figure 2.8: Components of FTIR

Radiation from the source is transmitted through an aperture. The aperture controls the amount emitted. This then passes through the interferometer which is a device that is responsible for the spectra “encoding”.

The beam is then directed to the sample which contains the molecules with functional groups to be determined. The beam is then transmitted through the sample or reflected by the detector where light is changed to electrical energy that can be measured and interpreted by computer that transforms it to a digital signal.

CHAPTER THREE

MATERIALS AND METHODS

3.1 Study site

Nairobi is the capital and largest city in Kenya. It is located in Nairobi County with latitude 1.4523-1.1657⁰ S and longitude 36.8219- 37.1601⁰ E. Nairobi occupies an area of 696 km². It is 1661 m above the sea level with tolerable temperatures throughout the year (CBS, 2001). Nairobi has a population of 4,410,000 (Kenya National Bureau of Statistics, 2017). Nairobi River, Ngong River and Mathare River are the major rivers which traverse through the County. It is the centre for executive and economic activities in Kenya (Alukwe, 2016). It is the home to industries such as food processing, fertilizer manufacturing, paints manufacturing, textile and clothing, battery manufacturing etc. Urban planning has been a problem in Nairobi, with most of the residents living in the informal settlements. On average there are 6336 people/km² in Nairobi (KNBS, 2017). According to UNEP, (2005), the high influx of people in Nairobi in search of employment has not only hindered development in the City but also greatly contributed to pollution. Increased industrialization has not only contributed heavily to soil but also air and water pollution. Figure 3.1 shows the map of Nairobi divided into divisions.

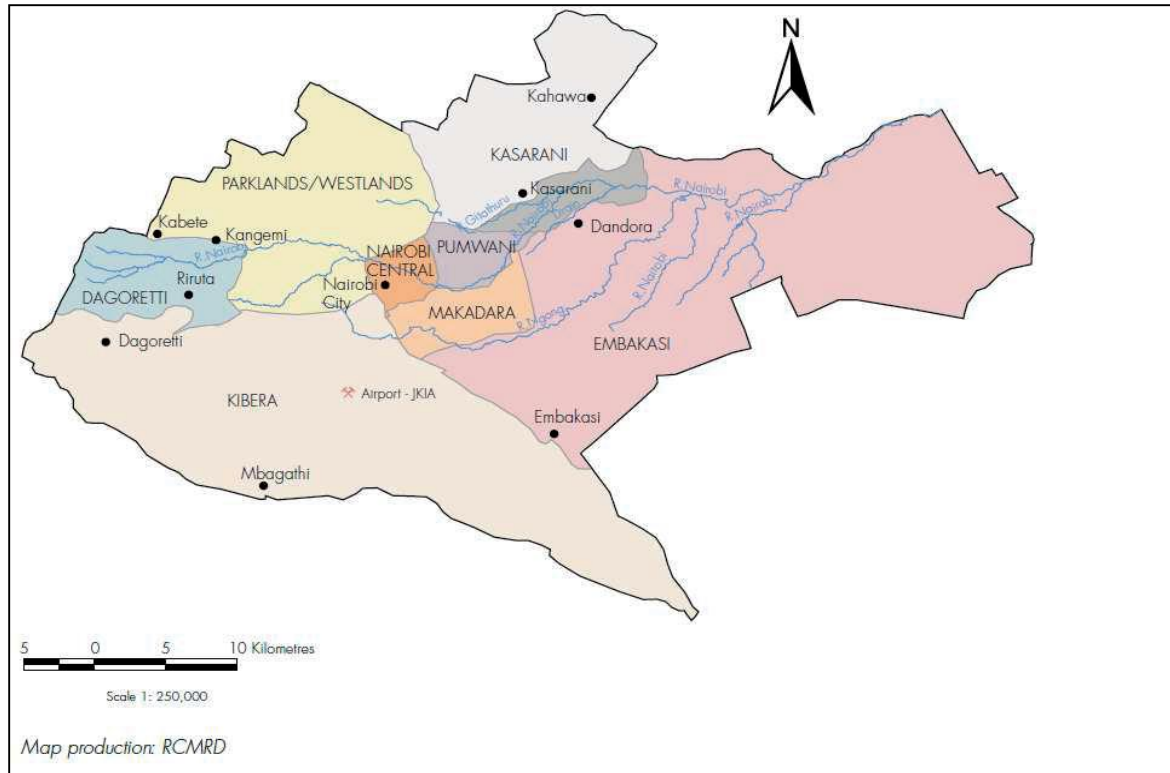


Figure 3.1: The map of Nairobi (Source: Alukwe, 2016)

3.2 Collection of the samples

Samples of wastewater were collected from Site A-Battery manufacturing Company (1.3052° S, 36.8537° E), Site B –Paints manufacturing Company (1.3120° S, 36.85490° E), Site C – Steel manufacturing Company (1.30726° S, 36.82841° E) and Site D- Plastics manufacturing Company (1.31854° S, 36.86530° E) located in Embakasi and Makadara Divisions in Nairobi County. The sampling sites are shown in Figure 3.2. Wastewater samples were collected at the exit points of the release tunnels from the industries.

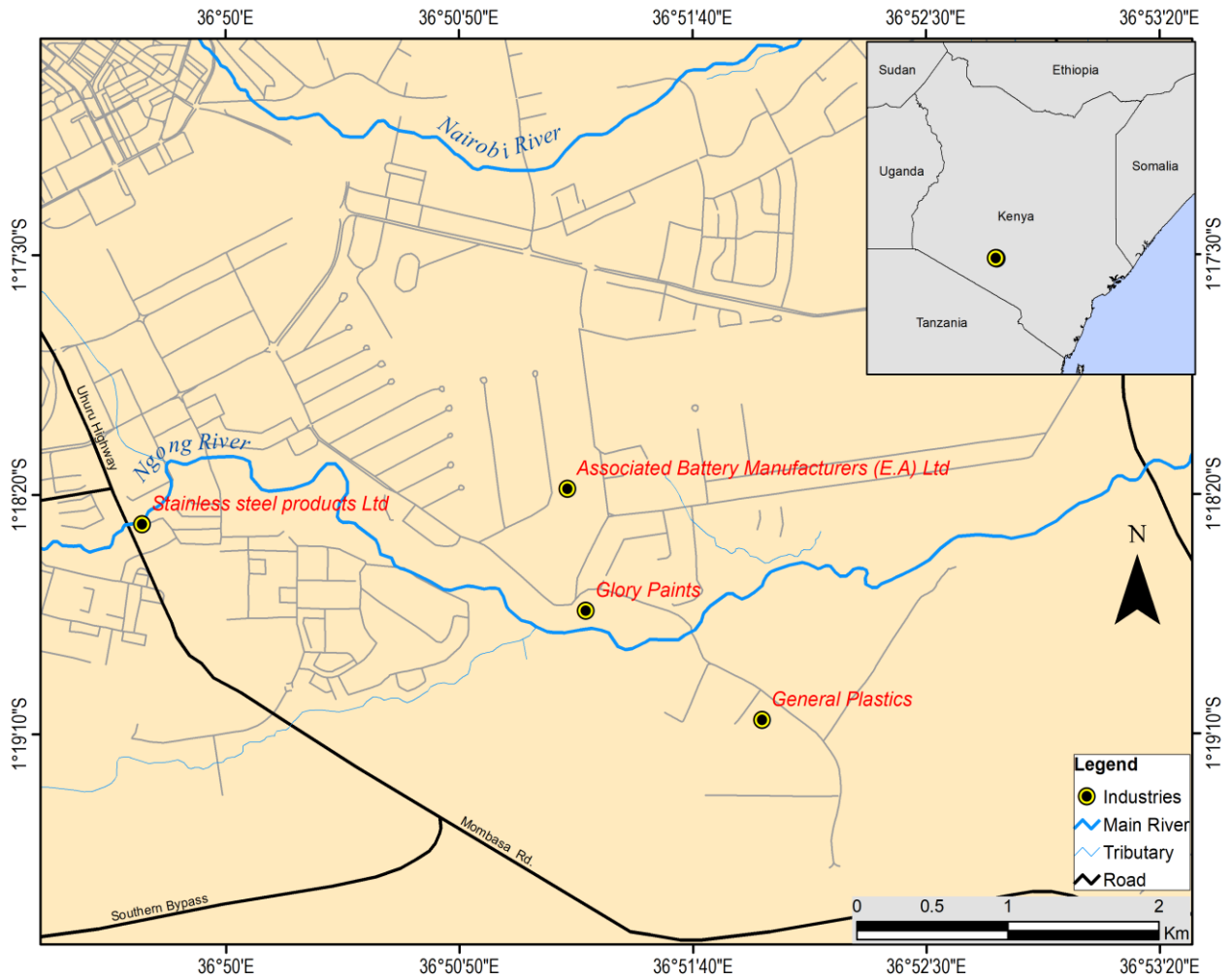


Figure 3.2 A map of sampling points in industrial area, Nairobi Kenya

Sampling was done using pre-cleaned polyethylene bottles that had been washed with distilled water and rinsed with HNO_3 and labeled (Sample A- for the sample collected from Battery manufacturing Company, sample B- for the sample collected from Paints manufacturing Company, C – for the sample collected from Steel manufacturing Company and sample D- for the sample collected from Plastics manufacturing Company). The samples were then stored in a refrigerator for subsequent analysis.

3.3 Adsorbent collection and preparation

Water hyacinth was collected from a beach point on Lake Victoria as shown in Figure 3.3.



Figure 3.3 Collection of water hyacinth from a point on Lake Vitoria

The water hyacinth stems were sliced into minute bits and cleaned completely with water in order to eliminate dust and other contaminants. Distilled water was then used to rinse and the stems dried until they were sufficiently dry. The water hyacinth pieces were further oven dried at 110 °C for a day to remove moisture completely. The dry fractions of the water hyacinth stem were ground into powder using mortar and pestle into various particle sizes. The particles were sieved and graded using three sieves (300, 425 and 2800 µm) and then stored for subsequent use. The ground water hyacinth is shown in Figure 3.4

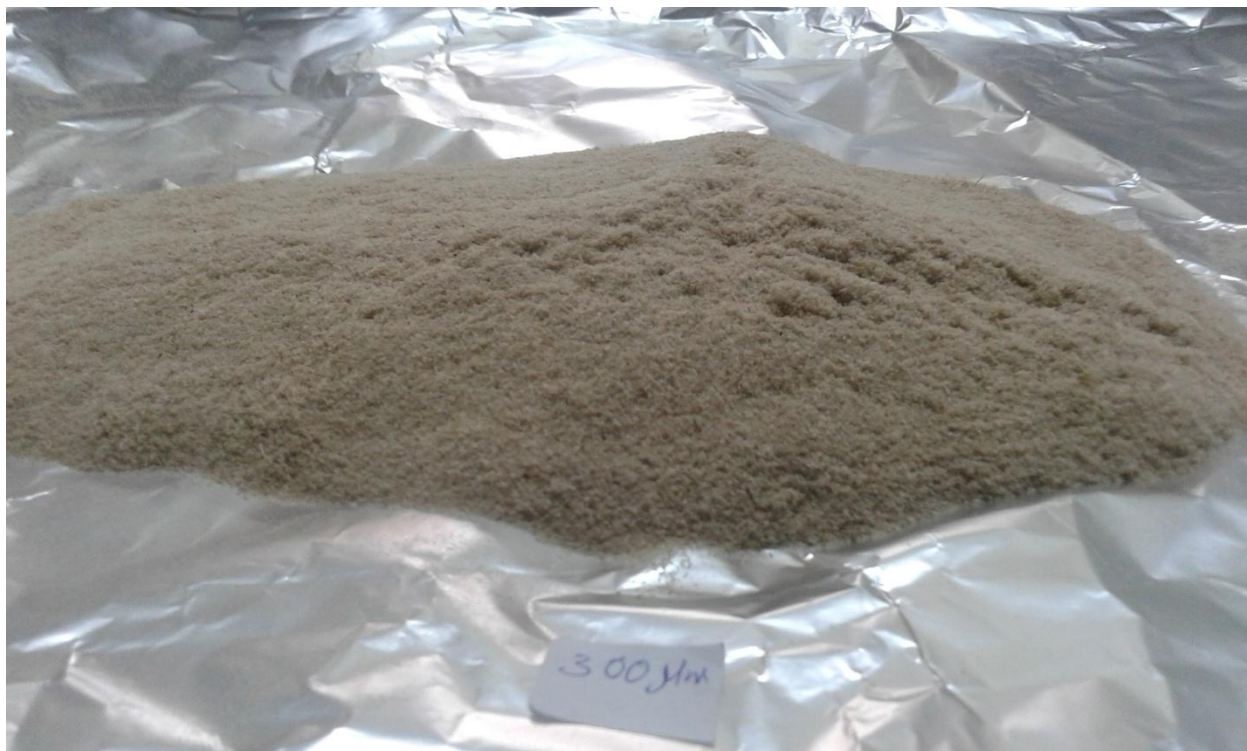


Figure 3.4: Ground water hyacinth sample (300 μm)

3.4 Apparatus and reagents

3.4.1 Apparatus

All volume measurements were done using pipette (20ml), volumetric flasks (100ml and 1000ml). 500 ml beakers were used for the adsorption processes. All the masses were weighed using an analytical balance (Model Mettler Toledo XS105). The pH measurements in the study were done using pH meter (Model HANNA HI 22091).

Samples in the study were stirred using SB 302 stirrer at 300 rpm. Gravity filtration of the samples was done using Whatmann Filter Paper No. 40. The filtrate was analyzed using Atomic Absorption Spectrometer (Model AA-6300 SHIMADZU). Mercury thermometer was used to monitor the temperature changes during the adsorption processes. Distilled water was used throughout the study.

3.4.2 Reagents

All reagents used in the study were of analytical grade. The reagents were provided by Chemoquip Limited. The reagents are summarized in Table 3.1

Table 3.1 Quantity and purity of the reagents used in the study

Reagent	Quantity	Purity
Pb (NO ₃) ₂	500 g	98%
Zn (NO ₃) ₂ . 6H ₂ O	500 g	96%
3CdSO ₄ .8H ₂ O	500 g	98%
Cr (NO ₃) ₃ . 9H ₂ O	500 g	97%
Ni (NO ₃). 6H ₂ O	500 g	98%
Whatmann Filter Paper No. 40	5 packets	-

3.5 Experimental procedure

3.5.1 Digestion of wastewater samples

300 ml of the wastewater samples were first treated with 3 ml dilute nitric acid, shaken thoroughly and allowed to stand for 24 hrs to allow the metal adsorbed to the walls of the container to re-dissolve. The samples were gravity filtered using Whatmann filter paper no. 40 and plastic filter funnels in order to eliminate turbidity. The filtrate was shaken and 100ml transferred into a beaker using a 100 ml volumetric flask. 3.0 ml of aquaregia was added to the 100 ml sample. The resulting mixture was covered with a watch glass. 100 ml of deionized water was transferred into a beaker, followed by 3.0 ml of aquaregia and covering the beaker with a watch glass to make a blank.

The samples were heated using hot plate (SB302) at 90 °C for 3 hrs in a fume hood until the volume of the sample was reduced to 20 ml. After digestion, the samples were allowed to stand for 30 minutes to cool and the fumes allowed to reduce. The watch glass was removed and the sample was dispensed into a 100 ml volumetric flask. Distilled water was added to the samples to make it to 100 ml. The samples were stirred using stirrer model SB302 (300 rpm, 25 ± 2 °C) to properly mix the sample. Gravity filtration was done using Whatmann Filter paper NO. 40 and

plastic filter funnels after which the concentration of the heavy metals in the samples was determined using Atomic Absorption Spectrophotometer.

3.5.2 Sample analysis using AAS

The standard solutions were used in the calibration of the AAS. The concentration of the standards used was from 0.1 to 1.0 ppm. The AAS was then switched on and set up to the working conditions as per the operational instructions. The standards were then aspirated into the instrument and the reading taken which were used to obtain the linear calibration curve for each metal. After which the samples were aspirated into the instrument and the absorbance of each metal in each sample determined. The concentrations of each metal in each sample were then recorded. Depending on the concentration values obtained, some of the samples were diluted to ascertain that the concentration lies within the concentration scope of the standards. The absorbance values obtained were fitted in $y = Mx + C$ (equation of the curve) to calculate the concentration of the samples (Where x = concentration; y =is absorbance; M = gradient). The calculated concentrations were recorded as C_1 (Table 4.1).

3.5.3 Preparation of the stock solutions

The formula (Equation 3.1) was used to calculate the amount of the salt to be dissolved in a liter of distilled water to make an aqueous solution whose concentration was 1000 ppm.

$$m = \frac{M_w}{A_w} \times \frac{100}{P} \times \frac{V}{1000} \quad (3.1)$$

where m = mass (g) of the soluble salt which was weighed, M_w = molecular weight of the salt, A_w = Atomic mass of the element of interest, V = volume of the stock solution to be made, P = percentage purity of the salt.

Calculation of the amount of metal salts for preparation of solution concentration.

Pb (NO₃)₂ (98% pure)

$$m = \frac{M_w}{A_w} \times \frac{100}{P} \times \frac{V}{1000}$$

Mw =331.2, Aw=207.2, p=98, V=1000

$$m = \frac{331.2}{207.2} \times \frac{100}{98} \times \frac{1000}{1000}$$

m=1.6311g

The calculated amount of metal salts which was weighed is shown in the Table 3.2.

Table 3.2 Amount of salts weighed (g) to make aqueous solution whose concentration was 1000 ppm

Metal	Molecular formula	Molecular weight	Amount weighed (g)
Lead	Pb (NO ₃) ₂	331.2	1.6311
Zinc	Zn (NO ₃) ₂ . 6H ₂ O	297.48	4.7396
Cadmium	3CdSO ₄ .8H ₂ O	769.56	6.9861
Chromium	Cr (NO ₃) ₃ . 9H ₂ O	400.15	7.9347
Nickel	Ni (NO ₃) ₂ . 6H ₂ O	290.80	5.0560

The amount weighed was then placed in a 1000 ml volumetric flask. 100 ml of distilled water was added and stirred using stirrer (Model: SB 302 at 300 rpm, 25 ± 2 °C) until all the salt had dissolved. 30 ml of 1M HNO₃ was added and the solution was swirled. Distilled water was added to make it to the mark using distilled water.

3.5.4 Working solutions

The working solutions were prepared through serial dilutions of the stock solution. The metallic concentrations of the working solutions prepared were based on the concentration of the same metal in the waste-water (Table 4.1). The following concentrations were prepared: 1.2, 3.2, 68.5 and 75.3 ppm for lead; 0.9, 1.0, 40.0 and 52.3 ppm for cadmium; 0.6, 0.8, 48.8 and 95.5 ppm for zinc; 0.1, 0.2 and 63.5 ppm for nickel and 0.4, 0.5, 12.6 and 87.6 ppm for chromium. The formula for dilution is shown in Equation 3.2.

$$C_1V_1=C_2V_2 \quad (3.2)$$

Where C_1 - concentration of the stock solution
 V_1 -volume to be taken from the stock solution
 C_2 -concentration intended to be made
 V_2 -the volume intended to be made

3.5.5 Removal of heavy metals from wastewater

100 ml of digested sample was added to 0.5 g of powdered water hyacinth (weighed using Mettler Toledo model XS105) contained in a series of beakers. The mixtures were stirred continuously using a stirrer (SB 302 at 300 rpm, 25 ± 2 °C) for 5 minutes and allowed to stand for 2 hours for adsorption to occur. The mixture was filtered using gravity filtration (using Whatman Filter Paper no. 40 and plastic filter funnels). The residual concentration (C_2) in the filtrate was established using the AAS. The recorded concentrations (C_1 and C_2) were used to compute the adsorption efficiency of water hyacinth in the adsorption of selected metallic ions from waste-water.

3.5.6 Calculation of adsorption efficiency and the adsorption capacity

The adsorption efficiency (q) by water hyacinth powder (<300 μm) was calculated based on the amount of adsorbate adsorbed in mg to concentration of metal ion originally present.

The formula for adsorption efficiency is shown in Equation 3.3.

$$q = \frac{c_1 - c_2}{c_1} \times 100 \quad (3.3)$$

where

q - adsorption efficiency

C_1 and C_2 - initial concentration and final concentration of the selected heavy metals in waste-water obtained from industrial area.

The concentration of lead in 100 ml of wastewater from a site was for example 60.5 ppm. Upon adsorption by 0.5 g of water hyacinth powder, the residual lead concentration was found to be 16.2 ppm

Sample calculation

$$\text{a) Adsorption efficiency} = \frac{C_1 - C_2}{C_1} \times 100$$

where $C_1 = 60.5$ ppm; $C_2 = 16.2$ ppm

$$\begin{aligned} \text{Adsorption efficiency} &= \frac{60.5 - 16.2}{60.5} \times 100 \\ &= 73.2\% \end{aligned}$$

The adsorption capacity (q) of powdered water hyacinth (<300 μm) calculated according to Equation 3.4

Calculation of % adsorbed and adsorptive capacity

b) Adsorption capacity

$$(q) = \frac{(C_1 - C_2)}{M} \times V \quad (3.4)$$

$C_1 = 60.5$ ppm; $C_2 = 16.2$ ppm; $m = 0.5$ g; $V = 0.1$ L

$$\begin{aligned} \text{Adsorption capacity (q)} &= \frac{60.5 - 16.2}{0.5} \times 0.1 \\ &= 8.86 \text{ mg/g} \end{aligned}$$

3.6 Removal of heavy metals from aqueous solution using water hyacinth

100 ml of an aqueous solutions whose concentrations varied with the metal (75.3 ppm for lead solution, 52.7 ppm for cadmium solution, 95.5 ppm for zinc solution, 63.5 ppm for nickel solution and 87.6 ppm for chromium solution) was added to 0.5g (<300 μm) of powdered water hyacinth (weighed using Mettler Toledo model XS105) contained in a series of 500 ml beakers. The mixtures were stirred continuously using a stirrer (SB 302 at 300 rpm, 25 ± 2 °C) for 5 minutes and allowed to stand for 2 hours for adsorption to occur. The mixture was filtered using gravity filtration (using Whatman Filter Paper no. 40 and plastic filter funnels). The concentrations (C_3) of selected heavy metal ions were determined in the filtrate using the Atomic

Absorption Spectrometer (AA-6300 SHIMADZU AAS). The recorded concentrations (C_1 and C_3) were used to determine the adsorption efficiency of water hyacinth (q).

3.7 The effect of selected parameters on heavy metal adsorption

The effects of pH, contact time, adsorbent dosage and particle size on heavy metal adsorption were determined as outlined below.

3.7.1 The effect of particle size on heavy metal removal

0.5 g (weighed using Mettler Toledo model XS105) of ground water hyacinth whose particle sizes was $<300 \mu\text{m}$ was placed in three, 500 ml beaker. To each beaker, 100 ml of metal ions (prepared in 3.5.4 above) was added. The mixtures were stirred continuously using a stirrer (SB 302 at 300 rpm, $25 \pm 2 \text{ } ^\circ\text{C}$) for 5 minutes and allowed to stand for predetermined time for adsorption to occur. The mixture was filtered using gravity filtration (using Whatman Filter Paper no. 40 and plastic filter funnels). The concentrations (C_3) of selected heavy metal ions were determined in the filtrate using the Atomic Absorption Spectrometer (AA-6300 SHIMADZU AAS). The above procedure was repeated using ground water hyacinth whose particle size was $>300<425 \mu\text{m}$ and $>425<2800 \mu\text{m}$. The efficiency of adsorption (q) of water hyacinth was calculated based on the amount of adsorbate adsorbed in mg to amount of adsorbent used for adsorption expressed in milligrams. The particle size that corresponded to the highest adsorption efficiency was established and was used during the study of the effects of pH, contact time and the adsorbent dosage.

3.7.2 Effect of pH on heavy metal adsorption on water hyacinth

0.5 g of ground water hyacinth (weighed using Mettler Toledo model XS105) of particle size $<300 \mu\text{m}$ was placed in six, 500 ml beakers. To each beaker, 100ml of aqueous solutions (prepared in 3.5.4) was added. The pH of the solution was regulated using 0.1 M NaOH or 0.1 M HNO_3 and read using bench top pH meter (Model: HANNA HI 22091). The mixtures were stirred continuously using a stirrer (SB 302 at 300 rpm, $25 \pm 2 \text{ } ^\circ\text{C}$) for 5 minutes and allowed to stand for predetermined time for adsorption to occur. Table 3.1 below shows the conditions which were set during the study on the effects of the pH.

Table 3.3 Conditions set for the investigation of the pH effects on adsorption of heavy metals using water hyacinth

Metal	pH range used	Speed of the stirrer (rpm)	Stirring time (minutes)	Adsorption Time (minutes)
Lead	2-7	300	5	120
Cadmium	2-7	300	5	120
Chromium	2-7	300	5	120
Zinc	2-7	300	5	120
Nickel	2-7	300	5	120

The mixture was filtered using gravity filtration (using Whatman Filter Paper no. 40 and plastic filter funnels). The concentrations (C_3) of selected heavy metal ions were determined in the filtrate using the Atomic Absorption Spectrometer (AA-6300 SHIMADZU AAS). The recorded concentrations (C_1 and C_3) were used to determine the adsorption efficiency of water hyacinth (q).

3.7.3 Effect of contact time on heavy metal removal

0.5 g of ground water hyacinth of $<300 \mu\text{m}$ was placed in twelve, 500 ml beakers. To each beaker, 100 ml of metal ion (prepared in 3.54) was added. The mixture was stirred continuously using stirrer (SB 302) at 300 rpm, $25 \pm 2 \text{ }^\circ\text{C}$ for 5 minutes. Adsorption was allowed to occur for predetermined time. The mixture was filtered using gravity filtration (using Whatman Filter Paper no. 40 and plastic filter funnels). The concentrations (C_3) of selected heavy metal ions were determined in the filtrate using the Atomic Absorption Spectrometer (AA-6300 SHIMADZU AAS). The efficiency of adsorption (q) of water hyacinth was calculated.

3.7.4 The effect of amount of water hyacinth on heavy metal removal

0.5 g of ground water hyacinth of size $<300 \mu\text{m}$ was placed in ten, 500 ml beakers. To each beaker, 100 ml of metal ion (prepared in 3.5.4) was added. The mixture was stirred continuously using stirrer (SB 302) at 300 rpm, $25 \pm 2 \text{ }^\circ\text{C}$ for 5 minutes. Adsorption was allowed to occur for predetermined time. The mixture was filtered using gravity filtration (using Whatman Filter

Paper no. 40 and plastic filter funnels). The concentrations (C_3) of selected heavy metal ions were determined in the filtrate using the Atomic Absorption Spectrometer (AA-6300 SHIMADZU AAS). The above procedure was repeated using 1.0, 1.5, 2.0, 2.5, 3.0, 3.5, 4.0, 4.5 and 5.0 g of water hyacinth powder. The efficiency of adsorption (q) of different water hyacinth dosages was calculated.

3.8 Adsorption equilibrium experiments

100 ml of aqueous solutions containing single metal ion (0.5-100 ppm) were added to 0.5 g of water hyacinth powder (<300 μm) in separate 500 ml beakers. The pH of the solutions was set (pH = 4 for lead and chromium, pH = 5 for nickel, cadmium and zinc) and the solutions stirred for 5 minutes. Adsorption was allowed to occur for 120 minutes. These experiments were performed at room temperature for every heavy metal ion that was investigated until the equilibrium was established. The mixture was filtered using gravity filtration (using Whatman Filter Paper no. 40 and plastic filter funnels). The concentrations (C_3) of selected heavy metal ions were determined in the filtrate using the Atomic Absorption Spectrometer (AA-6300 SHIMADZU AAS).

The data obtained from the experiment was fitted in Langmuir and Freundlich isotherms to characterize the reaction mechanism. The equilibrium adsorption capacity, q_e (mg/g) for water hyacinth was calculated using Equation 3.5.

$$q_e = \frac{(C_0 - C_e)v}{w} \quad (3.5)$$

The linear form of Langmuir isotherm that was used is shown in equation 3.6

$$\frac{1}{q_e} = \left(\frac{1}{qmb} \right) \cdot \frac{1}{C_e} + \frac{1}{qm} \quad (3.6)$$

where: C_0 and C_e are the initial concentration and final equilibrium concentration of the heavy metal (mg/L), v (L) and w (g) are volume of the sample and mass of the adsorbent used respectively.

q_e (mg/g) – equilibrium adsorption capacity

C_e (mg/l)- the amount of adsorbed heavy metal ion at equilibrium.

q_m (mg/g)- the highest amount of the heavy metal ion for every unit weight of water

hyacinth while b (l/mg)- Langmuir constant

$1/q_e$ was plotted against against $1/C_e$. The q_m and b values were determined graphically. The dimensionless factor R_L which is used to describe the Langmuir isotherm, was determined from Equation 3.7

$$R_L = \frac{1}{bC_0 + 1} \quad (3.7)$$

where ; $R_L < 1$ – adsorption is favorable,

$R_L > 1$ - adsorption is unfavorable

$R_L = 1$ – linear

$R_L > 1$ - adsorption is irreversible

Freundlich isotherm equation is based on the fact that adsorption occurs on a heterogeneous surface. It is an experiential model which takes into account the adsorptive energy at the surface of the adsorbent. It is expressed as shown in equation 3.8

$$q_e = K_F C_e^{1/n} \quad (3.8)$$

where q_e (mg/g) - amount of the heavy metal ion adsorbed per unit weight of water hyacinth bio-material.

C_e (mg/L)- the amount of un adsorbed heavy metal ion in the solution.

K_f - a constant indicating adsorption capacity

n - Adsorption intensity

The linear form of Freundlich isotherm equation which was used in the study is shown in Equation 3.9.

$$\log q_e = 1/n \log C_e + \log K_f \quad (3.9)$$

$\log q_e$ was plotted against $\log C_e$ and the gradient of $1/n$ and intercept of $\log K_f$ was used in comparing the correlation coefficient, r .

3.8.1 Batch experiments and Kinetic models of heavy metal adsorption on water hyacinth

The kinetic studies were conducted using 100 ml aqueous solutions of single metal at different concentrations (75.3 ppm for lead, 63.5 ppm for nickel, 52.7ppm for cadmium, 95.5 ppm for zinc and 87.6 ppm for chromium). 0.5 g (weighed using Mettler Toledo model XS105) of ground water hyacinth whose particle size was $<300 \mu\text{m}$ was added in separate 500 ml beakers. The pH value of the solutions in the beaker was set as follows: pH= 4 for lead and chromium solution, pH=5 for cadmium, nickel and zinc using a bench top pH meter model HANNA HI 22091, and were adjusted by adding 0.1M HNO_3 and 0.1 M NaOH . The mixtures were stirred continuously using stirrer (SB 302) at 300 rpm, 25 ± 2 °C) for 5 minutes. Adsorption was allowed to occur for 2 hours. The mixture was filtered using gravity filtration (using Whatman Filter Paper no. 40 and plastic filter funnels). The concentrations (C_3) of selected heavy metal ions were determined in the filtrate using the Atomic Absorption Spectrometer (AA-6300 SHIMADZU AAS). The recorded concentrations (C_1 and C_3) were used to determine the adsorption efficiency of water hyacinth (q). The data obtained was used to draw a plot that was used to determine the reaction order which described the adsorption of the heavy metal on water hyacinth bio material. Pseudo-first-order and pseudo-second-order which were applied are shown in Equations 3.10 and 3.11 respectively.

The linear pseudo-first-order equation is;

$$\text{Log}(q_e - q_t) = \log(q_e) - (K_1 t / 2.303) \quad (3.10)$$

The linear pseudo-second-order equation is;

$$t/q_t = 1/k_2 q_e^2 + t/q_e \quad (3.11)$$

where q_e (mg/g)- amount of heavy metal adsorbed on water hyacinth at equilibrium

K_1 (Min⁻¹) - rate constant of adsorption for pseudo-first-order

q_t (mg/g)- amount of heavy metal adsorbed on water hyacinth at time t

K_2 (g mg⁻¹min⁻¹) –rate constant of adsorption for pseudo-second-order

The adsorption rate constant (k_1) for pseudo-first-order was computed from the gradient of a linear plot of $\log(q_e - q_t)$ vs t while q_e was the value of the intercept. The adsorption rate constant for pseudo-second-order (k_2) and q_e were computed from the gradient and intercept of a linear plot of t/q_t vs t . The linear plot with the highest R^2 value was considered to describe the reaction best and was taken as the correct reaction order.

3.9 Fourier Transform Infrared Spectroscopic analysis of powdered water hyacinth before and after heavy metal adsorption.

Raw water hyacinth and metal loaded water hyacinth samples were prepared differently and scanned for various functional groups in the spectral range of $400-4000\text{ cm}^{-1}$ using the FTIR (Model: IR Affinity 1S class 1).

3.9.1 FTIR analysis of raw water hyacinth powder

Water hyacinth powder (prepared in 3.3) was mixed with a spatula of analytical grade KBr in a mortar. The mixture was fine ground. The sample was placed on 7mm collar and pressed to form a pellet by putting the set of metal die and a screw together. The collar containing the pellet was removed from metal die and a screw and it was placed in a cuvette. The machine was switched and the sample was scanned. Various bands in the spectrum were identified as corresponding to different bonds in different functional groups.

3.9.2 FTIR analysis of metal loaded water hyacinth powder

The water hyacinth residue after adsorption and filtration was further oven dried at $110\text{ }^{\circ}\text{C}$ for a day to remove moisture completely. 0.5 g of dry fractions of metal loaded water hyacinth were ground into powder using mortar and pestle. 1.0 g analytical grade KBr was mixed with the fine powder using a mortar. The mixture was fine ground. The sample was placed on 7 mm collar and pressed to form a pellet by putting the set of metal die and a screw together. The collar containing the pellet was removed from metal die and was placed on the sample holder. The machine was switched on and the sample was scanned. The spectra were compared with that of raw water hyacinth powder.

CHAPTER FOUR

RESULTS AND DICUSSION

4.1 Concentration of Heavy metals in wastewater

AAS was used to determine the absorbance of the samples. Appendices Ia, Ib, Ic, Id and Ie were used in the calculation of the concentration of metals. The results are presented in Table 4.1.

Table 4.1 Heavy metal concentrations (ppm) in wastewater

Site	Heavy metal concentration (ppm)				
	Pb	Cd	Zn	Ni	Cr
A	68.5 ± 0.1	52.7 ± 0.1	0.75 ± 0.01	0.2 ± 0.02	0.51 ± 0.01
B	75.3± 0.2	40.0 ± 0.5	95.5 ± 0.2	0.14 ± 0.06	12.6 ± 0.5
C	1.2 ± 0.03	0.98 ± 0.1	48.8 ± 0.3	63.5 ± 0.2	87.6 ± 0.5
D	3.2 ± 0.01	0.88 ± 0.6	0.58 ± 0.02	0.11 ± 0.03	0.38 ± 0.01

A= Battery manufacturing company; B=Paint manufacturing company; C=Steel manufacturing company and D= Plastics manufacturing company.

In site A, the order of metal concentration was lead>cadmium>zinc>chromium>nickel. The high concentration of lead in site A could be ascribed to the utilization of lead metal and lead oxide as electrodes during manufacturing of batteries (Saaidia *et al.*, 2017). The lofty concentration of cadmium in site A could be attributed to the use of Cadmium Oxide as a conductor in the manufacture of battery (Klein and Costa, 2007).

In site B, the order of metal concentration was zinc> lead>cadmium>chromium>nickel. The high zinc concentration in site B could be attributed to the use of ZnO and ZnCrO₄ as pigments in the manufacture of white and yellow paints respectively (Osmond, 2012). The high concentration could be attributed to the use of Pb(CO₃)₂ and PbCrO₄ to give fresh appearance and color respectively to the paints (Kessler, 2014). The concentration of Cadmium in site B (40.0 pm) was high as compared to the standards by NEMA (0.01 ppm). This could be because of the use of cadmium sulfide as a pigment in the manufacture of the yellow paints (Ogilo *et al.*, 2017). The high concentration of chromium in site B (12.6 ppm) could be attributed to the use of Cr₂O₃ and Cr₂O₃.H₂O as a colorant in chrome green paints (Sabty-Daily *et al.*, 2017).

In site C, the order of metal concentration was chromium>nickel>zinc> lead>cadmium. The high chromium levels (87.6 ppm) in site C could be as a result of chromium use in steel manufacturing (Nakamura *et al.*, 2017). The high nickel concentration could be attributed to the use of nickel in the manufacture of steel (Abdallah *et al.*, 2017). The high concentration of zinc in site C (48.8 ppm) could be as a result of manufacture of zinc-copper-titanium alloy. The high concentration could also be associated with the use of zinc in the galvanization of steel to prevent corrosion (Grillo *et al.*, 2014).

In site D, the order of metal concentration was lead>cadmium> zinc>chromium> nickel>. The high concentration of lead in site D could be attributed to the use of lead stabilizers for the manufacture of polyvinyl chloride products which are used for food packaging and manufacture of toys (Punjongharn *et al.*, 2017).

4.2 Adsorption efficiency and adsorption capacity of water hyacinth powder

The amount of heavy metals adsorbed (adsorption efficiency) on powdered water hyacinth (<300 μm) calculated according to Equation 3.3 and the adsorption capacity (q) according to Equation 3.4 and the results are provided in Table 4.2 (Sample calculation is provided in 3.5.6)

Table 4.2 Adsorption efficiency and adsorption capacity for the metals on water hyacinth powder from wastewater and for various concentrations at four sites compared to aqueous solution

Sites	Adsorption efficiency = $\frac{c_1-c_2}{c_1} \times 100$ %			Adsorption capacity (mg/g) $= \frac{(c_1-c_2)}{M} \times V$ mg/g	
Site	Heavy Metal	Wastewater	Aqueous solution	Wastewater	Aqueous solution
A	Lead (68.5 ppm)	76.4	84.2	10.5	11.5
	Zinc (0.8 ppm)	100	100	0	0
	Chromium (0.5 ppm)	100	100	0	0
	Cadmium (52.7 ppm)	68.9	76.9	7.3	8.1
	Nickel (0.2 ppm)	100	100	0	0
	B	Lead (75.3 ppm)	71.0	81.1	10.7
Zinc (95.5 ppm)		73.7	78.7	14.3	15.1
Chromium (12.6 ppm)		85.2	100	2.18	0
Cadmium (40.0 ppm)		65.5	83.5	5.2	6.7
Nickel (0.1 ppm)		100	100	0	0
C	Lead (1.2 ppm)	100	100	0	0
	Zinc (48.8 ppm)	81.8	89.1	8.0	8.7
	Chromium (87.5)	70.2	73.1	12.3	12.8
	Cadmium (1.0 ppm)	100	100	0	0
	Nickel (63.5 ppm)	60.4	65.7	7.7	8.4
D	Lead (3.2 ppm)	100	100	0	0
	Zinc (0.6 ppm)	100	100	0	0
	Chromium (0.3 ppm)	100	100	0	0
	Cadmium (0.8 ppm)	100	100	0	0
	Nickel (0.1 ppm)	100	100	0	0

From Table 4.2, the percent of metal ion adsorbed on water hyacinth varied with the concentrations and the media. The percent adsorbed was high both in wastewater and aqueous solution at low concentrations while at high metal concentrations the percent of metal ion adsorbed was low. At high percent of metal ion concentration the competition for the adsorption

site is high while at low concentration the competition is low (Medellin-Castillo *et al.*, 2017). The percent of adsorbed metal on water hyacinth was higher in aqueous solution compared to wastewater for a specific concentration. The low adsorption efficiency from wastewater could be attributed to external competition for adsorption sites by other metal ions in the wastewater (Park *et al.*, 2015). In the aqueous solution, only the single metal ions were available hence there was no external competition for the adsorption sites. The study showed that water hyacinth could effectively adsorb heavy metals from aqueous solution when there is no interference by other metals. Water hyacinth powder could be used to adsorb heavy metals from water at low concentrations.

4.3 Factors influencing the adsorption of heavy metals

The effects of pH, contact time, adsorbent dose and particle size on heavy metal adsorption on water hyacinth from an aqueous solution were investigated and the results are presented as below.

4.3.1 Effect of particle size on adsorption of zinc ions on water hyacinth

The quantity of zinc ions adsorbed from aqueous solution increased with decrease in particle size in the order $>425<2800$, $>300<425$ and <300 μm for the zinc concentrations of 95.5 ppm and 48.8 ppm respectively (Figure 4.1). The smaller particles had the highest adsorption efficiency. Appendix II was used to construct Figure 4.1

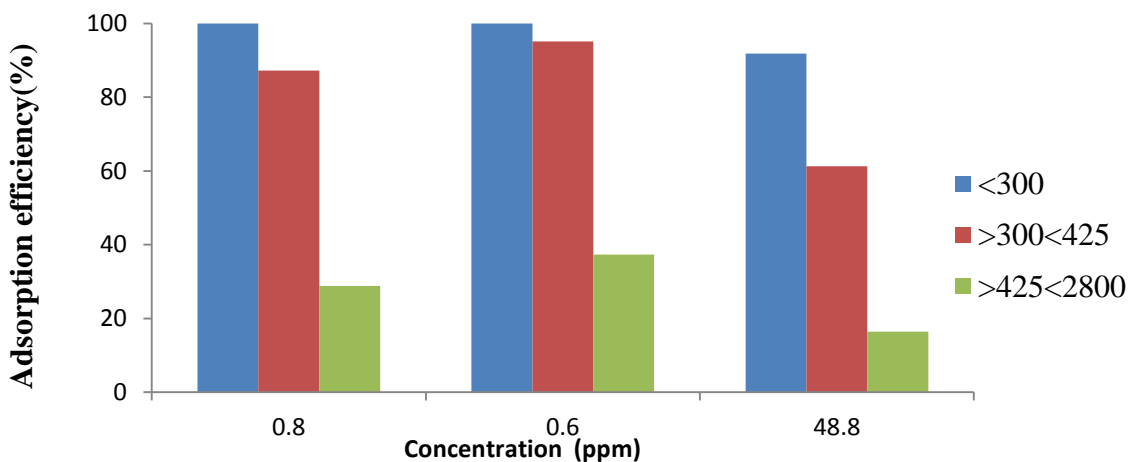


Figure 4.1 Effects of particle size on adsorption of zinc ions from aqueous solution (Adsorbent dose: 0.5g; pH=6.7; contact time 120 minutes; temperature $25 \pm 2^{\circ}\text{C}$)

Irrespective of the concentration used, the smaller particles adsorbed the highest amount of the heavy metal (Figure 4.1). This is so since they have a larger surface area for adsorption than the larger particles (Tembhukar and Dongre; 2006;Schalow *et al.*, 2007). The adsorption efficiency in low concentration (0.6 and 0.8 ppm) was 100% for particle size <300 μm . This could be ascribed to the availability of a larger area for adsorption (Punjongharm *et al.*, 2007). The high efficiency in 0.6 and 0.8 ppm aqueous solution further indicated that water hyacinth has the ability to adsorb zinc ions completely from a low concentration solution. The particle size which gave the highest percent of zinc ions adsorbed for all concentrations was <300 μm . The trend was similar to that of lead, cadmium, chromium and nickel is presented graphically in Appendix II.

4.3.2 Effect of pH on adsorption of zinc ions

The effects of pH on adsorption of zinc ions on water hyacinth powder at different concentrations are shown in Figure 4.2. The values in Appendix III were used to construct Figure 4.2

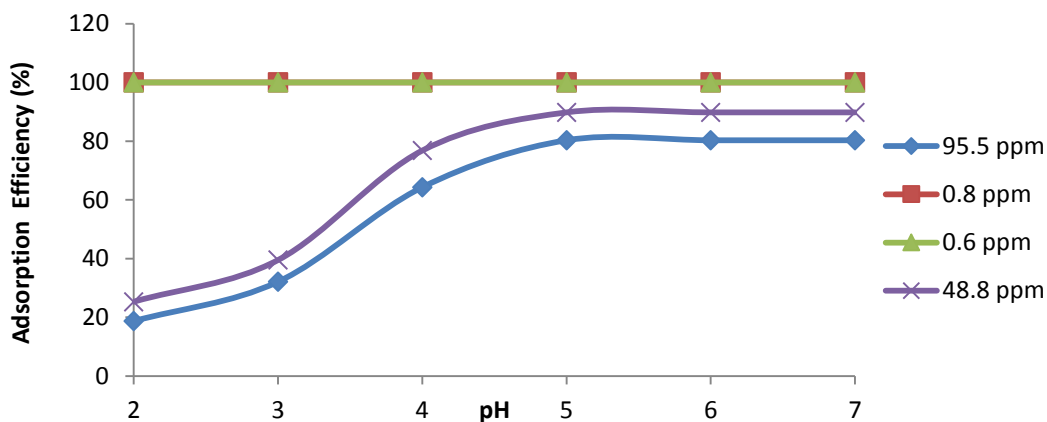


Figure 4.2: The effects of pH on adsorption of zinc ions on water hyacinth from aqueous solution. (Adsorbent dose: 0.5 g; particle size <300 μm ; contact time 120 minutes; temperature 25 ± 2 $^{\circ}\text{C}$)

The adsorption efficiency increased as pH increased from 2-5 for 95.5 ppm. However, there is slow increase in the amount of zinc ions adsorbed at the pH of 2-3. This could be attributed to the competition between zinc ions and hydrogen ions, for the exchange sites found at the outer surface of the adsorbent (Astuti *et al.*, 2017). In addition, the outer adsorbent layer has a positive

charge, which slowed down zinc ions approaching the adsorption spots owing to repulsion. From the pH of 3-5, adsorption of Zn increased rapidly. This might be because of reduced competition since the concentration of hydrogen ions which were hindering adsorption at lower pH was reduced. Optimum adsorption was observed at pH 5 while above pH 5, the slow increase could be because most of the adsorption sites were saturated with metal ions. The study showed that adsorption was optimum at a pH of 5. Similar results were obtained by Kumar, (2013) who used modified *Strychnos potatorum*. The effects of pH on the adsorption of lead, cadmium, chromium and nickel are presented graphically in Appendix III. The optimum pH for the adsorption of both lead and chromium was 4 while that of nickel, zinc, and cadmium was 5. The trend was similar for all the other heavy metals except lead and chromium in the pH range 6-7. Beyond the pH 6, the adsorption efficiency started declining. This could be due to precipitation of $Pb(OH)_2$ and $Cr(OH)_3$ respectively.

4.3.3 Effect of contact time on adsorption of zinc ions

The study showed that the percent zinc ion adsorbed by water hyacinth increased with contact time as shown Figure 4.3. At low concentrations of zinc ions (0.6 and 0.8 ppm), the percent zinc ions adsorbed increased rapidly within the first 10 minutes. The percent zinc ions adsorbed then remained at 100% from 10th minute to 120 minutes. This could be as a result of low concentrations of zinc ion hence less competition for the adsorption sites. It further showed that water hyacinth could adsorb zinc ions from an aqueous solution of low concentration completely. The curves for both 0.6 and 0.8 ppm appear together (Figure 4.3).

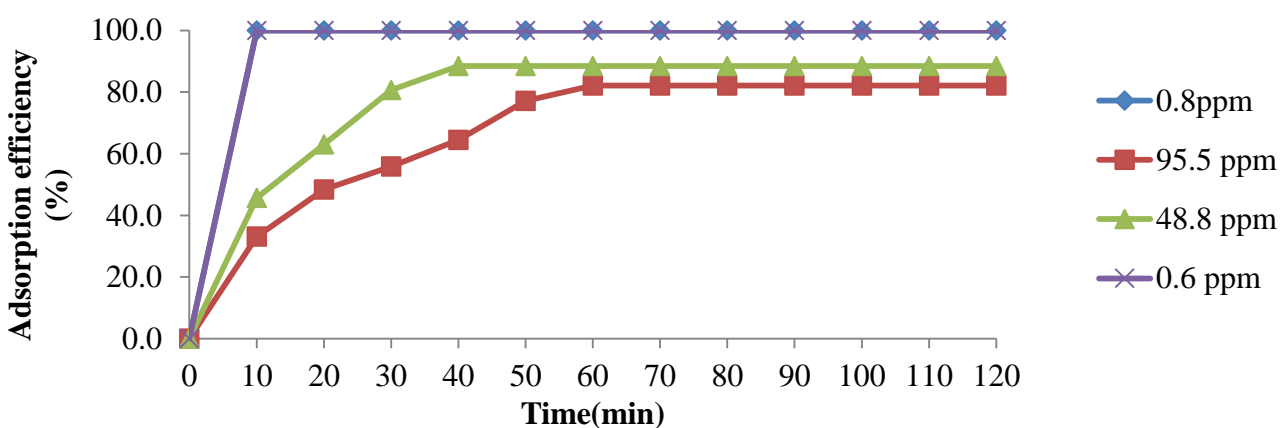


Figure 4.3. Effects of contact time on adsorption of zinc ions from aqueous solution. (Adsorbent dose: 0.5 g; pH = 6.7; particle size <300 μm ; temperature 25 ± 2 $^{\circ}\text{C}$)

When concentrations of 48.8 ppm and 95.5 ppm of zinc ions were used, it took time for the equilibrium to be established. This is because when the concentration was high, there was a competition for the adsorption sites. Adsorption efficiency reached a steady state at 40 and 60 minutes for 48.8 ppm and 95.5 ppm zinc solutions respectively. This could be because, as the time progressed, the repulsive force between cations bound on the adsorption site and the cations present in the solution became stronger hence slow establishment of equilibrium (Tchomgui-Kamga *et al.*, 2010; Igberase *et al.*, 2017). The trend was similar to the one obtained in the adsorption of lead, cadmium, nickel and chromium as shown in Appendix IV. The optimal time for the adsorption varied with the metal (30 for lead, 40 minutes for chromium, 80 minutes for nickel, and 60 minutes for both zinc and cadmium). Similar results were obtained by Igberase *et al.*, (2017) who used modified ligand.

4.3.4 Effect of adsorbent dosage on adsorption of zinc ions

The effects of adsorbent dosage on adsorption of zinc ions from an aqueous solution are shown in Figure 4.4. Appendix V was used to construct Figure 4.4.

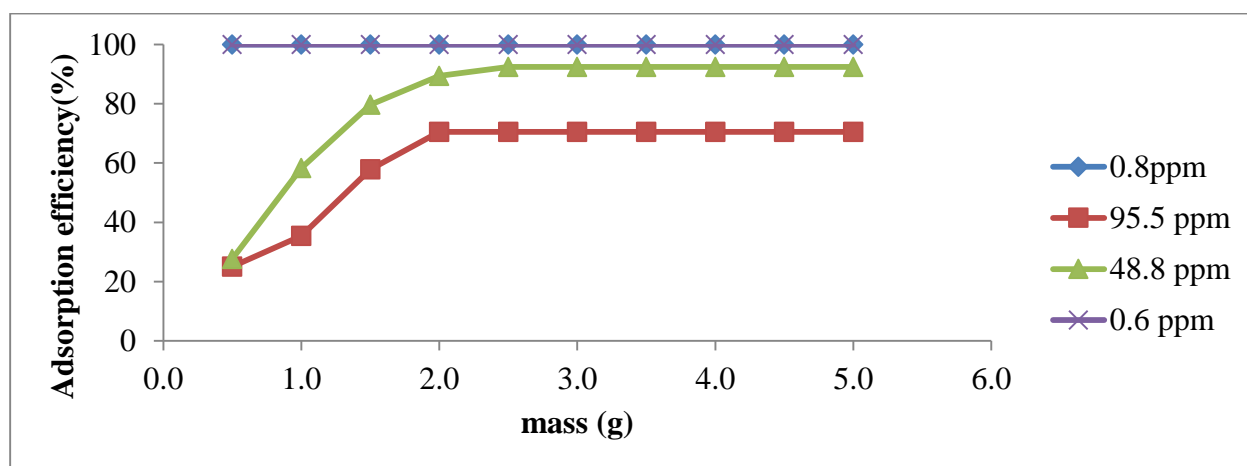


Figure 4.4: The effects of adsorbent dosage on adsorption of zinc ions (Adsorbent dose: 0.5 g; pH = 6.7; particle size <math><300\ \mu\text{m}</math>; contact time 120 minutes; temperature

The percent zinc ions adsorbed increased as the amount of adsorbent increased in both 48.8 ppm (27.7%-92.4%) and 95.5 ppm (25.1%-70.5%) as the dosage was increased from 0.5-2.5g and 0.5-2.0g respectively. The trend was the same for the two concentrations however optimum adsorption was reached at different doses of 2.0 g (for 95.5 ppm) and 2.5g (for 48.8 ppm).

The increase could be because of increased availability of vacant adsorption sites that increased with the quantity of adsorbent (Kumar *et al.*, 2010; Addagalla *et al.*, 2009). The percent zinc ions adsorbed then became steady with increase in adsorbent. This could have been because of the shielding effects among the cells (Gao *et al.*, 2009; Gundogdu *et al.*, 2012). This might have produced a block of cell active sites which increased as the adsorbent dose increased (Desta, 2013). The percent zinc ions adsorbed 100% for both 0.6 ppm and 0.8ppm solution. This might be because zinc ions which were present in the solutions were adsorbed completely by 0.5g of the adsorbent hence the curves formed a plateau together at adsorption efficiency 100%. The optimum adsorption for lead and nickel was 2.5g, cadmium was 3.0 g, chromium was 4.0g while nickel was 4.5g. The effects of adsorbent dosage on the adsorption of lead, cadmium, chromium and nickel are presented graphically in Appendix V.

4.4 Adsorption isotherms

In this study the amount of heavy metal adsorbed by water hyacinth powder was investigated using the Freundlich and Langmuir isotherms.

4.4.1 Adsorption isotherms for the adsorption of zinc ions

The data obtained (Appendix VI) from the studies were then fitted to both Langmuir and Freundlich isotherms (Figures 4.5 and 4.6).

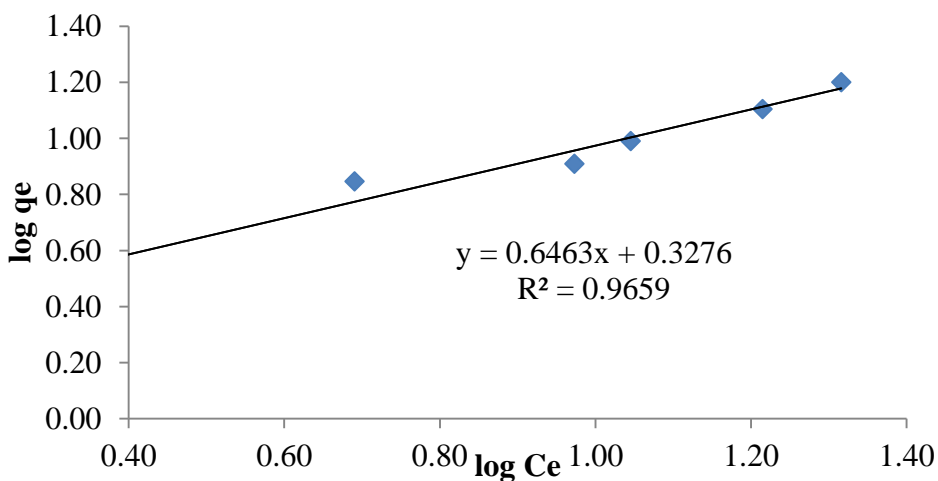


Figure 4.5 Linearized Freundlich plot for the adsorption of zinc ions onto water hyacinth powder

The logarithm of q_e (adsorption capacity at equilibrium) increased linearly to the logarithm of C_e (concentration at equilibrium)

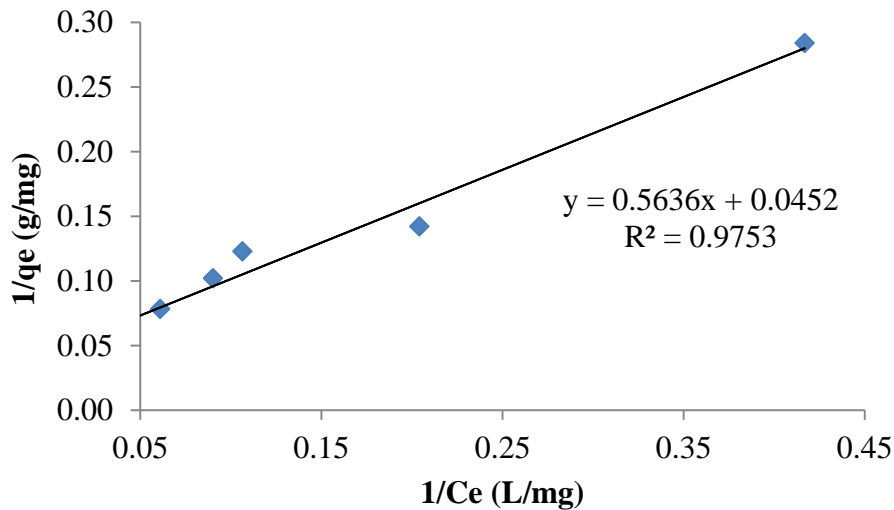


Figure 4.6: Linearized Langmuir plot for the adsorption of zinc ions onto water hyacinth powder

The reciprocal of q_e (adsorption capacity at equilibrium) increased linearly with the reciprocal of C_e (concentration at equilibrium). The Freundlich adsorption parameters (equilibrium constant (K_f), n and regression constant (R^2)) and the Langmuir parameters (regression constant (R^2 , q_m the highest amount of adsorbed per weight of water hyacinth, b -Langmuir constant) were determined graphically from Figure 4.5 while Figure 4.6 as shown in Appendix Vi and the results are presented in Table 4.3

Table 4.3: Parameters for Langmuir and Freundlich isotherms

Freundlich isotherm	Langmuir isotherm
$n = 1.5473$	b (L/mg) =0.0802
$K_f = 2.1262$	q_m (mg/g) =22.1239
$R^2 = 0.965$	$R^2 =0.975$

The use of water hyacinth powder on the adsorption of zinc ions correlated well with the Langmuir model in contrast to the Freundlich model based on the R^2 values. Results similar to

this were obtained by Chigondo *et al.*, (2013) where zinc ions were adsorbed using *Brachystegia spiciformis*. Langmuir isotherm describes the monolayer adsorption while Freundlich isotherm is an adsorption model that describes the multilayer adsorption.

4.4.2 Adsorption isotherms for the adsorption of lead ions

The data obtained from the studies (Appendix VI) were fitted to both Langmuir and Freundlich isotherms and the results are shown in Figures 4.7 and 4.8.

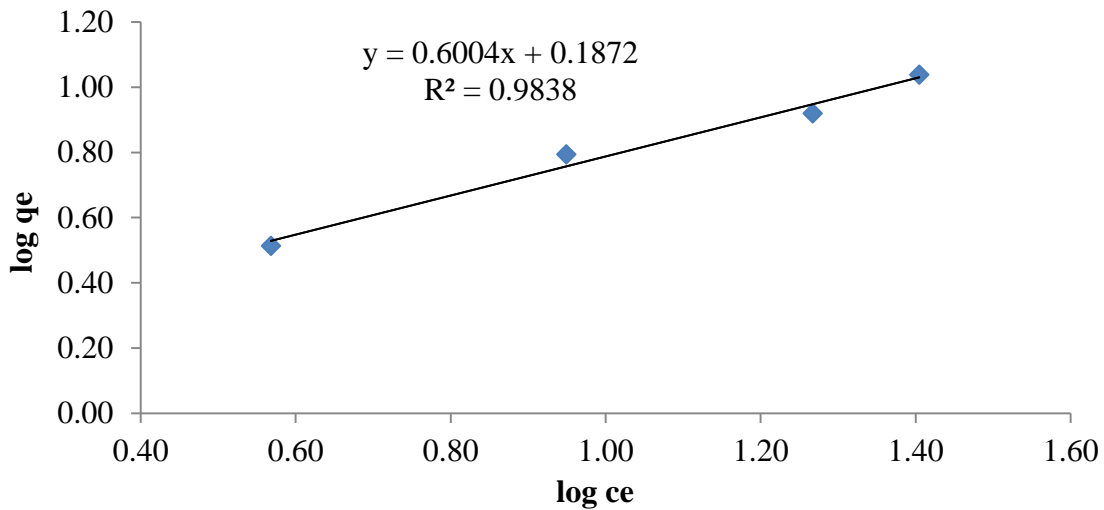


Figure 4.7 Linearized Freundlich plot for the adsorption of lead ions onto water hyacinth powder

The logarithm of q_e (adsorption capacity at equilibrium) increased linearly to the logarithm of c_e (concentration at equilibrium).

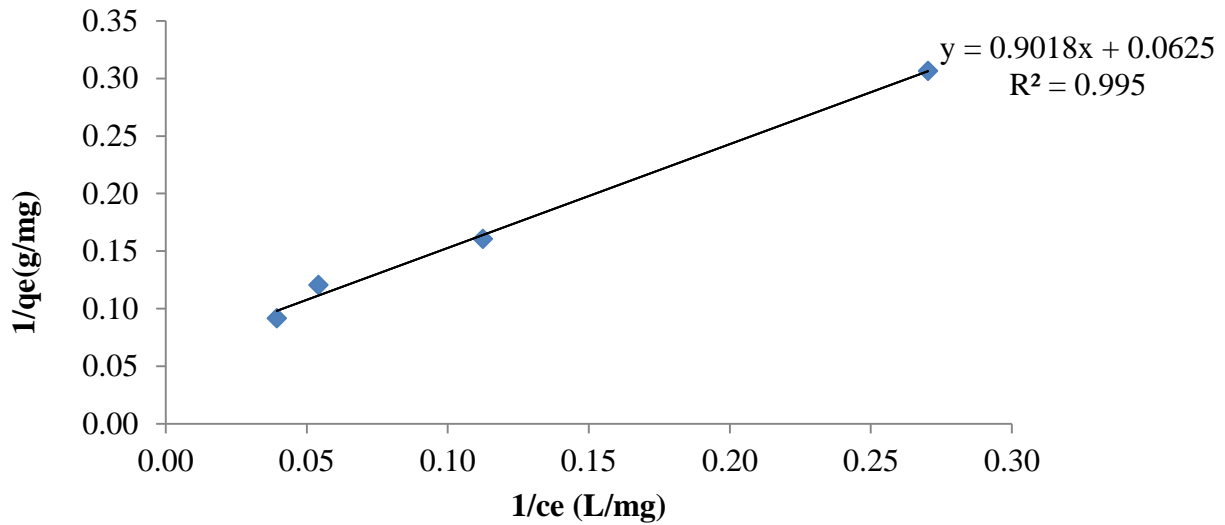


Figure 4.8: Linearized Langmuir plot for the adsorption of lead ions onto water hyacinth powder

The reciprocal of q_e (adsorption capacity at equilibrium) increased linearly with the reciprocal of c_e (concentration at equilibrium). The Freundlich adsorption parameters (equilibrium constant (K_f), n and regression constant (R^2)) and the Langmuir parameters (q_m -the highest quantity of the heavy metal ion for every entity weight of water hyacinth, b -Langmuir constant and regression constant (R^2)) were determined graphically from Figure 4.7 and 4.8 respectively as shown in appendix VI. The adsorption parameters are presented in Table 4.4.

Table 4.4 Langmuir and Freundlich isotherms parameters for adsorption of lead ions from aqueous solution ground using water hyacinth powder

Freundlich	Langmuir
$n = 1.6656$	$b \text{ (L/mg)} = 0.0693$
$K_f = 1.5389$	$q_m \text{ (mg/g)} = 16$
$R^2 = 0.983$	$R^2 = 0.995$

The use of water hyacinth powder on the adsorption of lead ions correlated well with the Langmuir model in contrast to the Freundlich model based on the R^2 values. Results similar to this were obtained by Liu *et al.*, (2009) where lead ions were adsorbed by steel slag.

4.4.3 Adsorption isotherms for the adsorption of nickel ions

The data obtained from the studies (Appendix VI) were then fitted to both Langmuir and Freundlich isotherms. The linearized Freundlich and Langmuir models are presented in Figures 4.9 and 4.10 respectively.

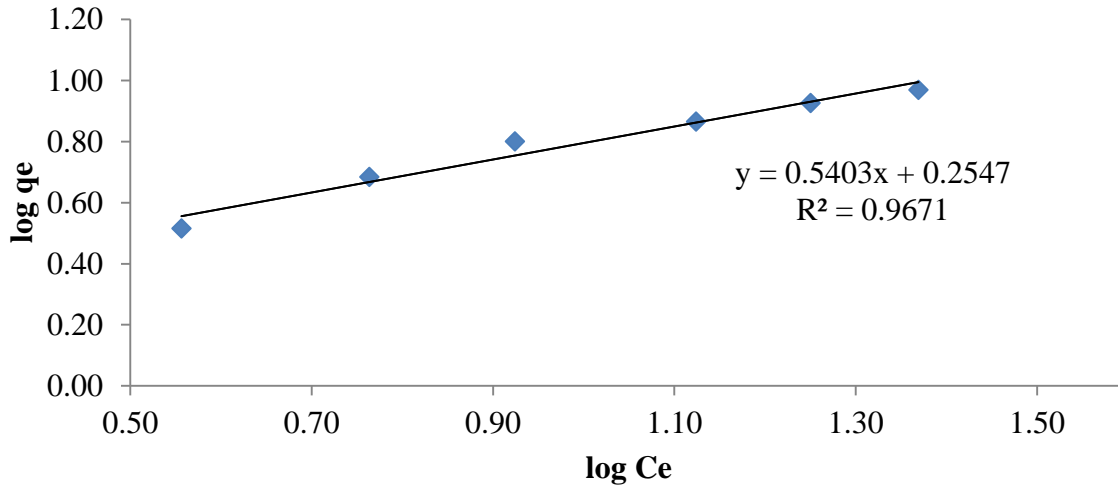


Figure 4.9: Linearized Freundlich plot for the adsorption of nickel ions on ground water hyacinth

The logarithm of q_e (adsorption capacity at equilibrium) increased linearly to the logarithm of c_e (concentration at equilibrium)

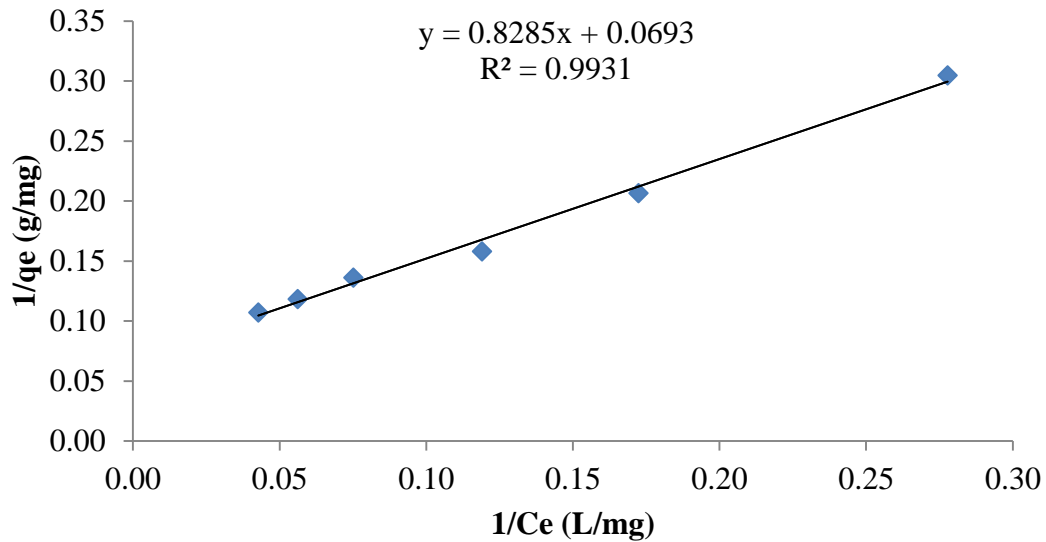


Figure 4.10: Linearized Langmuir plot for the adsorption of nickel ions on ground water hyacinth

The reciprocal of q_e (adsorption capacity at equilibrium) increased linearly with the reciprocal of C_e (concentration at equilibrium). The adsorption parameters for both Langmuir and Freundlich are presented in Table 4.5.

Table 4.5: Parameters for Langmuir and Freundlich isotherms for the adsorption of nickel ions

Freundlich	Langmuir
$n = 1.8508$	$b \text{ (L/mg)} = 0.0833$
$K_f = 1.7976$	$q_m \text{ (mg/g)} = 14.4928$
$R^2 = 0.967$	$R^2 = 0.993$

The Freundlich adsorption parameters (equilibrium constant (K_f), n and regression constant (R^2)) were determined graphically from Figure 4.9 and are presented in Table 4.5 while Figure 4.10 was used to model the Langmuir isotherm and to calculate the Langmuir parameters. The adsorption of nickel ions on water hyacinth powder was described better by Langmuir isotherm ($R^2 = 0.993$) compared to Freundlich isotherm ($R^2 = 0.967$).

4.4.4 Adsorption isotherms for the adsorption of cadmium ions

The data obtained (Appendix VI) were presented as shown in Figures 4.11 and 4.12

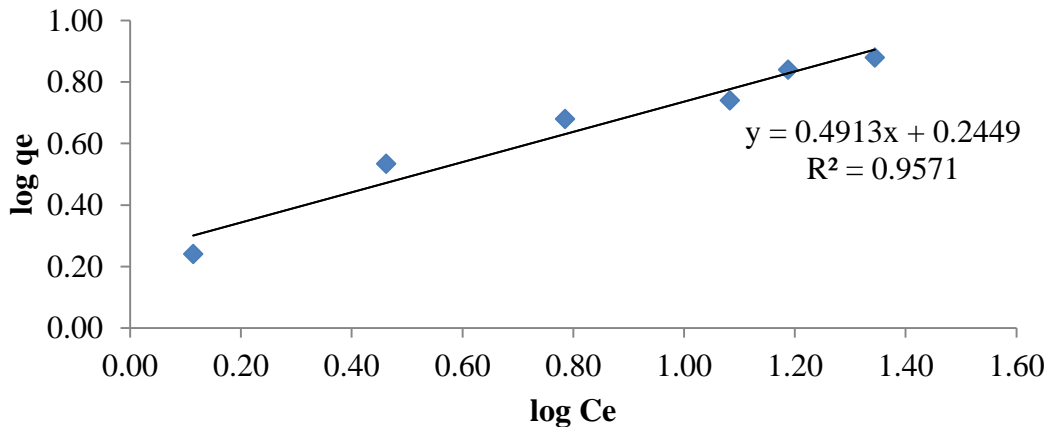


Figure 4.11 Linearized Freundlich plot for the adsorption of cadmium ions onto water hyacinth powder

The logarithm of q_e (adsorption capacity at equilibrium) increased linearly to the logarithm of C_e (concentration at equilibrium).

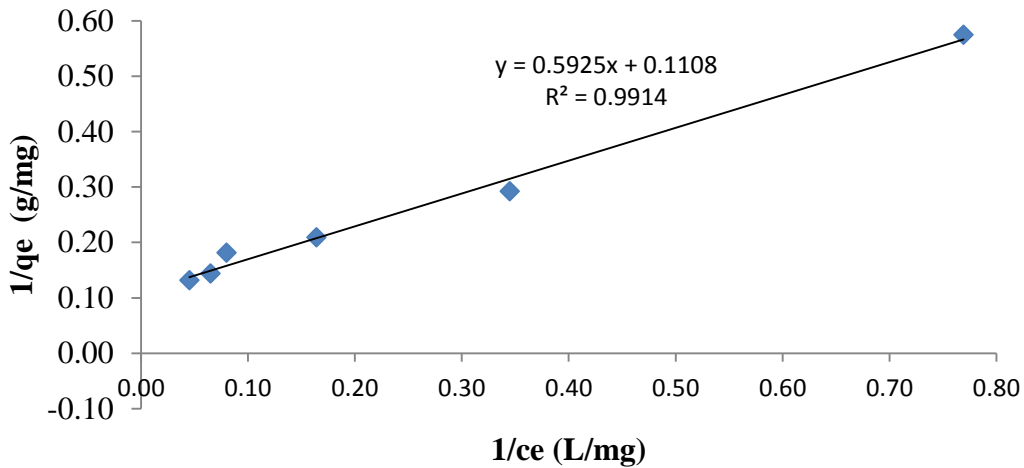


Figure 4.12: Linearized Langmuir plot for the adsorption of cadmium ions onto water hyacinth powder

The reciprocal of q_e (adsorption capacity at equilibrium) increased linearly with the reciprocal of c_e (concentration at equilibrium). The following parameters were applied for the Freundlich and Langmuir isotherms during adsorption (Table 4.6).

Table 4.6: Langmuir and Freundlich isotherms parameters for adsorption of cadmium ions from aqueous solution

Freundlich	Langmuir
$n = 2.0354$	$b \text{ (L/mg)} = 0.1870$
$K_f = 1.7575$	$q_m \text{ (mg/g)} = 9.0253$
$R^2 = 0.957$	$R^2 = 0.991$

Cadmium adsorption by water hyacinth powder correlated well with Langmuir than Freundlich isotherm model when fitted on the regression line as indicated by the R^2 values (Table 4.6).

4.4.4 Adsorption isotherms for the adsorption of chromium ions

The data obtained from the studies were then fitted into both Langmuir and Freundlich isotherms (Appendix VI). The isotherms are given in Figures 4.13 and 4.14

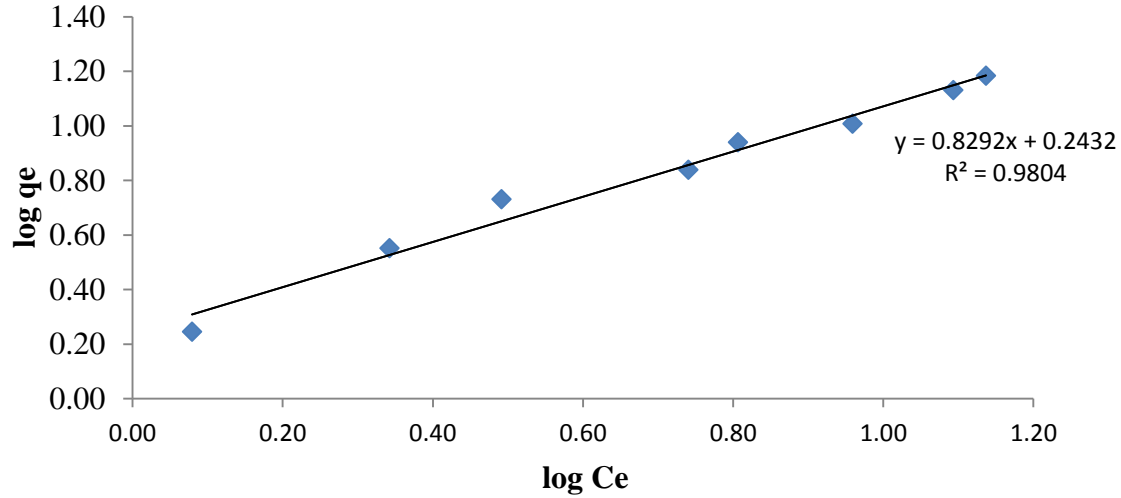


Figure 4.13: Linearized Freundlich plot for the adsorption of chromium ions onto powdered water hyacinth

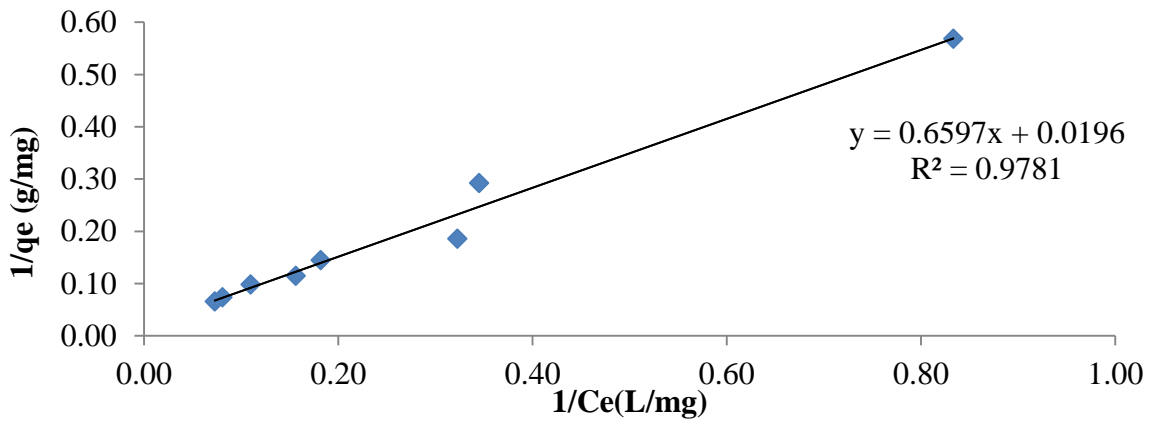


Figure 4.14: Linearized Langmuir plot for the adsorption of chromium ions onto water hyacinth powder

The reciprocal of q_e (adsorption capacity at equilibrium) increases linearly with the reciprocal of c_e (concentration at equilibrium). The Freundlich adsorption parameters (equilibrium constant

(K_f), n and regression constant (R^2) were determined graphically from Figure 4.13 and are presented in Table 4.7 while Figure 4.14 was used to model the Langmuir isotherm and to calculate the Langmuir parameters.

Table 4.7 Parameters for Freundlich and Langmuir isotherms for adsorption of chromium ions on water hyacinth powder

Freundlich isotherm	Langmuir isotherm
$n = 1.2060$	$b \text{ (L/mg)} = 0.0297$
$K_f = 1.7504$	$q_m = \text{(mg/g)} = 51.0204$
$R^2 = 0.980$	$R^2 = 0.978$

The values of R^2 were used to deduce the best model that would describe the adsorption on water hyacinth powder. Adsorption of chromium ions on water hyacinth powder correlated better with Freundlich Isotherm ($R^2 = 0.980$) than the Langmuir isotherm ($R^2 = 0.978$). Chromium adsorption on water hyacinth powder can therefore be described by the Freundlich Isotherm. The q_m (amount of metal ions adsorbed per unit mass of water hyacinth) value for chromium (51.0204) was higher than that of lead (16.0000), cadmium (9.0253), zinc (22.1239) and nickel (14.4928). The surface of water hyacinth is negatively charged. The oxidation state of chromium ions is +3 while that of lead, cadmium, zinc and nickel is +2. Therefore the affinity of adsorption sites to chromium ions is stronger compared to the affinity of adsorption sites to lead, cadmium, zinc and nickel ions.

4.5 Kinetic studies

The data obtained from this study were tested against the pseudo-first and pseudo second- order kinetic models.

4.5.1 Kinetic studies for the adsorption of zinc ions

The data obtained in Appendix VII was tested against the pseudo-first and pseudo second- order models and results are shown in Figures 4.15 and 4.16.

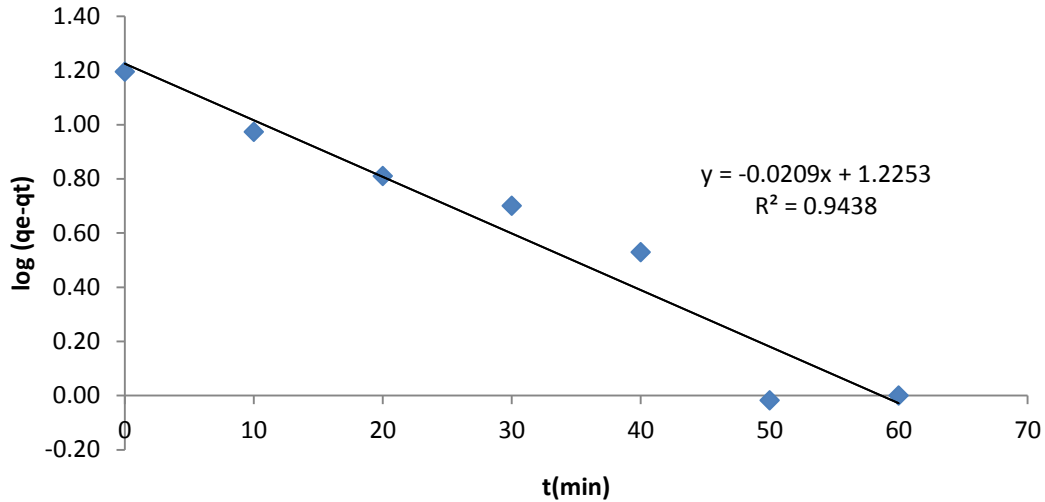


Figure 4.15: Pseudo-first-order for the adsorption of 95.5 ppm zinc ions onto water hyacinth powder

The logarithmic difference in adsorption capacity at equilibrium and at particular time ($\log q_e - q_t$) decreased linearly as the adsorption time increased.

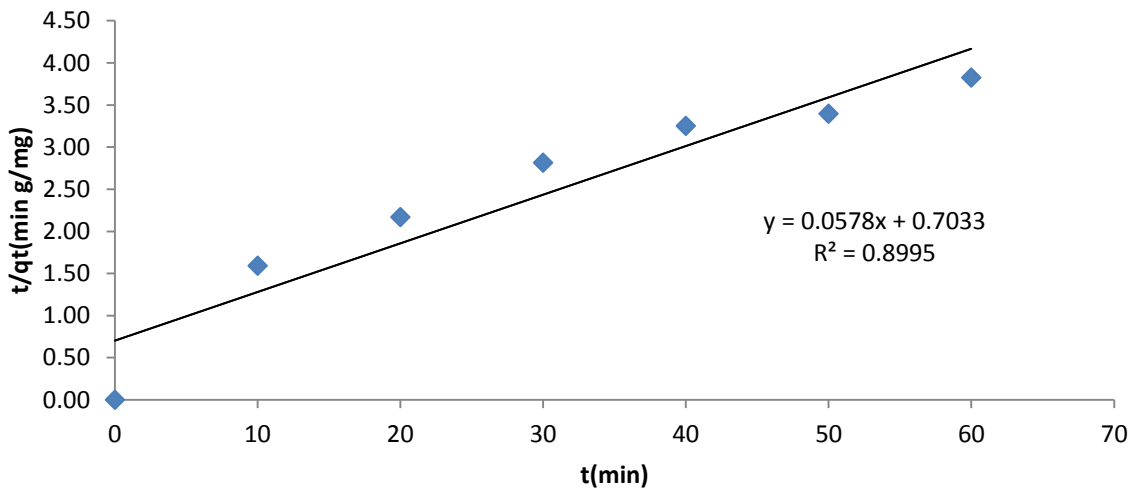


Figure 4.16: Pseudo-second-order for the adsorption of 95.5 ppm zinc ions onto water hyacinth powder

The quotient of t / q_t increased linearly with the adsorption time (Ngugi, 2015). The kinetic data for pseudo-first order and pseudo-second order parameters for the adsorption from (95.5 ppm

zinc ion solution, 75.3 ppm lead ion solution, 57.5 ppm cadmium ion solution, 63.7 ppm nickel solution and 87.6 ppm chromium) ionic solutions were calculated graphically (Appendix Vii).

The results are given in Table 4.8.

Table 4.8: The Pseudo first-order and Pseudo second-order kinetic parameters of adsorption of zinc, lead, cadmium, chromium and nickel ions on powdered water hyacinth

	Pseudo –first-order			Pseudo –second-order		
	Parameters			Parameters		
Metal ions	$K_1(\text{min}^{-1})$	$q_e(\text{mg/g})(\text{cal})$	R^2	$K_2(\text{g/mg/min/})$	$q_e(\text{mg/g})(\text{cal})$	R^2
Zinc ions	0.0481	16.80	0.944	0.0048	17.30	0.8995
Lead ions	0.0910	13.1735	0.929	0.0069	12.80	0.583
Nickel ions	0.0214	10.0485	0.969	0.0001	34.4828	0.543
Chromium ions	0.066	15.02	0.9897	0.0061	15.1515	0.771
Cadmium ions	0.0362	7.1895	0.989	0.0014	12.6262	0.949

It was observed that the R^2 value for the pseudo-first order in the adsorption of zinc ($R^2= 0.944$), lead ($R^2= 0.929$), nickel ($R^2= 0.969$), cadmium ($R^2= 0.989$) and chromium ions ($R^2= 0.9897$) were higher than that of pseudo-second order for the respective metal ions. This suggested that the adsorption kinetics of zinc, lead, nickel, cadmium and chromium ions on water hyacinth powder is better expressed by the pseudo first order model.

4.6 FTIR analysis for heavy metal adsorption on water hyacinth powder

The functional groups responsible for the adsorption of the metals (nickel, cadmium, lead, zinc and chromium) were investigated by FTIR (Model: IRA Affinity IS Class I) analysis. The spectra of the raw and metal loaded adsorbent are discussed below:

4.6.1 FTIR Spectra of water hyacinth powder

The spectra of raw water hyacinth powder and treated (metal loaded) water hyacinth powder for the metals nickel, cadmium, lead, zinc and chromium are provided in Figures 4.17-4.21.

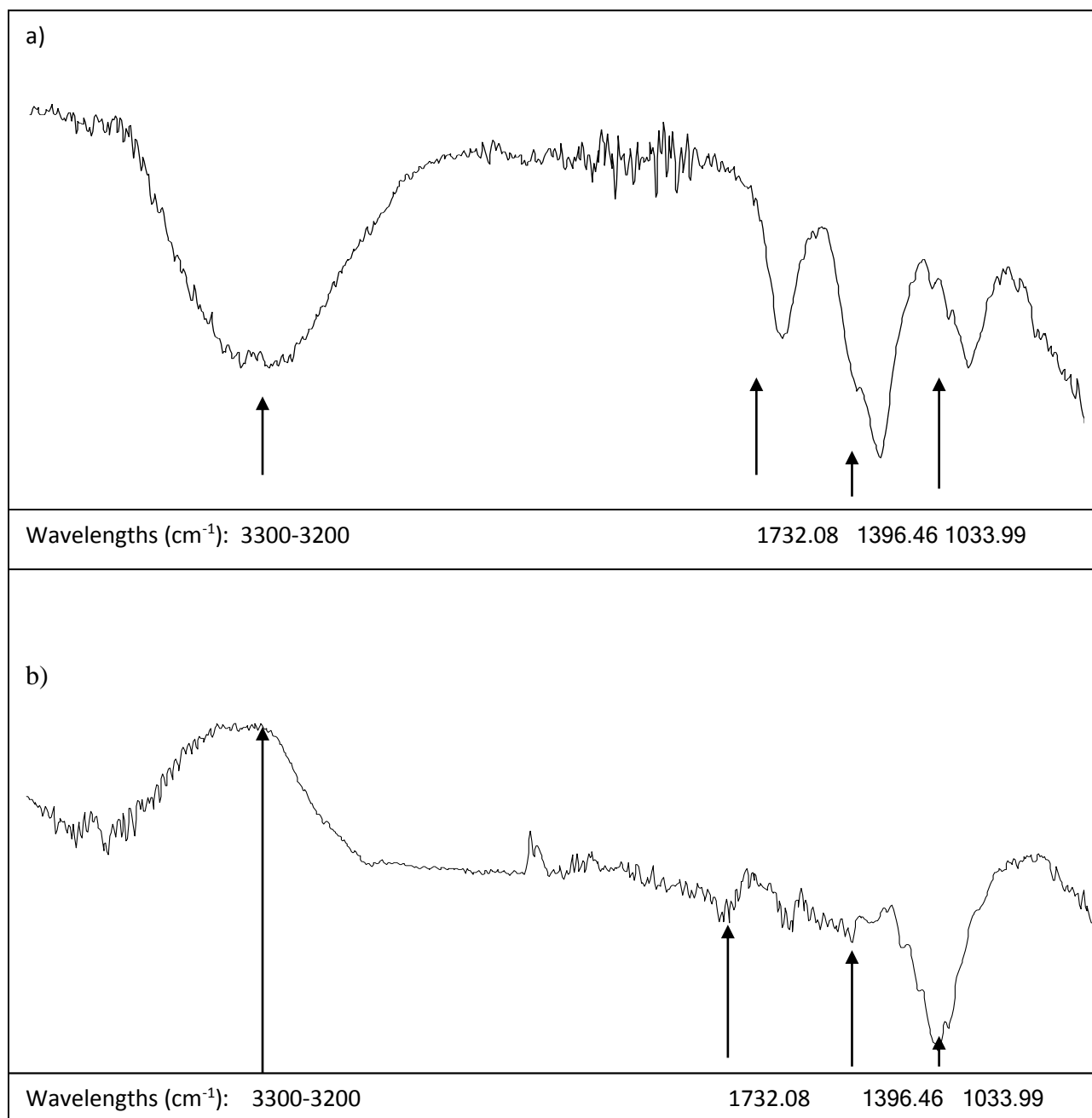


Figure 4.17: Spectra for water hyacinth powder before and after adsorption (a = spectrum for raw water hyacinth powder; b= spectrum of water hyacinth loaded with lead ions)

Figure 4.17a, it was observed that there was a strong broad absorption band in the region of 3200cm⁻¹ to 3300 cm⁻¹ for the raw water hyacinth powder. This was characteristic of O-H stretching attributed to alcohol, water, acid and phenols (Ibrahim *et al*, 2005). This peak is absent

in Figure 4.17b. The strong absorption band in the region of 1732 cm^{-1} was characteristic of C=O stretching bond structure which contained esters and carboxylic acids (Ibrahim, M, *et al.*, 2009). This peak is absent in Figure 4.17b. The disappearance of the peaks could be attributed to H atom present in the functional groups being substituted with lead ion (Mathias *et al.*, 2007). The strong band at absorption band 1396 cm^{-1} was characterized by bending of the C-H bonding in structures containing alkanes or both C-O stretch and O-H deformation in carboxylic acids (So *et al.*, 2003). The disappearance of this peak could be because lead ions are bound to hydroxyl, carboxyl and carbonyl functional groups (Nuhoglu and Malkoc, 2009). The strong band at 1033 cm^{-1} was characterized with C-O stretch in structures which contained carboxylic acids, ethers, ethers and alcohol (Hasan, *et al.* 2007). The band reduced in intensity upon adsorption of lead ions. The strong band at absorption band 1396 cm^{-1} is characterized by bending of the C-H bonding in structures containing alkanes or C-O stretch and O-H deform in structure containing carboxylic acids. Upon adsorption of lead ions the band reduced in intensity.

The water hyacinth powder spectra before and after adsorption of cadmium ions are presented in Figure 4.18.

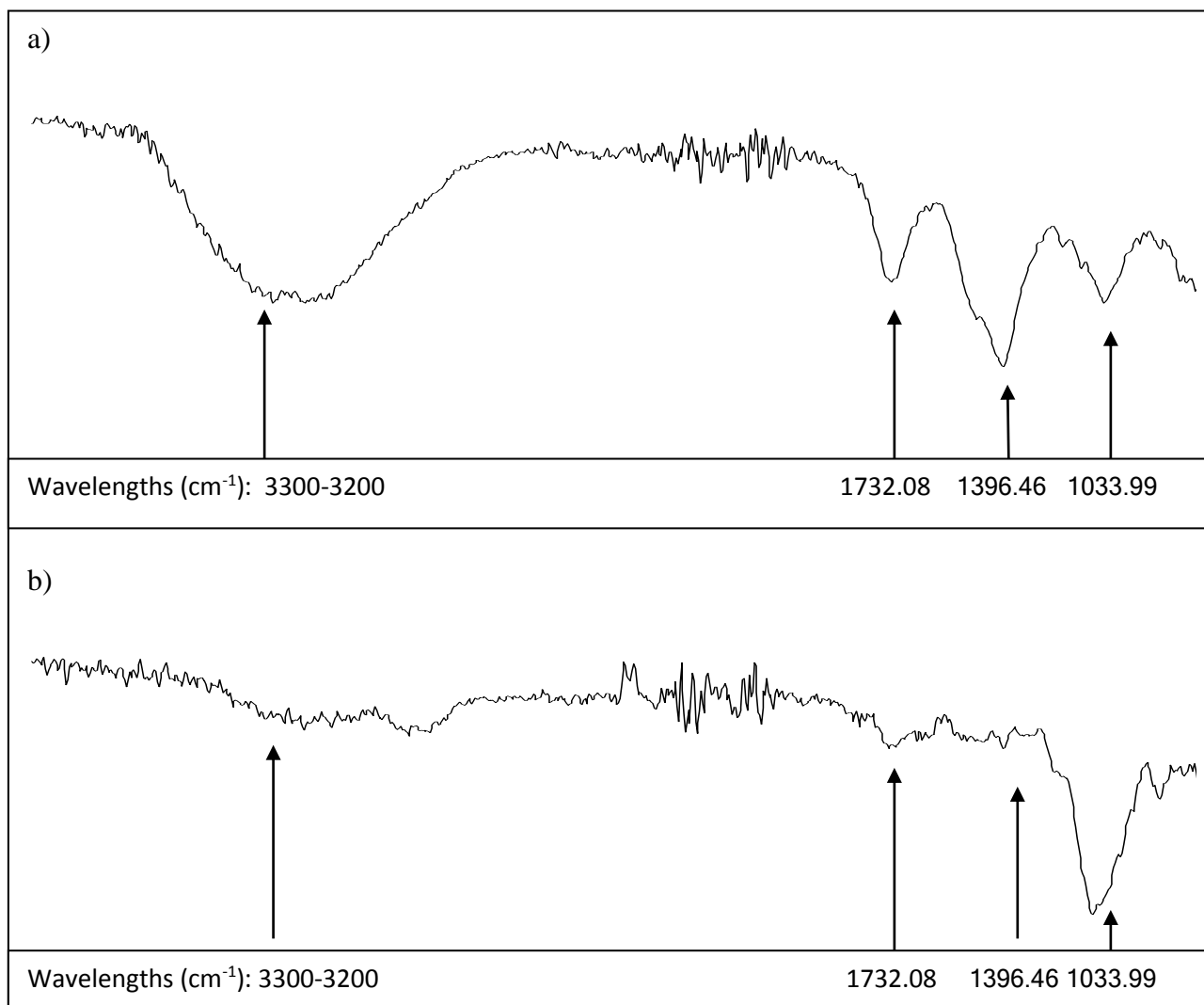


Figure 4.18: Spectra for water hyacinth powder before and after adsorption of cadmium ions (a = spectrum for raw water hyacinth powder; b= spectrum for cadmium loaded water hyacinth)

In Figure 4.18b, it was observed that the O-H (3200-3300 cm⁻¹) and C-H band disappeared. This could be due to participation of both alkyl and hydroxyl groups during cadmium adsorption (So *et al.*, 2003). The bands C=O and C-O were observed to reduce in intensity. This peak reduced in intensity when cadmium ions were adsorbed.

The strong peak at 1033 cm^{-1} is ascribed to the C-O stretch in structures which contained carboxylic acids, ethers, ethers and alcohol (Hasan, *et al.* 2007). The band reduced in intensity upon adsorption of cadmium ions.

The spectra of the water hyacinth powder before and after adsorption of nickel ions are presented in Figure 4.19

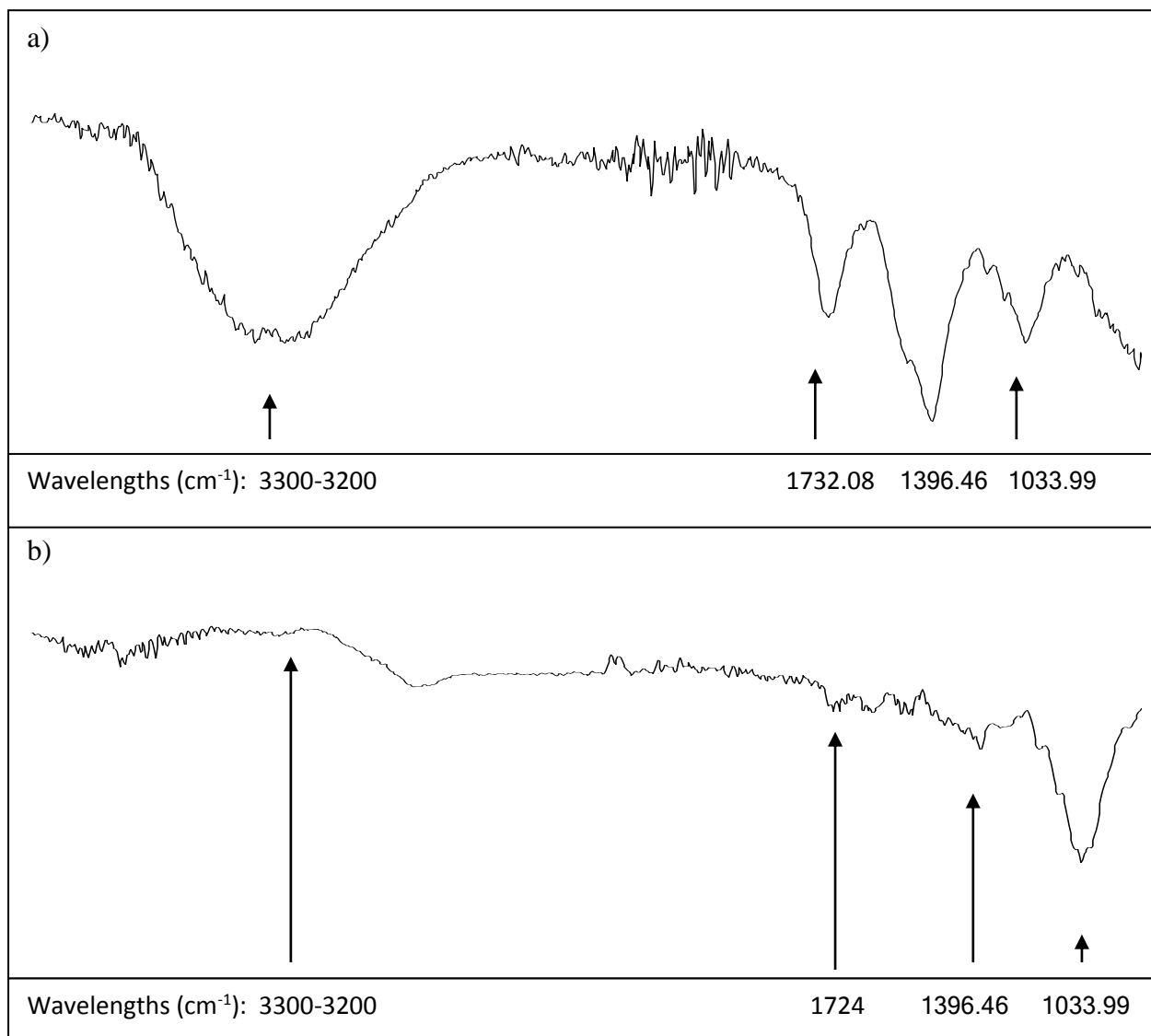


Figure 4.19: Spectra for water hyacinth powder before and after adsorption of nickel ions (a = spectrum for raw water hyacinth powder; b= spectrum for nickel loaded water hyacinth)

In Figure 4.19a, it was observed that there was a strong broad absorption band in the region of 3200cm^{-1} to 3300cm^{-1} for the raw water hyacinth powder. Loading of water hyacinth with nickel ions caused O-H band to disappear. The adsorption of nickel ions caused the C=O peak to shift from 1732cm^{-1} to 1724cm^{-1} . The adsorption peaks 1396cm^{-1} and 1033cm^{-1} to reduced in intensity after adsorption of nickel ions.

The spectra of the water hyacinth powder before and after adsorption of chromium ions are presented in Figure 4.20.

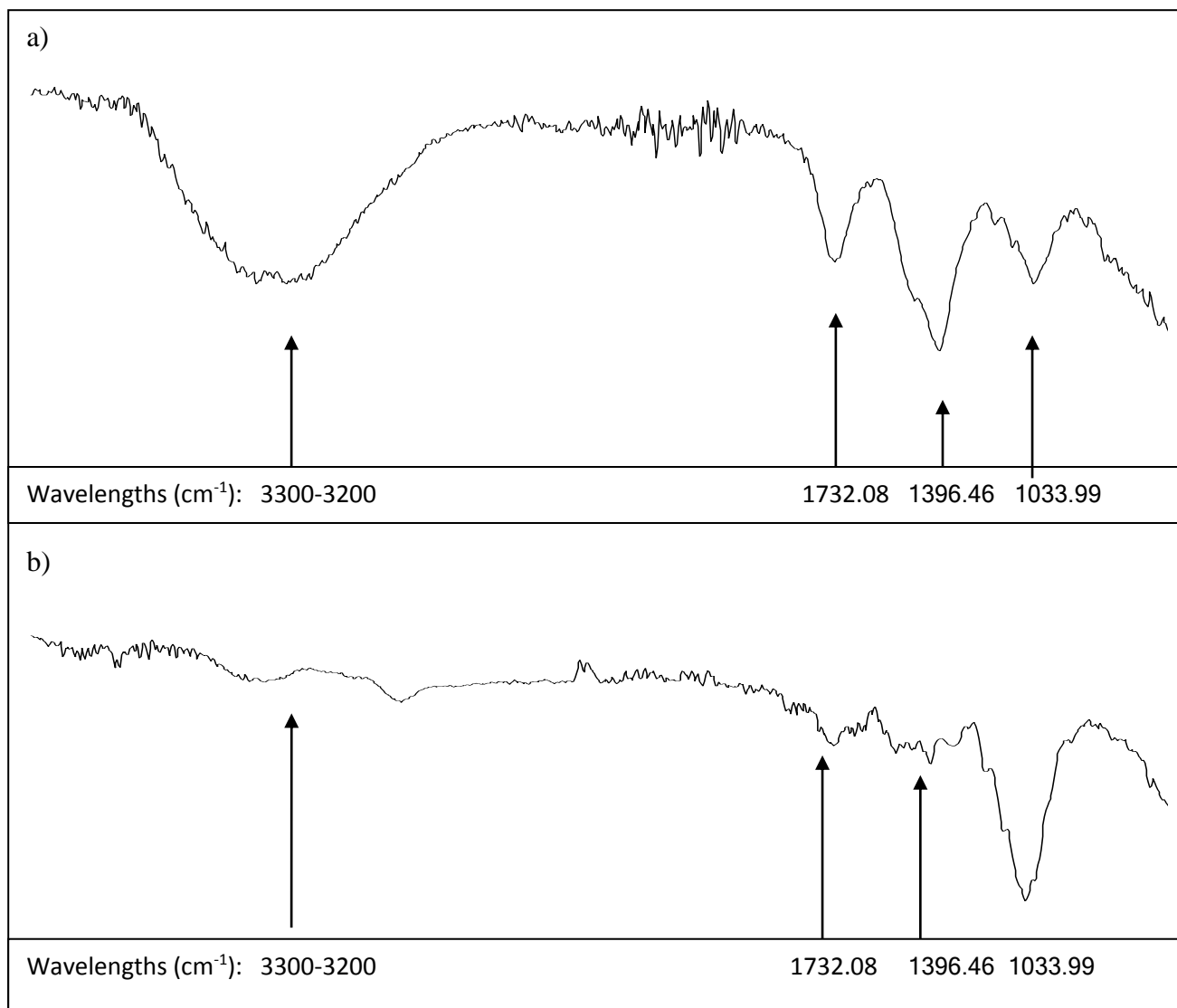


Figure 4.20: Spectra for water hyacinth powder before and after adsorption of chromium ions (a = spectrum for raw water hyacinth powder; b= spectrum for chromium loaded water hyacinth)

In Figure 4.20a, the adsorption of chromium ions caused the O-H band peak to disappear. Loading of water hyacinth with chromium ions caused the peak at 1396 cm^{-1} to disappear while the C=O peak reduced in intensity.

The spectra of the water hyacinth powder before and after adsorption of zinc ions are presented in Figure 4.21.

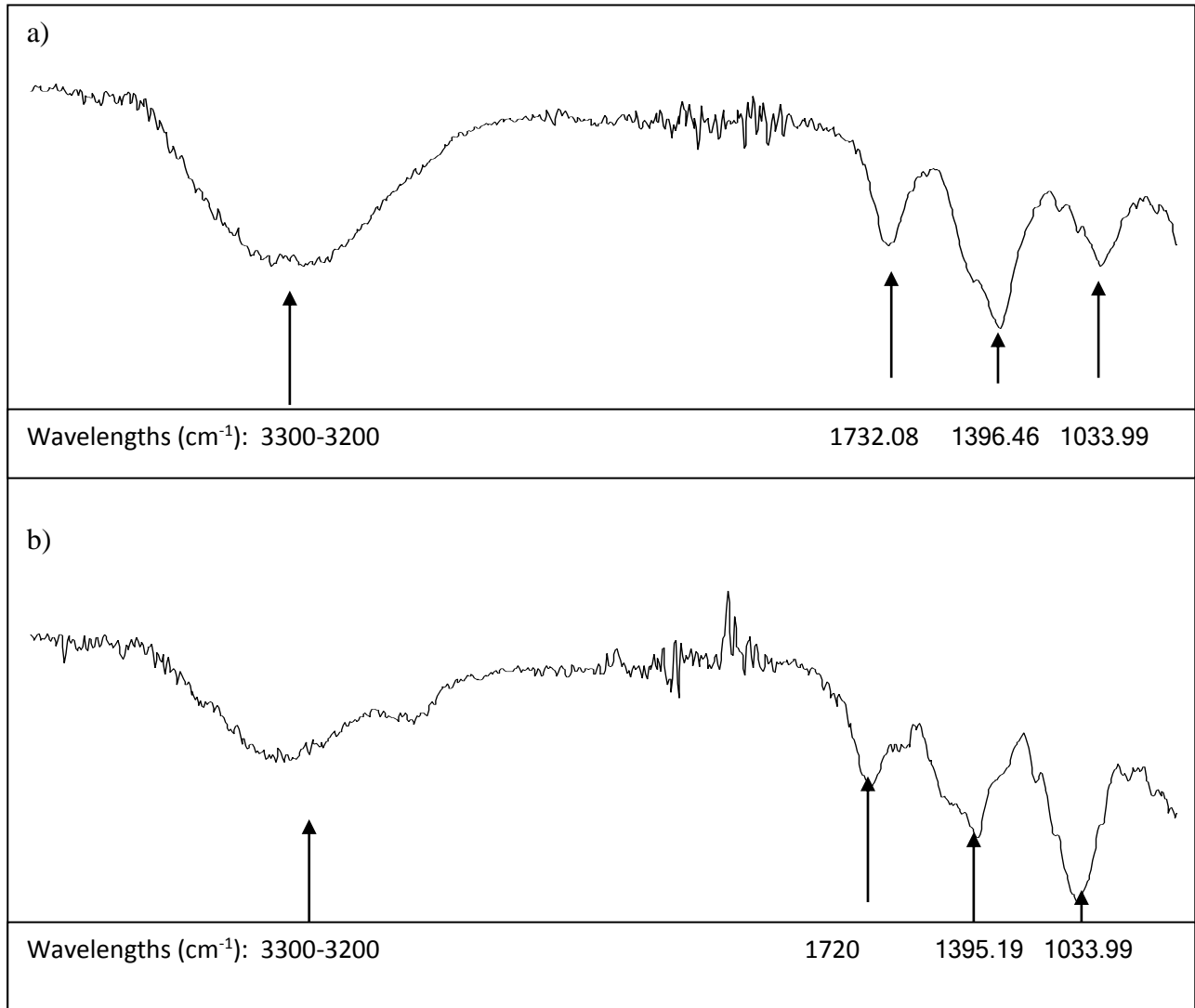


Figure 4.21: Spectra for water hyacinth powder before and after adsorption of zinc ions (a = spectrum for raw water hyacinth powder; b= spectrum for zinc loaded water hyacinth)

In Figure 4.21a, it was observed that adsorption of zinc ions caused the O-H band in the region of 3200 cm^{-1} to 3300 cm^{-1} to peak reduced in intensity. The reduction in intensity could be

attributed to zinc ions loaded on water hyacinth powder which reduced the peak height therefore the absorption band stretching to a lesser degree (Liu *et al.*, 2017). The uptake of Zinc ions caused C=O to shift from 1732 to 1720 cm^{-1} while the band at 1396 cm^{-1} shifted to 1395 cm^{-1} . The shifting of bands showed that heavy metals were adsorbed by the relevant functional groups (Njoki *et al.*, 2016). Uptake of zinc ions caused the C-O band to reduce in intensity upon adsorption of zinc ions. Comparison of the spectra for raw water hyacinth and metal loaded water hyacinth showed that the absorption bands either disappeared or reduced in intensity. Table 4.9. Summarizes the results.

Table 4.9 Effects of heavy metal adsorption on the water hyacinth spectra

Wavelength (cm^{-1})	Raw water hyacinth	Pb loaded	Ni loaded	Zn loaded	Cd loaded	Cr loaded
3200-3300	O-H carboxylic acid, alcohol, water, phenols	Disappeared	Disappeared	Reduced intensity	Disappeared	Disappeared
1732	C=O acid, esters	Disappeared	Shifted (1724)	Shifted (1720)	Reduced intensity	Reduced intensity
1396	C-H bending (alkanes) or C-O stretch and O-H deformation (acids)	Disappeared	Reduced intensity	Shifted (1395)	Disappeared	Disappeared
1033	C-O Alcohols, Acids, Esters, Ether	Reduced intensity	Reduced intensity	Reduced intensity	Reduced intensity	Reduced intensity

CHAPTER FIVE

CONCLUSIONS AND RECOMMENDATIONS

5.1 Conclusions

The levels of heavy metals in the wastewater were in the range of: 1.2-75.3 ppm for lead, 0.38-87.6 ppm for chromium, 0.11-63.5 ppm for nickel, 0.58-95.5 ppm for zinc and 0.88-52.7 ppm for cadmium and depended on the nature of industrial activities around the sampling sites. The levels of zinc, lead and cadmium in the wastewater were above the limit recommended by NEMA. Adsorption efficiency of heavy metals on water hyacinth (*E.crassipes*) powder was influenced by factors such as; adsorption time, dosage, pH and particle size of the adsorbent. The adsorption efficiency increased with increase in contact time after which a steady state was reached. The optimum adsorption time varied with the metal, for example optimum time for adsorption of Pb was 30 minutes, 40 minutes for Cr, 80 minutes for Ni and 60 minutes for both Cd and Zn. The study showed that adsorption increased with adsorbent dosage until an optimum adsorption dosage was reached which varied with the metal. The adsorbent dosage for adsorption of Pb and Zn was 2.5 g, Cd was 3.0 g, Cr was 4.0 g and while Ni was 4.5 g. The adsorption of all the metal ions increased with decrease in particle size in the order $>425 < 2800$, $>300 < 425$ and $<300 \mu\text{m}$ for each of the concentrations. The adsorption was within the pH range of 2-6, however the pH range for adsorption varied with the metal. The pH range for adsorption of Pb, Cr and Cd was 2-5 and 2-6 for Ni and Zn after which a plateau was reached and then the adsorption efficiency dropped. The adsorption data for zinc, cadmium, nickel and lead from the aqueous solution fitted well in Langmuir model while the adsorption data for chromium fitted well in the Freundlich model. Kinetics study showed that adsorption process for chromium, zinc, cadmium, nickel and lead was described well by the pseudo first order reaction kinetic model. The FTIR study showed that the loading of the water hyacinth powder with metal ions led to the specific bands shifting to either lower or higher wave numbers, reduced intensity or the disappearance of some peaks which could be attributed to the adsorption process at these particular functional groups: C-H, O-H, C=O or C-O. The results of this study showed that water hyacinth is a suitable low cost adsorbent for heavy metals since they contain functional groups where the

metals could attach and that at low concentrations, the adsorption efficiency of heavy metals by the water hyacinth powder was at 100%.

5.2 Recommendations

1. The wastewater should be analyzed at various points to monitor the changes in the heavy metal concentration as they are released into the environment from plastic manufacturing industries, steel manufacturing industries, paint manufacturing industries and battery manufacturing industries (or nearby water bodies)
2. Analysis of wastewater from other industries should be conducted.
3. Activated carbon prepared from water hyacinth should be tested to determine its effectiveness in heavy metal removal from aqueous media.
4. Recovery studies should be conducted on metal-laden water hyacinth powder to determine their stability for reuse in adsorption studies.

REFERENCES

- Abbas, A., Abussaud, B.A, Ihlsanullah, Al-Baghli, N.A.H. and Redhwi, H.H. (2017) Adsorption of Toluene and Paraxylene from aqueous solution using pure and iron oxide impregnated carbon nanotubes: Kinetics and isotherm studies. *Biorganic chemistry and applications* **17**:2-12
- Abdallah, M., AL Jahdaly, B.A., Salem, M.M., Fawzy, A. and Abdel, A.A. (2017) Pitting corrosion of Nickel alloys and stainless steel in chloride solutions and its inhibition using some inorganic compounds. *Journal of material and environmental sciences* **8**:2599-2607
- Abdel, S. O., Reiad, N. A. and ElShafei, M.M. (2011,) Removal of heavy metals from waste water using agricultural and industrial waste. *Journal of Advanced Research* **2**: 297-303
- Abdullar, A. (2015) Sources of metal pollution in the urban atmosphere. *Journal of environmental health science and engineering* **13**: 79-82
- Achparaki, M., Thessalonikeos, E., Tsoukali, H., Mastrogianni, O., Chatzinikolaou, F., Vasilliades, N. and Raikos N. (2012) Heavy metals toxicity. *Aristotle university medical journal* **39**:29-34
- Addagalla, V.A., Darwish, N.A. and Hilal, N. (2009). Studies of various parameters in the biosorption of heavy metals on activated sludge. *World applied sciences journal* **5**:32-40
- Agarwal, A. and Vaishiali (2017) Chiosan based adsorbent;A remedy to handle industrial waste water. *The international journal of engineering and sciences* **6**:34-49
- Ahenda, O.S., Kithure, G.N.J., Njenga, H., Wangeci, N.A. and Nyang'au, O.J. (2019) Characterization and adsorption of Heavy Metals in industrial effluents from paints and coating industries in Nairobi, Kenya. *International journal of Engineering Applied Science and Technology* **4**:41-46
- Akbari, M Hallajisani, A., Keshtkar, A.R.,Shahbeig, H., and Ghorbanian, S.A. (2015). Equilibrium and Kinetic study and modeling of Cu(II)and Co(II) synergistic biosorption from Cu(II)-Co(II) single and binary mixtures of brown algae *C.indica*. *Journal of environmental chemical engineering* **3**:140-149
- Anah, L. and Astrini, N.(2018) Isotherm adsorption studies of Ni(II) ion removal from aqueous

- solutions by modified carboxymethyl cellulose hydrogel. *Earth and Environmental science* **160**: 1-8
- Angelovicova, L. and Fazekasova, D. (2014) Contamination of the soils and water environment by heavy metals in the former mining areas of Rudnany (Slovakia) *soil and water resources* **9**:18-24
- Amzeze, D. A., Onyari, J. M., Shiundu, P. M. and Gichuki, J. W. (2014) Equilibrium and kinetics studies for biosorption of aqueous Cd(II) ions onto *Eichhornia crasippes* biomass. *Journal of applied chemistry* **7**:29-37
- Alben, J. (1996) Fourier transform infrared spectroscopy of enzyme systems. *In: Mantsch H. H. And Chapman D (eds) infrared spectroscopy of Biomolecules*, pp.19-38. New York: Wiley
- Aleixo, P.C., Santos, D., Tomazelli, A.C., Rufini, I.A., Berndt, H. and Krug, F.J. (2004). Cadmium and lead determination in food by injection flame furnace atomic absorption spectrometry after ultra sound assisted sample preparation. *Analytical chemistry acta* **512**:329-337
- Alukwe, I.A. (2016) Urban drainage and sanitation, A case study of Nairobi-Kenya. *International journal of recent engineering research and development (IJRERD)* **02**:61-66
- Arif, T. J., Mudsser, A., Kehkashan, S., Arif, A., Inho, C. and Qazi, M. R. H (2015) Heavy metals and human health. *Journal of molecular sciences* **16**:29592-29630
- Arshadi, M., Amiri, M. J and Mousavi, S. (2014) Kinetics, equilibrium and thermodynamic investigations of Ni(II), Cu (II), Cd(II) and Co(II) adsorption on barley straw ash. *Water resources and industry* **6**:1-17
- Astuti, W., Martiani, W. and Khair, I.N. (2017) Competitive adsorption of Pb²⁺ and Zn²⁺ ions from aqueous solutions by modified coal fly ash. *American institute of physics* **18**: 1-6
- Astrini, N., Anah, L. and Haryadi, H.R. (2015) Adsorption of Heavy metals ions from aqueous solution using cellulose based hydrogel composite. *Macromolecule symposia* **3** **53**:191-197
- Azimi, A., Azari, A., Rezakazemi, M. and Ansarpour, M. (2017) Removal of heavy metals from industrial waste water: A review. *ChemBioEng* **11**:1-2
- Babae, Z., Nikoopour, H. and Safafar, H. (2007) A comparison of commercial Nickel catalyst effects on hydrogenation of soybean oil. *World of applied sciences journal* **2**:621-626

- Bai, Y. and Bartkiewicz, B. (2009) Removal of Cadmium from wastewater using ion exchange resin amberjet 1200H columns. *polish journal of environmental studies* **18**:1191-1195
- Balkhair, S.K. and Ashraf, A.M. (2015) Field accumulation risks of heavy metals in soils and vegetables crop irrigated with sewage water in western region of Saudi Arabia. *Saudi journal of biological sciences* **23**:32-44
- Barakat, M.A. (2011). New trends in removing heavy metals from industrial wastewater. *Arabian Journal of Chemistry* **4**: 361-377.
- Baran, A. and Tarnawski, M. (2015) Assessment of heavy metals mobility and toxicity in Contaminated sediments by sequential extraction and a battery of bioassays. *PubMed Central* **24**:1279-1293
- Benhoft, A.R (2013) "Cadmium toxicity and treatment" *The scientific world journal* vol. **2013**: 1-7
- Cameron, K.S., Buchner, V. and Tchounwou, P.B. (2011) Exploring the molecular mechanisms of nickel induced Genotoxicity and carcinogenicity. A literature review. *PubMed Central* **26**:81-92
- CBS (2001). "Counting people for development" *population and housing census* **01**: 23-31
- Chen, S.H., Zhang, J., Zhang, C.L., Yue, Q.Y., Li, C. (2010) Equilibrium and kinetic studies of methyl orange and methyl violet adsorption on activated carbon derived from *Phragmites australis*. *Desalination* **252**:149-156
- Chiba, W., Passerini, M.D. and Tundisi J.G. (2011) Metal contamination in Benthic macrovertebrates in sub-basin in southeast of Brazil. *Brazil journal of biology* **71**:391-399
- Chibuikwe, G.U. and Obiora, S.C. (2014) Heavy metals polluted soils: Effects on plants and Bioremediation methods. *Applied and environmental science* **2014**:1-12
- Chigondo, F., Nyambuya, T. and Chigondo, M.(2013) Removal of Zinc(II) ions from aqueous solution using msasa tree(*Brachystegia spiciformis*) leaf powder: Equilibrium studies. *Journal of asian scientific research* **3**:140-150
- Clark, A.P., Pinedo, C.A., Fatus, M. and Capuzzi, S. (2012) Slow sand water filter: Design, implementation, accessibility and sustainability in developing countries. *Medical science* **18**:105-117

- Daping, S., Dafang, Z., Dong, J., Jingying, F. and Qiao, W. (2015) Integrated health risk assessment of heavy metals in Suxian County, South China. *International journal of environmental research and public health* **12**:7100-7117
- Deshpande, J.D., Joshi, M.M. and Giri A.P. (2012) Zinc: The trace element of major importance in the human nutrition and health. *International journal of medicine science and public health* **2**:1-6
- Desta, M.B. (2013) Batch sorption experiments: Langmuir and Freundlich isotherm studies for the adsorption of textile metal ions onto Teff straw (Eragrostis tef) Agricultural waste. *Journal of thermodynamics* **58**:30-38
- Dipak, P. (2017) Research on heavy metal pollution of River Ganga. *Annals of Agrarian science* **15**: 278-286.
- Donati, G.L., Nascentes, C.C., Nogueira, A.R.A, Arruda, M.A.Z. and Nobrega, J.A.(2006). Acid extraction and cloud point preconcentration as sample preparation strategies for the determination of biological materials by thermospray flame furnace atomic absorption spectrometry. *Microchemistry journal* **82**:189-195
- Echem, O.G. (2014) Determination of the levels of heavy metal (Cu, Fe, Ni, Pb and Cd) up take of pumpkin (*Telfairia occidentalis*) leaves cultivated on contaminated soils. *Journal of applied science* **18**:71-77
- Fashola, M.O., Ngole-jeme, M.V. and Babalola, O.O (2016) Heavy metal pollution from Gold mines: Environmental effects and bacteria strategies for resistance. *PublicMed journal* **13**: 1047-1048
- Fil, B. A., Yilmaz, A.E., Boncukcuoglu, R. and Bayar, S. (2012) Removal of divalent heavy metal ions from aqueous solutions by Dowex HCR-S sythetic resin. *Bulgarian chemical communications* **44**: pp 201-207
- Frohne, T., Rinklebe, J., Langer, U., Laing, D.G., Mothes, S. and Wennrich, R. (2012) Biogeochemical factors affecting mercury methylation rate in two contaminated floodplains soils. *Biogeo sciences* **9**:493-507
- Gao, Z., Bandosz, T.J., Zhao, Z. and Qui, J (2009) Investigation of factors affecting adsorption of transition metals on oxidized carbon nanotubes. *ScienceDirect* **267**:357-365
- Garba, Z.N., UgbagaN.I. and Abdullahi, A.K. (2016) Evaluation of optimum adsorption

- conditions for Ni(II) and Cd(II) removal from aqueous solution by modified plantain peel (MPP). *Seni-suef university journal of basic and applied sciences* **5**:170-179
- Garbuio, J.F., Horward, L.J. and Marcedo, L.(2012). Impact of Human activities on Soil contamination. *Applied and environmental soil science* **101**:72-88
- García , R. and Baez, A.P (2012). Atomic Absorption Spectroscopy. *Intechopen journal* **81** 7:1-13
- Gaspar, A. and Berndt, H. (2000). Beam injection flame furnace atomic absorption spectrometry: A new flame method. *Analytical chemistry* **72**:240-246
- Gernand, A.D., Schulze, K.J., Stewart, C.P., West, K.P. and Christian, P. (2016) *PubMed Journal* **12**:274-289.
- Grillo, F.F., Coleti, J.L., Espinosa, D.R.C., Oliveira, J.R. and Tenorio, J.A.S. (2014). Zn and Fe recovery from electric arc furnace dusts. *Material transactions* **55**:351-356
- Gisi, S.D., Lofrano, G., Grassi, M. and Notarnicola, M. (2016) Characteristics and adsorption capacities of low cost sorbents for waste-water treatment. *Sustainable material and technologies* **9**:10-40
- Goormaghtigh, E., Ruyschaert, J.M. and Raussens, V. (2006) Evaluations of the information content for the protein secondary structure determination. *Biophysical journal* **90**:2946-2957
- Govind, P. and Madhuri, S. (2014) Heavy metals causing toxicity in animals and fishes. *Research journal of animal, veterinary and fisheries science* **2**:17-23
- Gower, S.D., Corniola, R.S., Morgan, T.J. and Levenson C.W. (2013) Zinc deficiency regulates hippocampal gene expression and impairs neural differentiation. *PMC Journal* **16**:174-182.
- Griffiths, P.R and Holmes, C. (2002) *Handbook of vibrational spectroscopy, Vol.* Chichester John Wiley and Sons.
- Griffiths, P. and de Hasseths, J.A (2007). Fourier transform infrared spectrometry (2nd ed.) Wiley -Blackwell. ISBN 0-471-19404-2
- Guan, Y., Shao, C. and Ju, M. (2014) Heavy metal contamination and a partition for industrial and mining gathering areas. *International journal of environmental research and public health* **11**:7286-7303
- Gunatilake, S. K. (2015). Methods of removing heavy metals from industrial waste water.

- Gundogdu, A., Duran, C., Senturk, H.B., Soylak, M., Ozdes, D., Serencam, H. and Imamoglu, M. (2012) Adsorption of phenol from aqueous solution on a low-cost activated carbon produced from tea industry waste: Equilibrium, Kinetic and thermodynamic study. *Journal of chemical engineering* **57**: pp 2733-2743
- Guo, E.L. and Katta, R. (2017) Diet and hair loss: Effects of nutrients deficiency and supplement use. *Dermatology practical concept journal* **7**:1-10.
- Gupta, P., Roy, S. and Mahindrakar, A. (2012) Removal of heavy metals from waste water using water hyacinth. *Resources and environment* **2**:202-215
- Hameed, B.H., Salman, J.M., and Ahmad, A.L. (2009). Adsorption isotherm and kinetic modeling of 2, 4-D pesticide on activated carbon derived from date stones. *Journal of hazardous materials* **163**:121-126
- Hasan, S.H., Talat, M. and Rai, S. (2007) Sorption of Cadmium and zinc from aqueous solution by water hyacinth (*Eichhornia crassipes*). *Bioresources technology* **98**:918-928
- Hegazi, H. A. (2013). Removal of the characteristics of heavy metal from waste-water by low-cost adsorbents. *HBRC Journal* **9**:276-282.
- Henry, J.B., Ian, B., Ramakrishna, B.S. and Graeme, P.Y. (2014) Oral rehydration therapy in second decade of twenty first century. *PubMed journal* **16**:376-377
- Ibrahim, M, Nada, A. and Kamal, D.E. (2005) DFT and FTIR spectroscopic study of carboxyl group. *Indian journal of pure and applied physics* **43**:911-917
- Ibrahim, H.S., Ammar, N.S., Soylak, M. and Ibrahim, M. (2009) Removal of Cd(II) and Pb(II) from aqueous solutions using dried water hyacinth as a biosorbent. *Elsevier* **96**:413-420
- Ibrahim, M., Kuhn, O. and Scheytt, T. (2009) Molecular spectroscopic study of water hyacinth dry matter. *The open chemical physics journal* **2**:1-6
- Igberase, E., Osifo, P. and Ofomaja, A. (2017) Adsorption of Pb, Zn, Cu, Ni, and Cd by modified ligand in a single component aqueous solution: Equilibrium, Kinetic, thermodynamic and desorption studies. *International journal of analytical chemistry* **2017**:27-42
- Jaishankar M., Tseten, T., Anbalagan, N., Mathew, B.B. and Beergowda, N.K. (2014) Toxicity, mechanism and health effects of some heavy metals. *Interdisciplinary toxicology* **7**: 60-72

- Jeppu, G.P. and Clement, T.P. (2012). A modified Langmuir-Freundlich isotherm model for simulating pH-dependent adsorption effects. *Journal of contaminat hydrology* **129**:46-53
- Jiao, X., Teng, Y., Zhan, Y., Wu, J. and Lin, X. (2015) Soil heavy metal pollution and risk assessment in Shenyang industrial district, northeast China. *PLOS One* **10**:1-10
- Johri, N., Juacquillet, G. and Unwin, R. (2010) Heavy metal poisoning: The effects of Cadmium on the kidney. *PubMed* **23**:783-792
- Kamar, F.H., Craciun, M.E. and Nechifor A.C. (2014) Heavy metals: Sources, health effects, environmental effects, removal methods and natural adsorbent material as low cost adsorbent. *International journal of scientific engineering and technology research* **3**: 2974-2979
- Kandziora-Ciupa, M., Nadgorska-Socha, A., Barczyk, G. and Ciepal, R. (2017) Bioaccumulation of heavy metals and ecophysiological responses to heavy metals stress in selected population of *vaccinium myrtillus* L and *vaccinium vitis-idaea* L. *Ecotoxicology* **26**:966-980
- Kant, R. (2012) Textile dyeing industry an environmental hazard. *Natural science* **4**:22-26.
- Kanwal, F., Rehman, R., Mahmud, T., Anwar, J. and Ilyas, R. (2012) Performance of Egg shell and fish scale as adsorbent material for chromium (vi) removal from effluents of Tannery industries in Eastern Uganda. *Journal of Chilean chemical society* **57**:1058-1063
- Kayastha, S. P. (2014). Heavy metal pollution of agricultural soils and vegetables of Bhaktapur district, Nepal. *Scientific world* **12**:48-55
- Kenya National Bureau of Statistics (2017). Population distribution by sex, number of households, area and density County and district. *Keeping you informed* **17**:1-5
- Kessler, R. (2014) Lead based decorative paints: Where are they still sold and why? *Environmental health perspective* **122**: 96-103
- Khurana, R. and Fink, A.L. (2000) Do parallel beta helix proteins have unique Fourier transform infrared spectrum. *Biophysical journal* **78**:994-1000
- Kilpimaa, S., Runtti, H., Kangas, T., Lassi, U., and Kuokkanen, T. (2014) Removal of phosphate and nitrate modified carbon residue from biomass gasification. *ScienceDirect* **10**:1923-1933
- Klein, C., and Costa, M. (2007). Nickel. In G.F. Nordberg, B.A. Fowler, M. Nordberg, & L. Friberg (EDS.), *Handbook on toxicology of metals* (3rd ed., pp. 743-758).

Academic Press Inc.

- Kragovic, M., Dakovic, A., Markovic, M., Krstic, J., Gatta, D. and Rotiroti, N. (2013) Characterization of lead sorption by the natural and Fe (iii)-modified zeolite. *ScienceDirect* **283**:764-774
- Kumar, S.P. (2013) Adsorption of Zn(II) ions from aqueous environment by surface modified *strychnos potatorum* seeds, a low cost adsorbent **15**:35-41
- Kumar, O., Pradhan, S., Sehgal, P., Singh, Y. and Vijayaraghavan, R (2010). Denatured Ricin can be detected as native Ricin by immunological methods, but nontoxic. *journal of forensic science* **55**:801-807
- Lane, E.A., Canty, M.J. and More, S.J. (2015) Cadmium exposure and consequences for health and productivity of farmed ruminants. *Research in veterinary science* **101**:132-139
- Lissy, M. and Madhu, G. (2011) Removal of heavy metals from waste-water using water Hyacinth. *International journal on transportation and urban development* **1**:48-52
- Liu, S.Y., Gao, J., Qu, B. and Yang, Y.J. (2009) Kinetic models for the adsorption of lead ions by steel slag. *Waste management research* **28**:748-753
- Liu, T., Hou, J.H., Wang, J.B., Wang, W., Wang, X.Y. and Wu, J.L.(2017) Bio-sorption of Heavy metals from Aqueous solution by the novel *Biosorbent pectobacteriu* Sp.ND2. *Enviromental progress and sustainable energy* **100**: 56-64
- Mahurpawar, M. (2015) Effects of heavy metals on Human health. *International journal of research Granthaalayah* **2**:2394-2306
- Mamybaev, A. A, Dzharkenov, T. A., Imangazina, Z. A. and Satybaldieva, U. A. (2015) Mutagenic and carcinogenic actions of chromium and its compounds. *Enviromental health and preventive medicine* **20**:159-167
- Mathias, E., Evangelou, M.W.H. and Scaeffler, A. (2007) A cyanide phytoremediation by water hyacinth (*Eichhornia crassipes*). *Chemosphere* **66**:816-823.
- Mbui, D., Orata, D.O., Jackson, G. and Kariuki, D. (2014) Investigation of Kenyan bentonite in adsorption of some heavy metals in aqueous solution systems using cyclic voltammetric techniques. *Academic Journals* **9**:102-108

- Mebrahtu, G. and Zerabruk, S. (2011) Concentration and health implication of heavy metals in drinking water from urban areas of tigray region, Northern Ethiopia. *Momona Ethiopian journal of science* **3**:1-8
- Medellin-Castillo, N.A., Padilla-Ortega, E., Regeles-Martinez, M.C, Ocampo-Perez, R., Leyva-Ramos, R. and Carranza-Alvarez, C. (2017) Single and competitive adsorption of Cd(II) and Pb(II) ions from aqueous solution onto industrial chili seeds (*Capsicum annum*) waste. *Sustainable environment research* **27**:61-69
- Michaela, S., Ahrmad, I., Meryers, J., Russell, B., Dorrah, K. and Defreese, C. (2016) The effects of the heavy metal nickel on LINE 1 endonuclease. *The FASEB journal* **30**:607-611
- Monachese, M., Burton, J.P. and Reid G. (2012) Bioremediation and tolerance of Humans to heavy metals through microbial processes: potential role of probiotics. *Applied and environmental microbiology* **78**:6397-6404
- Mousavi, H.Z., Hossynifar, A., Jahed, V., Dehghani, S.A.M. (2009) Removal of lead from aqueous solution using waste tire rubber ash as an adsorbent. *Journal of chemical engineering* **27**: pp 79-87
- Mulamu, L.O. (2014) Heavy metals contamination of land and water around Nairobi City Dandora Dumpsite, Kenya. *Global journal of environmental science and technology* **2**:360-367.
- Murithi, G., Onindo, C.O., Wambu, E.W. and Muthakia, G.K. (2014) Removal of Cadmium (II) ions from water by adsorption using water hyacinth (*Eichornia crassipes*) biomass. *BioResources* **9(2)**:3613-3631
- Nakamura, S., Kondo, Y., Nakajima, K., Ohno, H. and Pauliuk, S.(2017) Quantifying recycling and losses of Cr and Ni in steel throughout multiple life cycles using MaTrace-Alloy. *Environmental science and technology* **51**:9469-9476
- National Environment Management Authority (2006). Guidelines on drinking water quality and effluents monitoring. *prime journals* **3**:1033-1042
- Ndeda, L. A. and Manohar, S. (2014). Determination of heavy metals in Nairobi Dam water, Kenya. *IOSR journal of environmental science toxicology and food technology* **8**: 68-73
- Ngah, W. and Hanafiah, M.A.K.M. (2008a) Removal of heavy metals from waste water by

- chemically modified plant waste as adsorbent: A review. *Bioresources technology* **99**:3935-3948
- Ngugi, F. (2015) Equilibrium and Kinetics studies for the adsorption of aqueous Cu(II) ions onto Mangroves Biomass. *International journal of Science and Research* **4**:355-360
- Nicolas, H. B., Annemie, B. and Jose, A.C.B (2013). Atomic spectroscopy. *ACS publications* **85**:670-704
- Nimibofa, A., Agustus, N.E. and Donbebe, W. (2017) “Modelling and interpretation of Adsorption isotherms,” *Journal of chemistry* vol. **2017**, Article ID 3039817, 17 pages, 2017
- Njagi, J. M., Akunga D. N., Njagi, M. M., Ngugi, P. M. and Njagi, E. M. N. (2016). Heavy Metal Pollution of the Environment by Dumpsites: A Case of Kadhodeki. *International journals of life science scientific research* **2**:191-197
- Njoki, M.A., Mercy, G., Nyagah, G. and Gachanja, A. (2016) Fourier transform infrared spectrophotometric analysis of functional groups found in *Ricinus communis*. L and *Cucurbita maxima Lam*. Roots, Stems and Leaves heavy metal adsorbent. *International journal of science environment*.**5**:861-871
- Nuhoglu, Y. and Malkoc, E. (2009). Thermodynamics and kinetics studies for the environmentally friendly Ni (II) biosorption using waste pomace of olive oil factory. *Bioresources technology* **100**:2375-2380
- Ogilo, J.K., Onditi, A.O., Salim, A.M. and Yusuf, A.O. (2017) Assessment of levels of heavy metals in paints from interior walls and indoor dust from residential houses in Nairobi City County, Kenya. *Chemical Science Journal* **21**:1-7
- Ogunkule, C.O., Mustapha, K., Oyedeji, S and Fatoba, O.P. (2016). Assessment of metallic pollution status of surface water and aquatic macrophytes of earthen dams in Ilorin, north-central of Nigeria as indicators of environmental health. *Sciencedirect* **28**:324-331
- Ojedokun, A.T. and Olugbenga S.B. (2016). Sequestering of heavy metals from wastewater using cow dung. *Science direct* **13**:7-13
- Onyatta, J. O. and Huang, P. M. 2005. Phosphate-induced cadmium release from soils. In. P. M. Huang, A. Violante, J.-M. Bollag, and P. Vityakon (Eds.), *Soil Abiotic and Biotic*

- Interactions and the Impact of the Ecosystem and Human Welfare*. Enfield, NH USA: Science Publishers, pp. 343-371.
- Onyatta, J. O., Chepkwony, C. K. and P. O. Ongoma (2009) The impact of urban activities on heavy metal distribution and bioavailability index in selected tropical urban soils. *In J. Xu and P. M. Huang (eds.), Molecular Environmental Soil Science at the Interfaces in the Earth's Critical Zone*. Zhejiang University Press, Published in Springer-Verlag GmbH, pp. 100-102.
- Osmond, G (2012).Zinc white: A review of zinc oxide pigment properties and implications for the stability in oil based paintings. *Australian institute for the conservation of cultural material* **33**:20-29
- Oves, M., Saghir, K.M., Hunda, Q.A., Nadeem F.M. and Almeelbi, T. (2016) Heavy metals: Biological importance and detoxification strategies. *Journal of bioremediation and biodegradation* **7**: 334- 340
- Park, J. D. and Zheng, W. (2012) Human exposure and health effects of inorganic and elemental mercury. *Journal of preventive medicine & public health* **46**:344-352
- Park, J. H., Cho, J. S., Ok, Y. S., Kim, S. H., Kang, S. W., Choi, I. K., Heo, J. S., Delaune, R. D. and Seo , D.C.(2015) Competitive adsorption and selectivity sequence of heavy metals by chicken bone-derived biochar: Batch and column experiment. *Journal of environmental science and health* **50** :1-11
- Parmar, M. and Thankur, L. S. (2013) Heavy metal Cu, Ni and Zn: Toxicity, health hazards and their removal techniques by low cost adsorbents. *International journal of plant, animal and environmental sciences* **3**:146-157
- Peng, W., Chenghui, L., Chengbingz, Z. and Xiandeng, H. (2012). Determination of cadmium in biological samples:An update from 2006 to 2011. *Applied spectroscopy reviews* **45**:327-370
- Pereira-Filho, E. R., Berndt, H. and Arruda, M.A.Z. (2002). Simultaneous sample digestion and determination of Cd,Cu and Pb in biological samples using thermospray flame furnace atomic absorption spectrometry(TS-FF-AAS) with slurry sample introduction. *Journal of atomic atmospheric spectrometry* **17**:1308-1315

- Plum, L.M., Rink, L. and Haase, H. (2010). Essential toxin: Impact of zinc on Human health. *International. Journal of environmental research and public health* **7**:1342-1365.
- Punjongharn, P., Meevasana, K. and Pavasant, P. (2017) Influence of particle size and salinity on adsorption of basic dyes by agricultural waste: dried seagrape (*Caulepa lentillifera*). *Journal of environmental science* **20**:760-768
- Rehman, K., Fatima, F., Waheed, I. and Akash, M.S.H. (2018) Prevalence of exposure of heavy Metals and their impact on health consequences. *Journal of cellular Biochemistry* **119**:157-184
- Sabty-Daily, R.A., Harris, P.A., Hinds, W.C. and Froines, J.R. (2017). Size distribution and speciation of chromium in paints spray aerosols at an aerospace facility. *Annals of occupational hygiene* **49**:47-59
- Saaidia, S., Delimi, R., Benredjem, Z., Mehellou, A., Djemel, A. and Barbari, K. (2017) Use of a PbO₂ electrode of lead-acid battery for the electrochemical degradation of methylene blue. *Separation science technology* **52**:1602-1614
- Sarin, V. and Pant, K.K. (2006) Removal of chromium from industrial waste using eucalyptus bark. *Bioresource technology* **97**:15-20
- Schalow, T., Brandt, B., Starr, D.E., Laurin, M., Shaikhutdinov, S.K., Shauermann, S.M. Libuda, J and Freund, J.H. (2007) Particle size dependent adsorption and reaction kinetics on reduced and partially oxidized Pd nanoparticles. *Physical chemistry chemical physics* **9**:1347-1361
- Shaban, N.S., Abdou K.A. and Hassan, N.E. (2016) Impact of toxic heavy metals and pesticides residue in herbal products. *Journal of basic and applied sciences* **5**:102-106
- Singh, D., Gupta, R. and Tiwari, A. (2011). Phytoremediation of lead from waste-water using aquatic plants. *International journal of biomedical research* **7**:411-421
- Singh, M. and Susan, V. P. (2016) Conventional and innovative techniques for removal of Heavy metals from electroplating industry waste water. *International journal of engineering sciences and research technology* **5**:150-159
- So, L.M., Chu, L.M. and Wong P.K. (2003) Microbial enhancement of Cu²⁺ removal capacity of *Eichhornia crassipes* (Matt) *Chemosphere* **52**:1499-1503
- Sun, H., Brocato, J. and Costa, M. (2015) Oral chromium exposure. *PubMed central* **2**:295-303

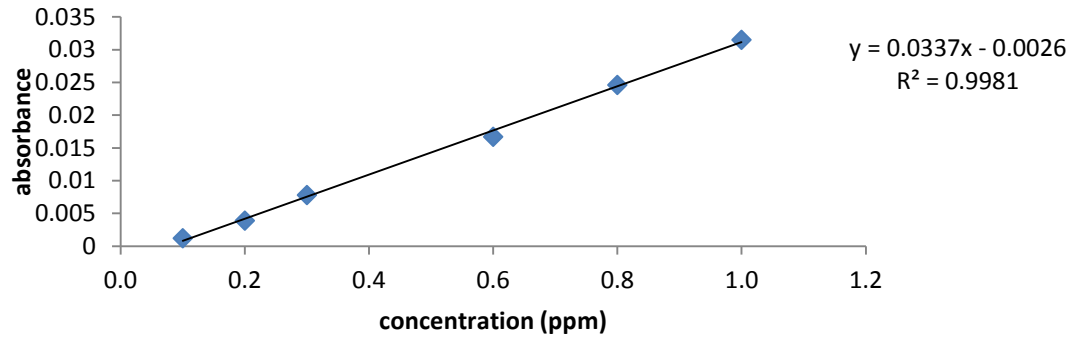
- Tang, Y., Yang, Q., Lu, J., Zhang, X., Suen, D., Tan, Y., Jin, L., Xiao, J., Xie, R., Rane, M., Li, X. and Cai, L. (2010). Zinc supplementation partially prevents renal pathological changes in diabetic rats. *Journal of nutritional biochemistry* **21**:237-246
- Tasker, S.Z., Standley, E.A. and Jamison T.F. (2014) Recent advances in Nickel Catalysis. *PubMed Central* **15**:299-309
- Tchomgui-kamga, E., Alonzo, V., Nansou-Njiki, C.P., Audebrand, N., Ngameni, E. and Darchen, A (2010). Preparation and characterization of charcoal that contained dispersed aluminium oxide as adsorbent for removal of fluoride from drinking water. *ScienceDirect* **48**: 333-343
- Tchounwou, P.B., Yedjou, C.G., Patlolla, K.A. and Sutton, D. J. (2012) Heavy metals toxicity and the environment. *PubMed central journals* **101**:133-164
- Tembhukar, A.R. and Dongre, S (2006) Studies on fluoride removal using adsorption process. *Journal of environmental science and engineering*.**143**:151-156
- Terdkiatburana, T., Wang, S. and Tade, M.O. (2009) Adsorption of heavy metals ions by natural and synthesized zeolites for wastewater treatment. *International journal of environment and waste management* **3**: 328-334
- Tripathi, A. and Manju, R.R. (2015) Heavy metal removal from waste-water using low cost adsorbents. *Bioremediation and biodegradation* **6**:1-5.
- United Nations Environment programmes (2005). Unep global environmental alert services. *OARE research in the environment* **70**:798-803
- United Nations Environment programmes (2013). Unep global environmental alert services. *OARE research in the environment* **65**:766-783
- Velazquez, N.A., Gonzalez, I., Bujaidar, M.E. and Cevallos, C.C. (2013) Amelioration of Cadmium-produced teratogenicity and Genotoxicity in Mice given *Arthrospira maxima* (Spirulina) treatment. *PubMed journal* **49**:143-148
- Villamagna, A.M. and Murphy B.R. (2010) Ecological and socio-economic impacts of invasive water hyacinth (*Eichhornia crassipes*) A review. *Fresh water biology* **55**:282-298
- Vodyanitskii, Y.N. (2016) Standards for the content of Heavy metals in the soils of some states. *Annal agrarian science* **14**: 257-263.

- Wani, A.L., Ara, A., and Usmani J.A. (2015) Lead toxicity: A preview. *PubMed central* **8**:55-64
- Waseem, A., Arshad, J., Iqbal, F.,Sajjad, A., Mehmood, Z. and Murtaza, G. (2014) pollution status of Pakistan: Heavy metal contamination of water, soil and vegetables. *BoiMed research international***13**: 21-29
- Wauna, R.A. and Okieimen, F.E. (2011) Heavy metals contaminated soils: A review of sources, chemistry, risk and best available strategies for remediation. *International scholarly research notices* **36**: 1-A20
- World Health Organisation (2011) Recommendations on the management of diarrhea and pneumonia in HIV-infected infants and children. *community based management of severe aceute malnutrition* **20**:11-19
- Zimmermann, L.T., Santos, D.B., Naime, A.A., Leal, B.R., Dorea, JG., Barbosa, F., Aschner, M., Batista, J.T.R. and Farina, M. (2013) Comparative study on methyl and ethyl mercury-induced In C6 glioma cells and the potential role of LAT-1 in mediating mercurial-thiol complexes uptake. *Neurotoxicology* **38**:1-8

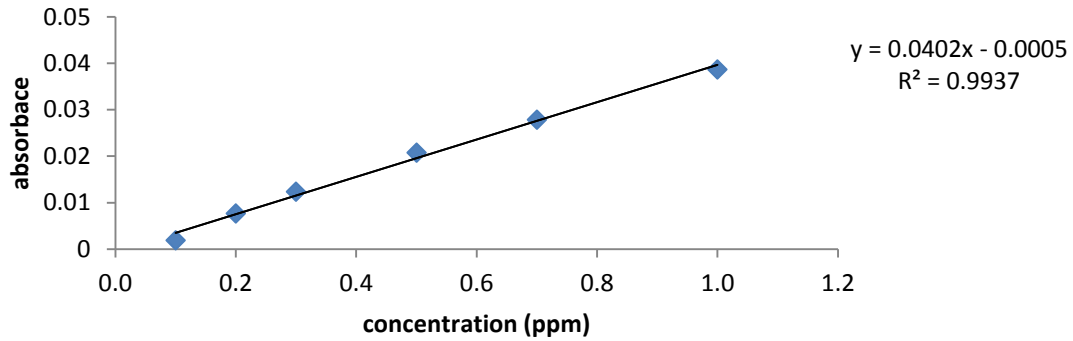
APPENDICES

Appendix I: Calibration curves

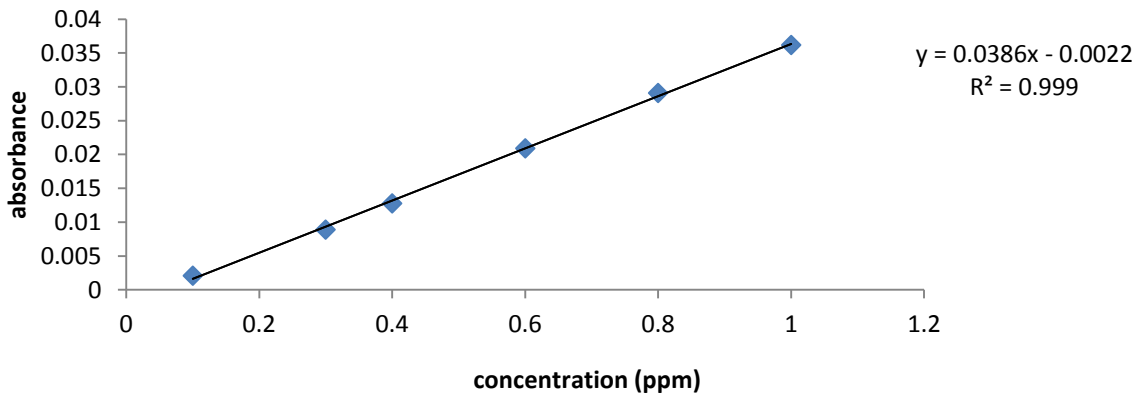
Appendix Ia: Calibration curve for Cadmium



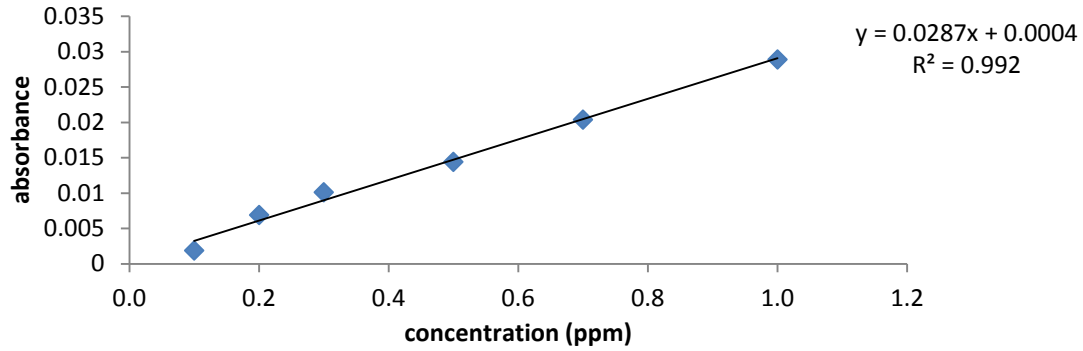
Appendix Ib: Calibration curve for Lead



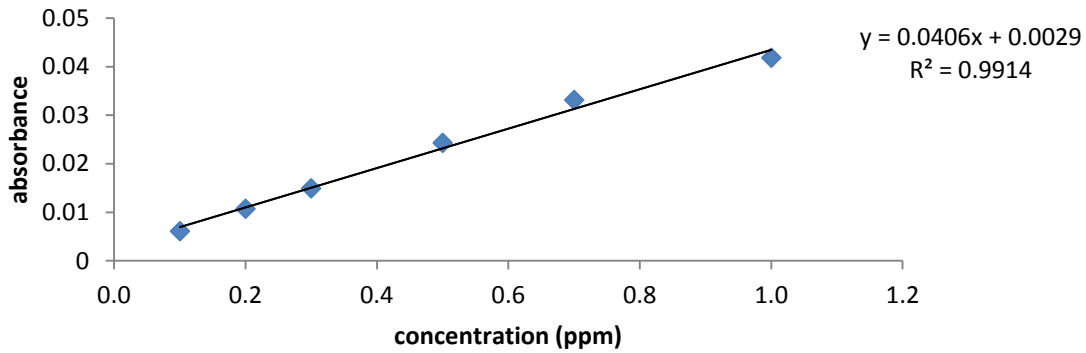
Appendix Ic: Calibration curve for Chromium



Appendix Id: Calibration curve for Nickel



Appendix Ie: Calibration curve for Zinc



Appendix If: Absorbance for the waste-water samples

Source	Pb	DF	Cd	DF	Zn	DF	Ni	DF	Cr	DF
Site A	0.2750	10	0.1750	10	0.0334	ND	0.0062	ND	0.0176	ND
Site B	0.3022	10	0.1322	10	0.3906	10	0.0046	ND	0.0464	10
Site C	0.0480	ND	0.0304	ND	0.0201	10	0.1827	10	0.3361	10
Site D	0.1280	ND	0.0271	ND	0.0265	ND	0.0037	ND	0.0125	ND

DF-Dilution Factor

ND-not diluted

Calculation of sample concentration

The equation for calibration curve for cadmium was $y = 0.0337x - 0.0026$. The absorbance for cadmium in site A was 0.1750. Concentration(x) was calculated as follows:

$$X = \frac{y + 0.0026}{0.0337}$$

Where y= absorbance

$$X = \frac{0.1750 + 0.0026}{0.0337}$$

$$= 5.27$$

The sample was diluted to a factor of 10.

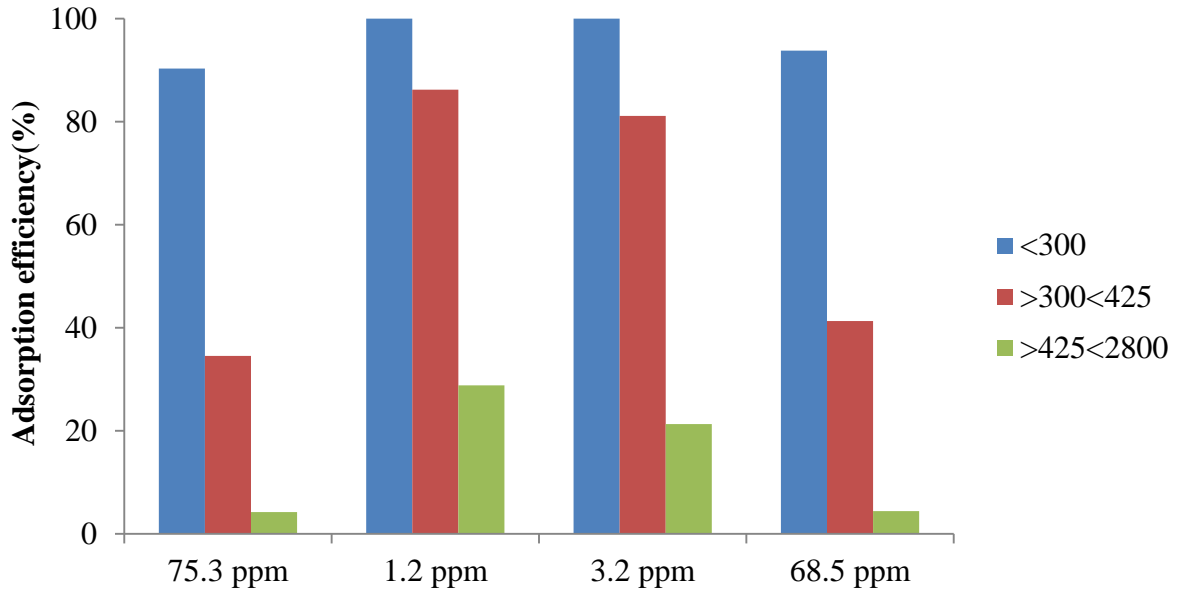
Therefore the real concentration was

$$5.27 \times 10 = 52.7 \text{ ppm}$$

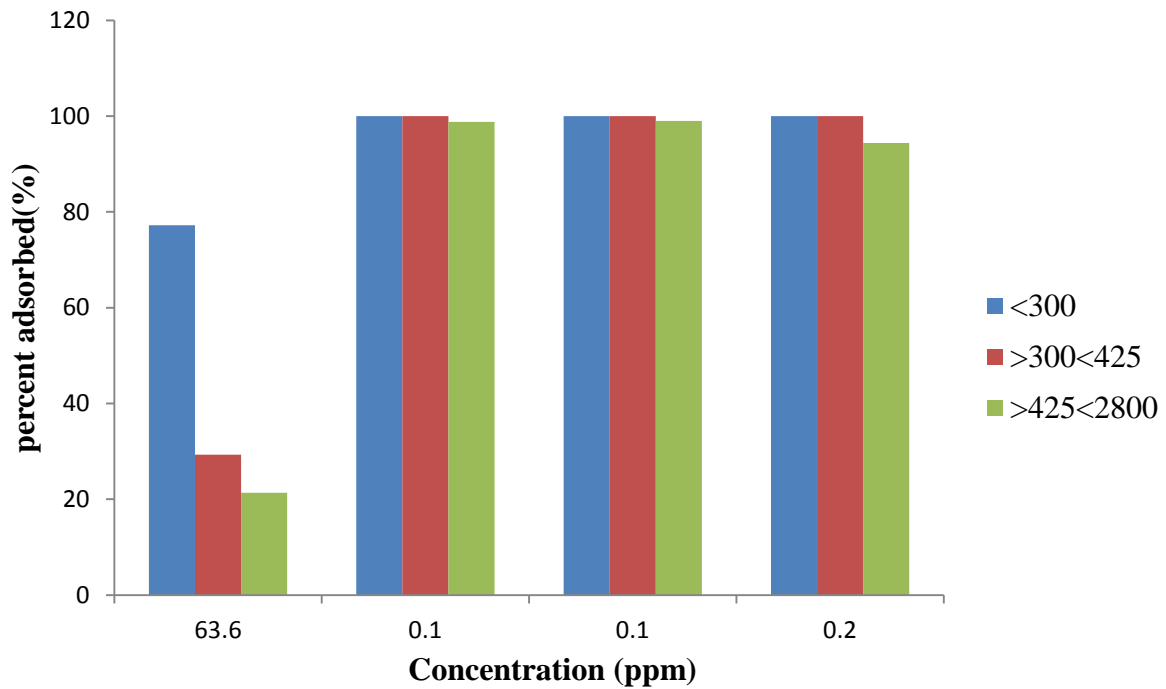
Appendix II: Adsorption efficiency (%) vs particle size (μm) for Zn, Pb, Ni, Cd and Cr

Zinc				
% adsorbed at:				
particle sizes (μm)	95.5 ppm	0.8 ppm	0.6 ppm	48.8 ppm
<300	81.3	100	100	91.8
>300<425	46.5	87.2	95.1	61.3
>425<2800	7.2	28.8	37.3	16.4
Lead				
particle sizes	75.3 ppm	1.2 ppm	3.2 ppm	68.5 ppm
<300	90.3	100	100	93.8
>300<425	34.5	86.2	81.1	41.3
>425<2800	4.2	28.8	21.3	4.4
Nickel				
particle sizes	63.5 ppm	0.1 ppm	0.1 ppm	0.2 ppm
<300	77.2	100	100	100
>300<425	29.3	100	100	100
>425<2800	21.4	98.8	99	94.4
Chromium				
Particle sizes	87.6 ppm	12.6 ppm	0.5 ppm	0.3 ppm
<300	70.5	92.7	100	100
>300<425	17.6	69.1	100	100
>425<2800	2.3	45.8	100	100
Cadmium				
Particle sizes	52.7 ppm	40.0 ppm	1ppm	0.9 ppm
<300	78.2	88.4	100	100
>300<425	28.3	42.1	100	100
>425<2800	1.5	6.8	100	100

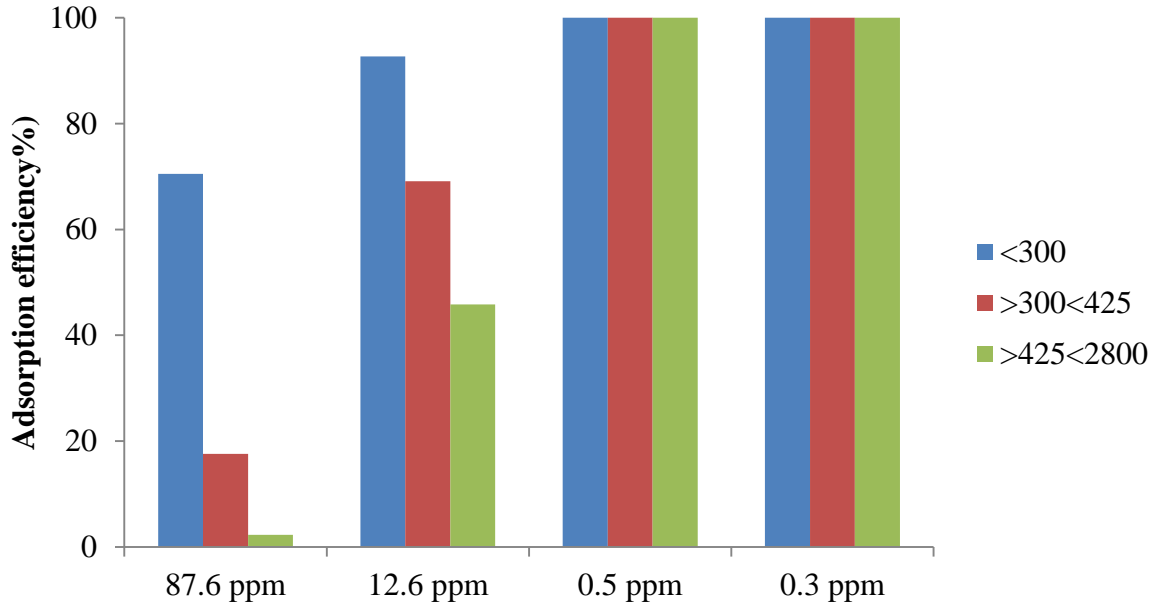
Appendix II a: Effect of particle size on adsorption of lead ions



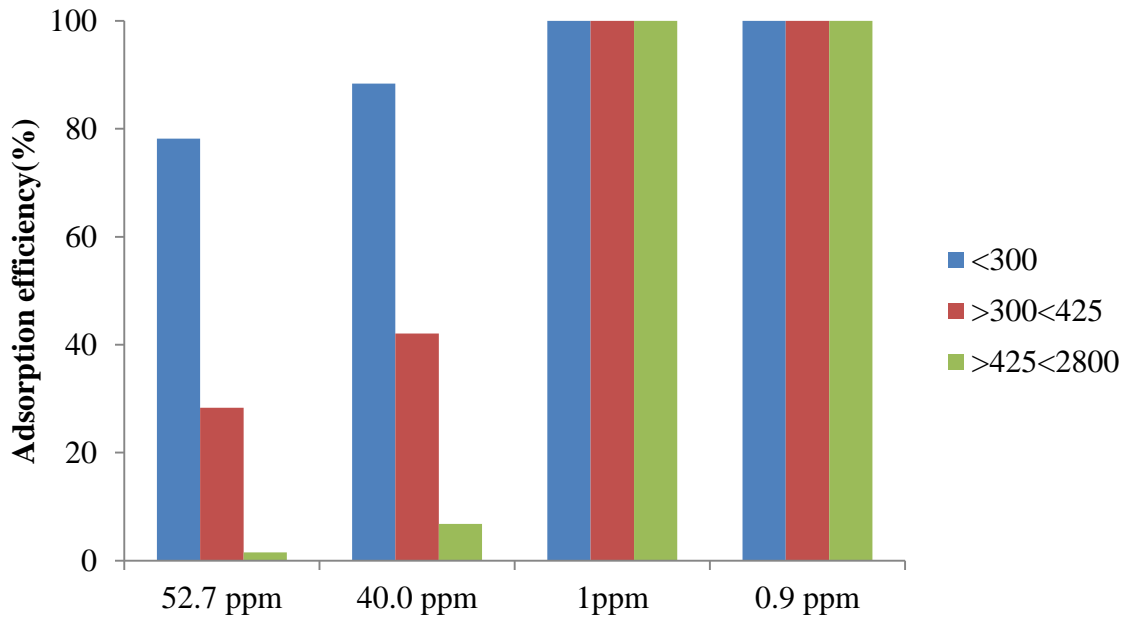
Appendix II b: Effect of particle size on adsorption of nickel ions



Appendix II c: Effect of particle size on adsorption of chromium ions



Appendix II d: Effect of particle size on adsorption of cadmium ions

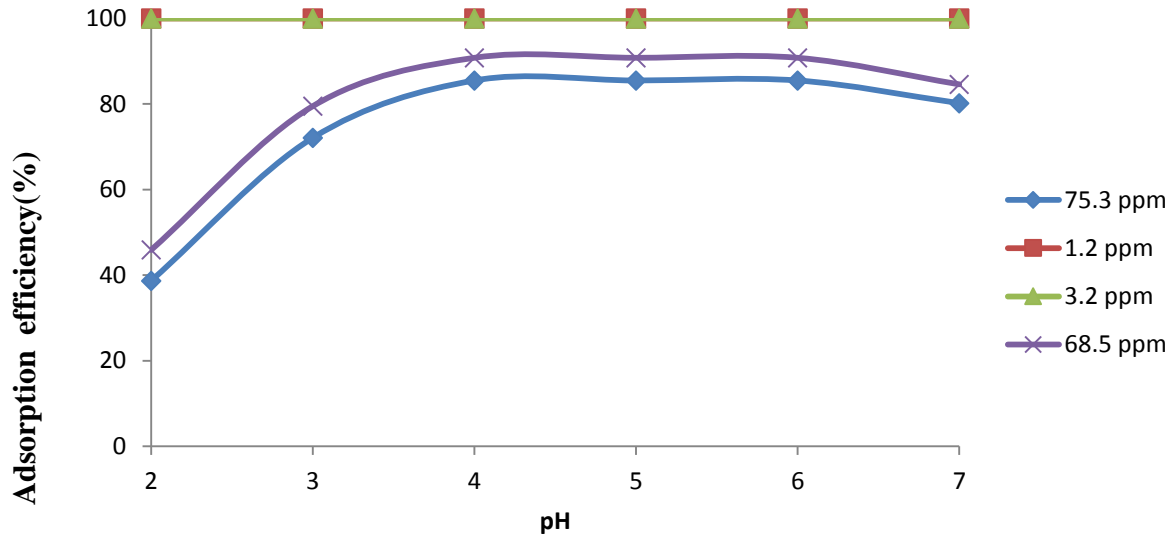


Appendix III: Adsorption efficiency (%) vs pH for Zn, Pb, Ni, Cd and Cr

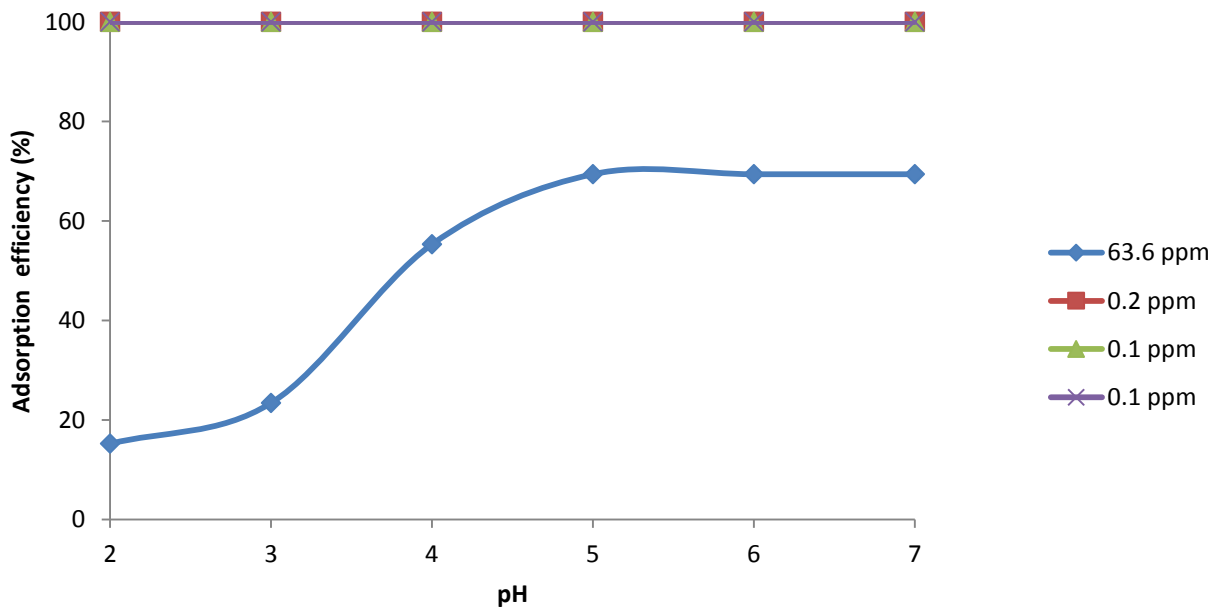
Zinc				
% adsorbed at:				
pH	95.5 ppm	0.8 ppm	0.6 ppm	48.8 ppm
2	18.7	100	100	25.3
3	32.1	100	100	39.5
4	64.3	100	100	76.8
5	80.3	100	100	86.8
6	80.3	100	100	86.8
7	80.3	100	100	86.9
Lead				
pH	75.3 ppm	1.2 ppm	3.2 ppm	68.5 ppm
2	38.7	100	100	45.9
3	72.1	100	100	79.5
4	85.5	100	100	90.8
5	85.5	100	100	90.8
6	85.5	100	100	90.8
7	80.2	100	100	84.6
Nickel				
pH	63.5 ppm	0.2 ppm	0.1 ppm	0.1 ppm
2	15.2	100	100	100
3	23.4	100	100	100
4	55.3	100	100	100
5	69.4	100	100	100
6	69.4	100	100	100
7	69.4	100	100	100
Chromium				
pH	87.6 ppm	12.6 ppm	0.5 ppm	0.3 ppm
2	14.6	36.7	100	100
3	56.4	68.5	100	100

4	79.1	84.8	100	100
5	79.1	84.8	100	100
6	79.1	84.8	100	100
7	73.2	79.3	100	100
Cadmium				
pH	52.7 ppm	40.0 ppm	1.0 ppm	0.9 ppm
2	27.4	31.3	100	100
3	57.1	61.7	100	100
4	74.3	79.5	100	100
5	83.9	90.6	100	100
6	83.9	90.6	100	100
7	83.9	90.6	100	100
Zinc				
pH	95.5 ppm	0.8 ppm	0.6 ppm	48.8 ppm
2	18.7	100	100	25.3
3	32.1	100	100	39.5
4	64.3	100	100	76.8
5	80.3	100	100	86.8
6	80.3	100	100	86.8
7	80.3	100	100	86.9

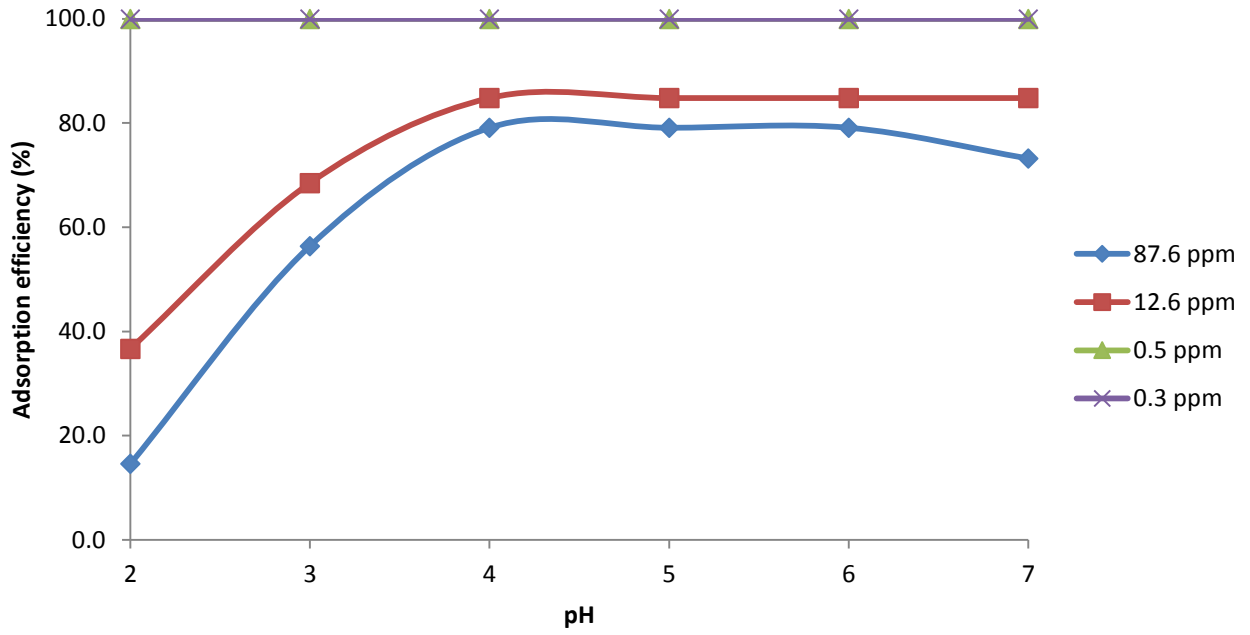
Appendix IIIa: Effect of pH on adsorption of lead ions



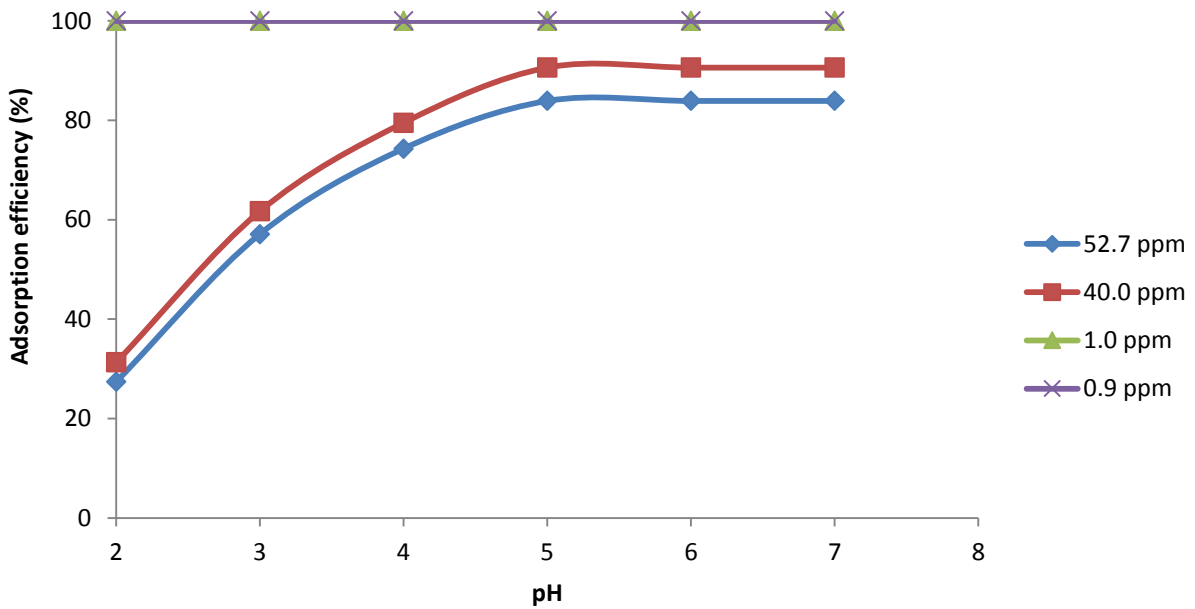
Appendix IIIb: Effect of pH on adsorption of nickel ions



Appendix IIIc: Effect of pH on adsorption of chromium ions



Appendix IIIId: Effect of pH on adsorption of cadmium ions



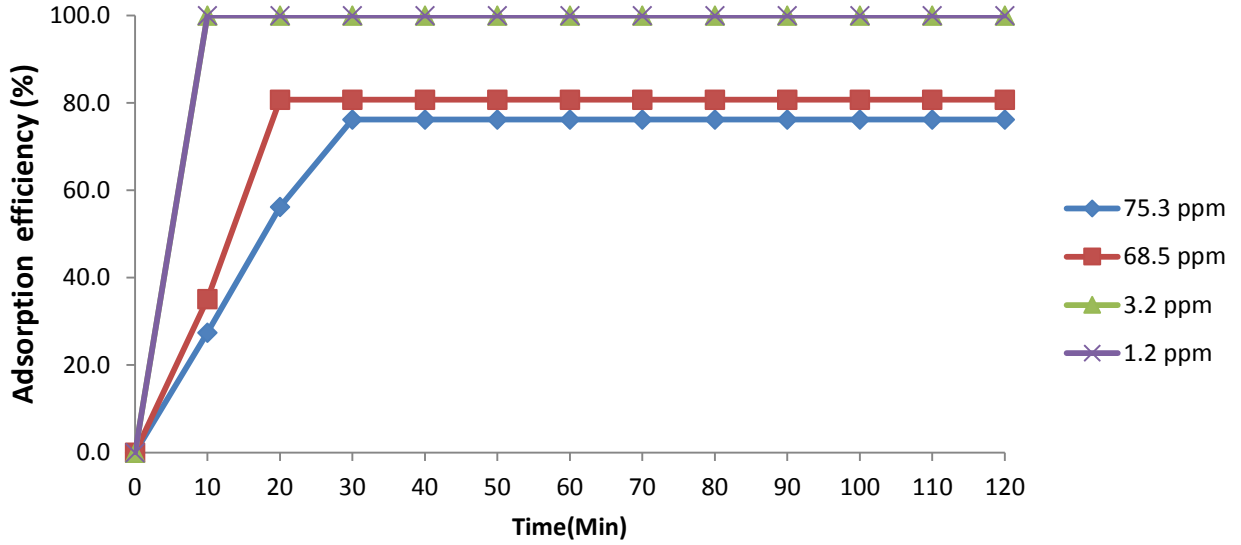
Appendix IV: Adsorption efficiency (%) vs contact time (min) or Zn, Pb, Ni, Cd and Cr

Lead				
% adsorbed at:				
Time	75.3 ppm	68.5 ppm	3.2 ppm	1.2 ppm
0	0.0	0.0	0.0	0.0
10	27.4	35.1	100	100
20	56.2	80.7	100	100
30	76.2	80.7	100	100
40	76.2	80.7	100	100
50	76.2	80.7	100	100
60	76.2	80.7	100	100
70	76.2	80.7	100	100
80	76.2	80.7	100	100
90	76.2	80.7	100	100
100	76.2	80.7	100	100
110	76.2	80.7	100	100
120	76.2	80.7	100	100
Zinc				
Time	0.8ppm	95.5 ppm	48.8 ppm	0.6ppm
0	0.0	0.0	0.0	0.0
10	100	33.1	45.7	100
20	100	48.4	63	100
30	100	55.9	80.7	100
40	100	64.5	88.4	100
50	100	77.1	88.4	100
60	100	82.1	88.4	100
70	100	82.1	88.4	100
80	100	82.1	88.4	100
90	100	82.1	88.4	100
100	100	82.1	88.4	100

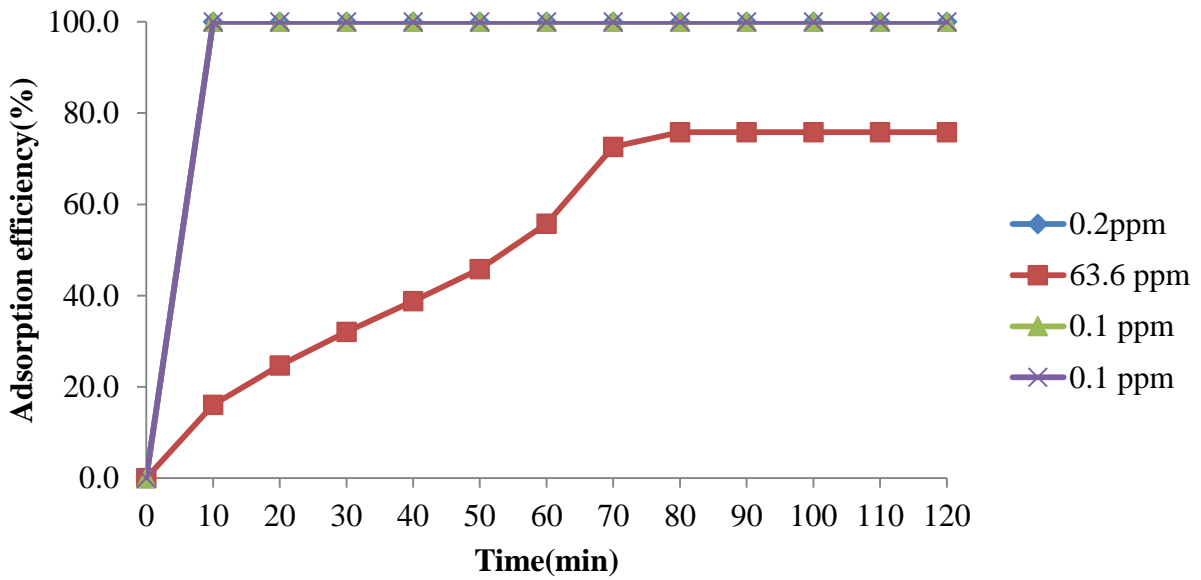
110	100	82.1	88.4	100
120	100	82.1	88.4	100
Chromium				
Time	87.6ppm	0.5 ppm	12.6 ppm	0.3ppm)
0	0.0	0.0	0.0	0.0
10	26.4	100	62.9	100
20	49.7	100	88.7	100
30	63.2	100	88.7	100
40	75.4	100	88.7	100
50	75.4	100	88.7	100
60	75.4	100	88.7	100
70	75.4	100	88.7	100
80	75.4	100	88.7	100
90	75.4	100	88.7	100
100	75.4	100	88.7	100
110	75.4	100	88.7	100
120	75.4	100	88.7	100
Nickel				
Time	0.2ppm	63.5 ppm	0.1 ppm	0.1ppm
0	0.0	0.0	0.0	0.0
10	100	16.1	100	100
20	100	24.7	100	100
30	100	32.1	100	100
40	100	38.8	100	100
50	100	45.8	100	100
60	100	55.8	100	100
70	100	72.6	100	100
80	100	75.8	100	100
90	100	75.8	100	100
100	100	75.8	100	100

110	100	75.8	100	100
120	100	75.8	100	100
Cadmium				
Time	1.0ppm	(52.7 ppm	40.0 ppm	0.9ppm
0	0.0	0.0	0.0	0.0
10	100	20.1	24.7	100
20	100	30.7	53.3	100
30	100	42.1	60.8	100
40	100	48.3	69.4	100
50	100	55.8	73.4	100
60	100	65.8	73.4	100
70	100	65.8	73.4	100
80	100	65.8	73.4	100
90	100	65.8	73.4	100
100	100	65.8	73.4	100
110	100	65.8	73.4	100
120	100	65.8	73.4	100

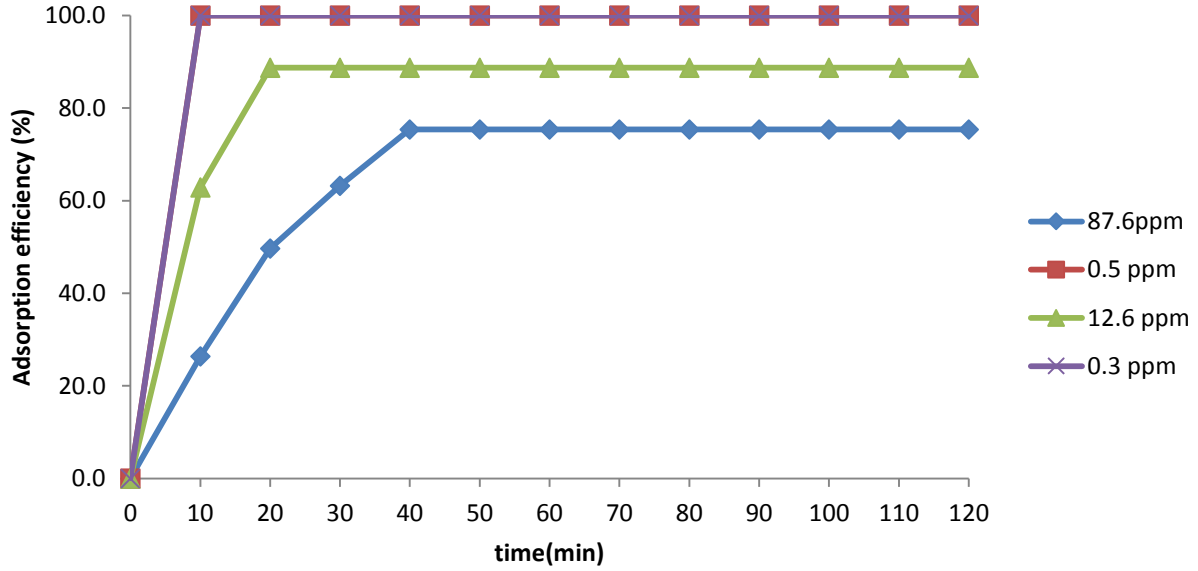
Appendix IVa : Effect of contact time on adsorption of lead ions



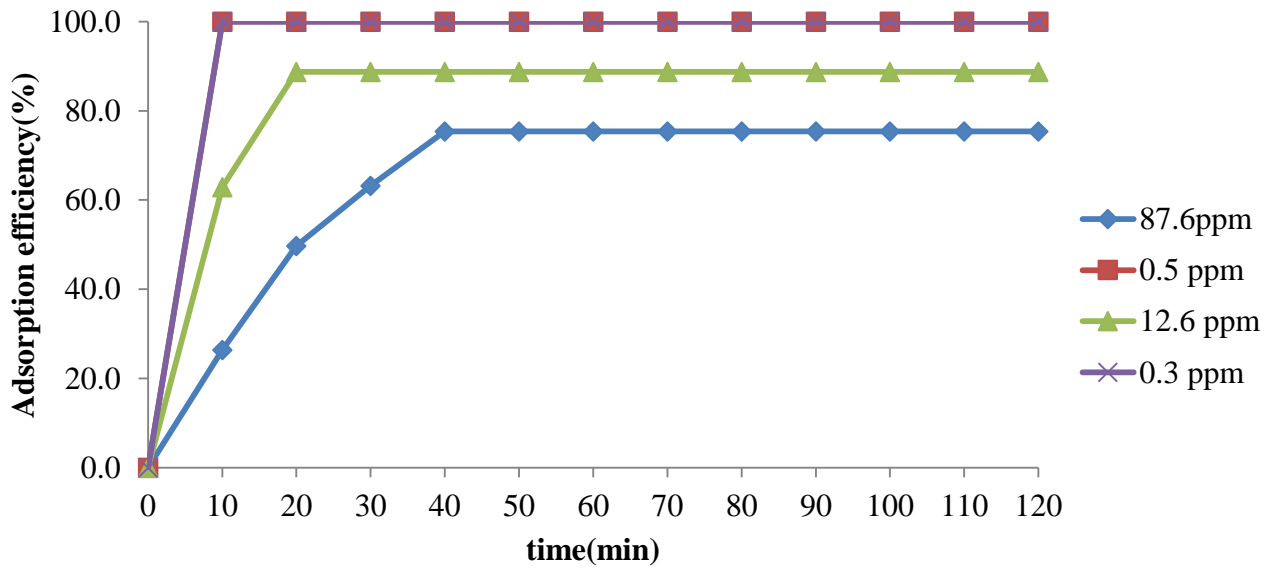
Appendix IVb : Effect of contact time on adsorption of nickel ions



Appendix IVc : Effect of contact time on adsorption of chromium ions



Appendix IVd : Effect of contact time on adsorption of cadmium ions



Appendix V: Adsorption efficiency (%) vs adsorbent dosage (g) for Ni, Cd, Cr, Zn and Pb

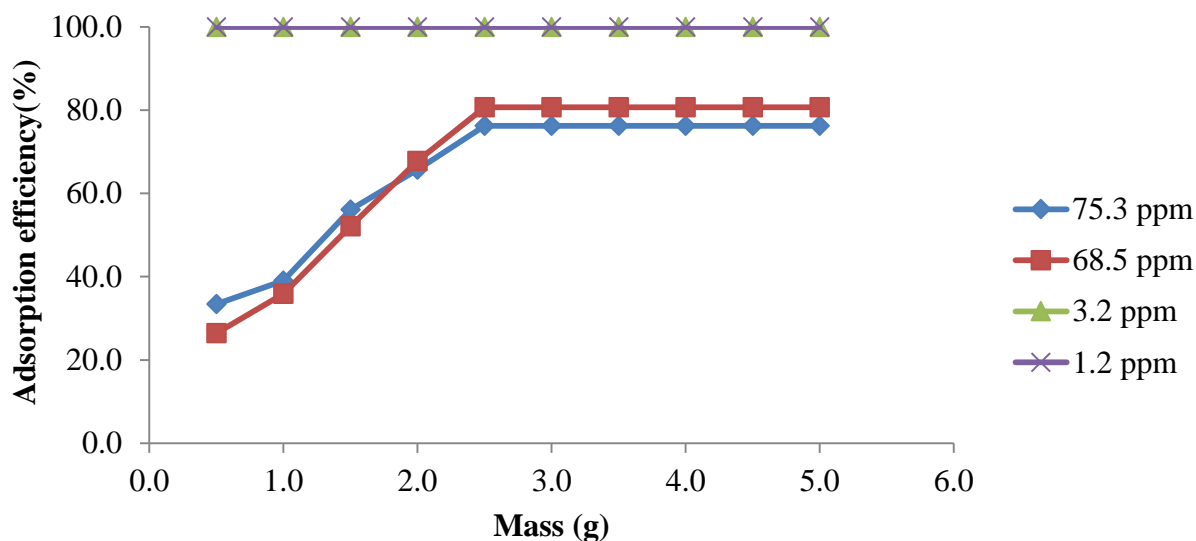
The table below shows how efficiencies varies with mass of the adsorbent for each metal at different concentrations

Lead				
adsorption efficiency at:				
Mass(g)	75.3 ppm	68.5 ppm	3.2 ppm	1.2 ppm
0.5	33.4	26.4	100	100
1.0	39.0	35.9	100	100
1.5	56.1	52.1	100	100
2.0	65.7	67.8	100	100
2.5	76.2	80.7	100	100
3.0	76.2	80.7	100	100
3.5	76.2	80.7	100	100
4.0	76.2	80.7	100	100
4.5	76.2	80.7	100	100
5.0	76.2	80.7	100	100
Zinc				
Mass(g)	0.8ppm	95.5 ppm	48.8 ppm	0.6ppm
0.5	100	25.1	27.7	100
1.0	100	35.4	58.3	100
1.5	100	57.9	79.7	100
2.0	100	70.5	89.4	100
2.5	100	70.5	92.4	100
3.0	100	70.5	92.4	100
3.5	100	70.5	92.4	100
4.0	100	70.5	92.4	100
4.5	100	70.5	92.4	100
5.0	100	70.5	92.4	100
Chromium				

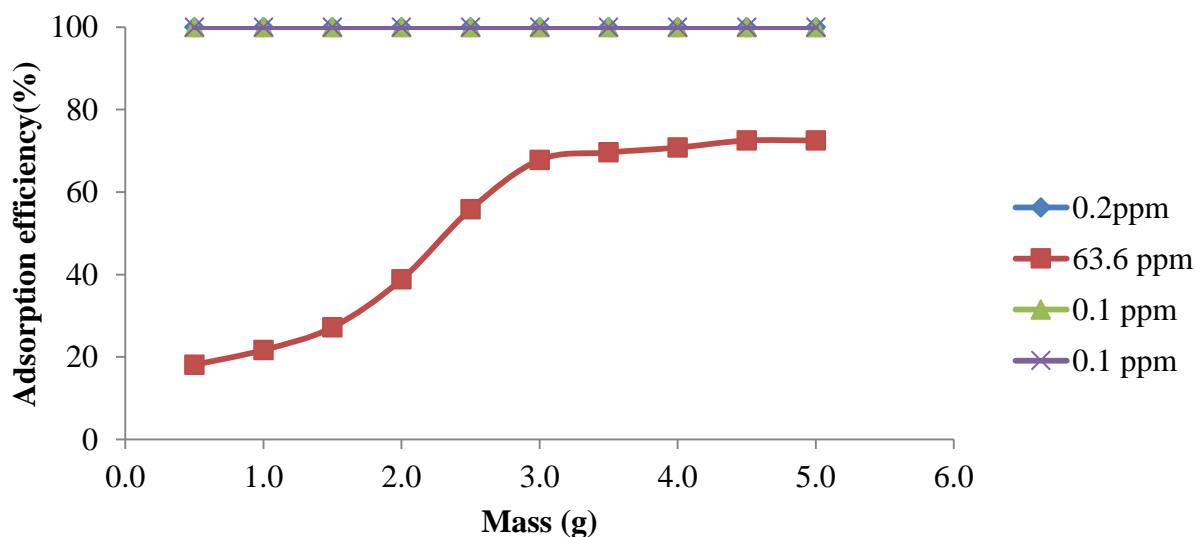
Mass(g)	87.6ppm	0.5 ppm	12.6 ppm	0.3ppm)
0.5	10.4	100	63.4	100
1.0	12.7	100	88.3	100
1.5	15.2	100	90.5	100
2.0	28.4	100	100	100
2.5	47.4	100	100	100
3.0	60.4	100	100	100
3.5	66.4	100	100	100
4.0	72.4	100	100	100
4.5	72.4	100	100	100
5.0	72.4	100	100	100
Nickel				
Mass(g)	0.2ppm	63.5 ppm	0.1 ppm	0.1ppm
0.5	100	18.1	100	100
1.0	100	21.7	100	100
1.5	100	27.2	100	100
2.0	100	38.8	100	100
2.5	100	55.8	100	100
3.0	100	67.8	100	100
3.5	100	69.6	100	100
4.0	100	70.8	100	100
4.5	100	72.5	100	100
5.0	100	72.5	100	100
Cadmium				
Mass(g)	1.0ppm	(52.7 ppm	40.0 ppm	0.9ppm
0.5	100	24.7	20	100
1.0	100	28.3	23.7	100
1.5	100	34.1	30.8	100
2.0	100	45.3	49.4	100
2.5	100	60.8	67.4	100

3.0	100	68.8	80.3	100
3.5	100	68.8	80.3	100
4.0	100	68.8	80.3	100
4.5	100	68.8	80.3	100
5.0	100	68.8	80.3	100

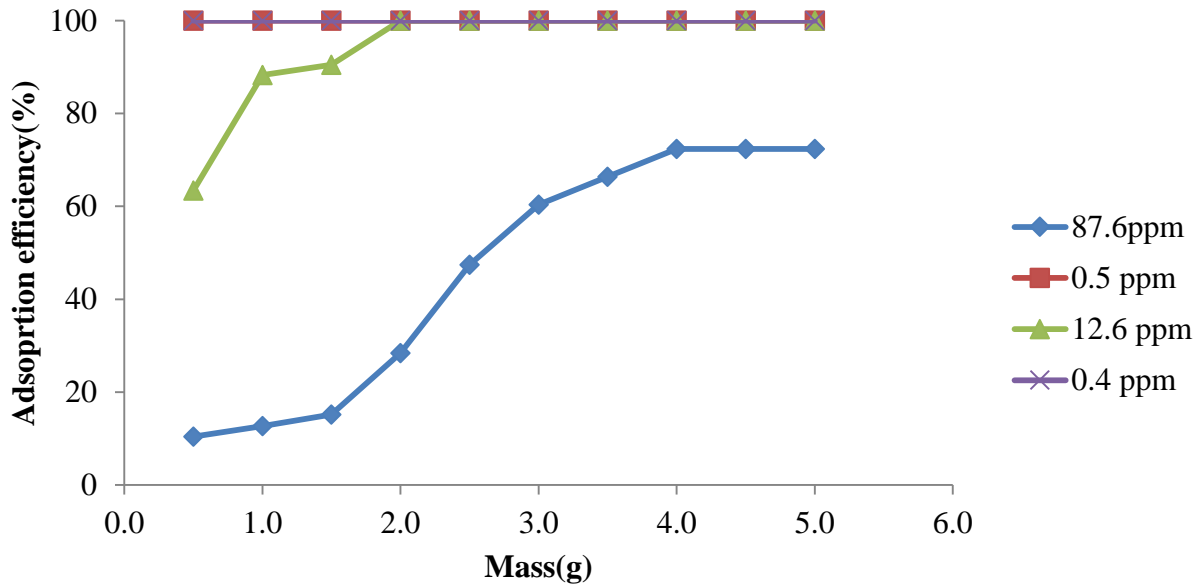
Appendix Va: Effect of adsorbent dosage on adsorption of lead ions



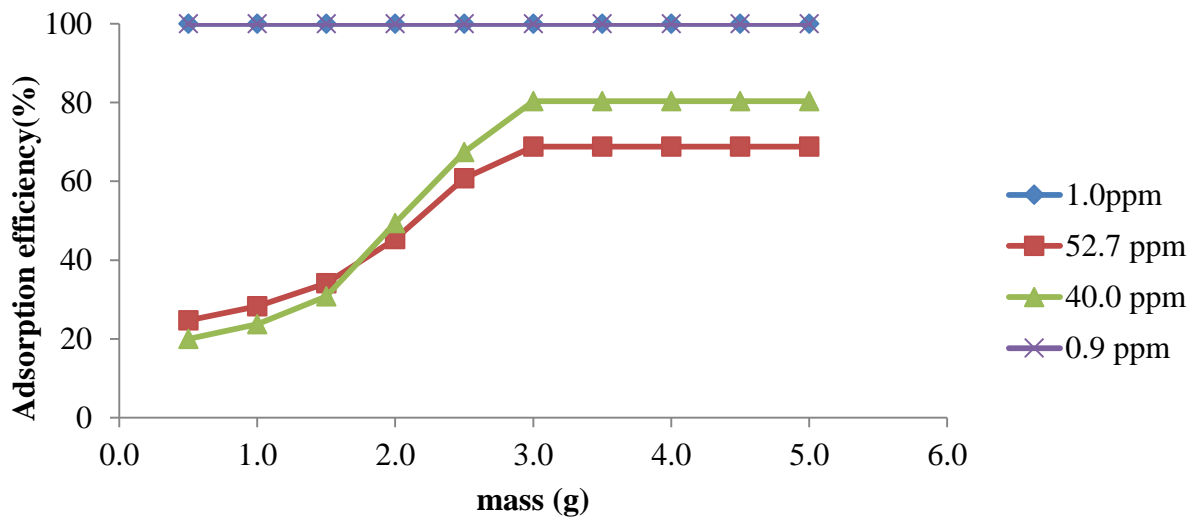
Appendix Vb: Effect of adsorbent dosage on adsorption of nickel ions



Appendix Vc: Effect of adsorbent dosage on adsorption of chromium ions



Appendix Vd: Effect of adsorbent dosage on adsorption of cadmium ions



Appendix VI: Equilibrium data for Pb²⁺, Cd²⁺, Cr³⁺, Zn²⁺ and Ni²⁺.

Equilibrium data for Pb²⁺						
C _o	C _e	1/C _e	q _e	1/q _e	log q _e	log C _e
0.5	0	Error	0.1	10	-1.0000	Error
1	0	Error	0.2	5	-0.6990	Error
10	0	Error	2	0.5	0.3010	Error
20	3.7	0.2703	3.26	0.3067	0.5132	0.5682
40	8.9	0.1124	6.22	0.1608	0.7938	0.9494
60	18.5	0.0541	8.3	0.1205	0.9191	1.2672
80	25.4	0.0394	10.92	0.0916	1.0382	1.4048
Equilibrium data for Cd²⁺						
C _o	C _e	1/C _e	q _e	1/q _e	log q _e	log C _e
0.5	0	0.1000	Error	10.0000	Error	-1.0000
1	0	0.2000	Error	5.0000	Error	-0.6990
10	1.3	1.7400	0.7692	0.5747	0.1139	0.2405
20	2.9	3.4200	0.3448	0.2924	0.4624	0.5340
30	6.1	4.7800	0.1639	0.2092	0.7853	0.6794
40	12.5	5.5000	0.0800	0.1818	1.0828	0.7404
50	15.4	6.9200	0.0649	0.1445	1.1875	0.8401
60	22.1	7.5800	0.0452	0.1319	1.3444	0.8796
Equilibrium data for Cr³⁺						
C _o	C _e	1/C _e	q _e	1/q _e	log q _e	log C _e
0.5	0	0.1000	Error	10.0000	Error	-1.0000
1	0	0.2000	Error	5.0000	Error	-0.6990
10	1.2	1.7600	0.8333	0.5682	0.0792	0.2455
20	2.2	3.5600	0.4545	0.2809	0.3424	0.5514
30	3.1	5.3800	0.3226	0.1859	0.4914	0.7308
40	5.5	6.9000	0.1818	0.1449	0.7404	0.8388

50	6.4	8.7200	0.1563	0.1147	0.8062	0.9405
60	9.1	10.1800	0.1099	0.0982	0.9590	1.0077
80	12.4	13.5200	0.0806	0.0740	1.0934	1.1310
90	13.7	15.2600	0.0730	0.0655	1.1367	1.1836
Equilibrium data for Zn²⁺						
C _o	C _e	1/C _e	q _e	1/q _e	log q _e	log C _e
0.5	0	0.1000	Error	10.0000	Error	-1.0000
1	0	0.2000	Error	5.0000	Error	-0.6990
10	0	2.0000	Error	0.5000	Error	0.3010
20	2.4	3.5200	0.4167	0.2841	0.3802	0.5465
40	4.9	7.0200	0.2041	0.1425	0.6902	0.8463
50	9.4	8.1200	0.1064	0.1232	0.9731	0.9096
60	11.1	9.7800	0.0901	0.1022	1.0453	0.9903
80	16.4	12.7200	0.0610	0.0786	1.2148	1.1045
100	20.7	15.8600	0.0483	0.0631	1.3160	1.2003
Equilibrium data for Ni²⁺						
C _o	C _e	1/C _e	q _e	1/q _e	log q _e	log C _e
0.5	0	0.1000	Error	10.0000	Error	-1.0000
1	0	0.2000	Error	5.0000	Error	-0.6990
10	0	2.0000	Error	0.5000	Error	0.3010
20	3.6	3.2800	0.2778	0.3049	0.5563	0.5159
30	5.8	4.8400	0.1724	0.2066	0.7634	0.6848
40	8.4	6.3200	0.1190	0.1582	0.9243	0.8007
50	13.3	7.3400	0.0752	0.1362	1.1239	0.8657
60	17.8	8.4400	0.0562	0.1185	1.2504	0.9263
70	23.4	9.3200	0.0427	0.1073	1.3692	0.9694

Example on calculation of Langmuir and Freundlich parameters.

The initial concentration of Pb²⁺ was 60 ppm while the final concentration was 18.5 ppm. Using the data in appendix VI and equation in figures 4.7 and 4.8.

Comparing equation 3.6 with equation from the graph (Figure 4.8)

$$y = 0.9018x + 0.0625$$

$$\frac{1}{q_m} = 0.0625 \quad \text{hence } q_m = 16$$

$$\frac{1}{q_m \cdot b} = 0.9018 \quad \text{replacing } q_m \text{ we get } b = 0.0693$$

Comparing equation 3.9 with equation from the graph (Figure 4.7)

$$y = 0.6004x + 0.1872$$

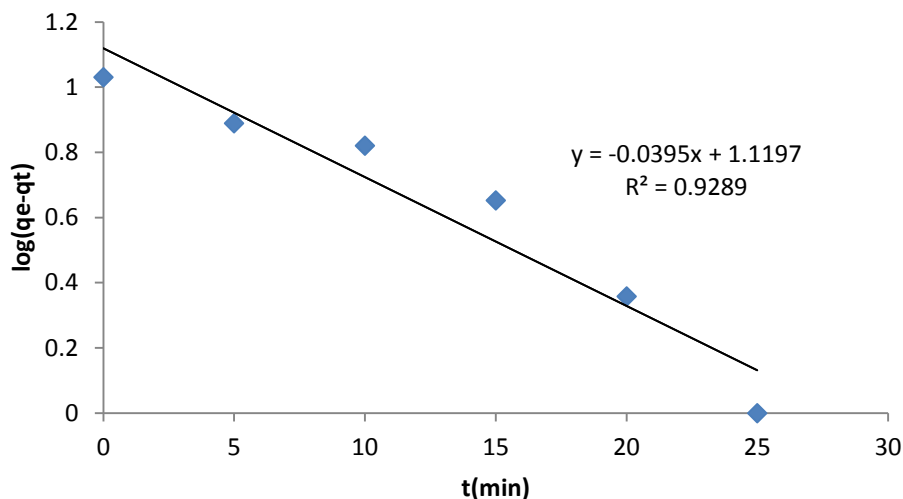
$$\log K_f = 0.1872 \quad \text{hence } K_f = 1.5389$$

$$1/n = 0.6004 \quad \text{hence } n = 1.6656$$

Appendix VII: Kinetic graphs for Equilibrium data for Pb²⁺, Cd²⁺, Cr³⁺, Zn²⁺ and Ni²⁺.

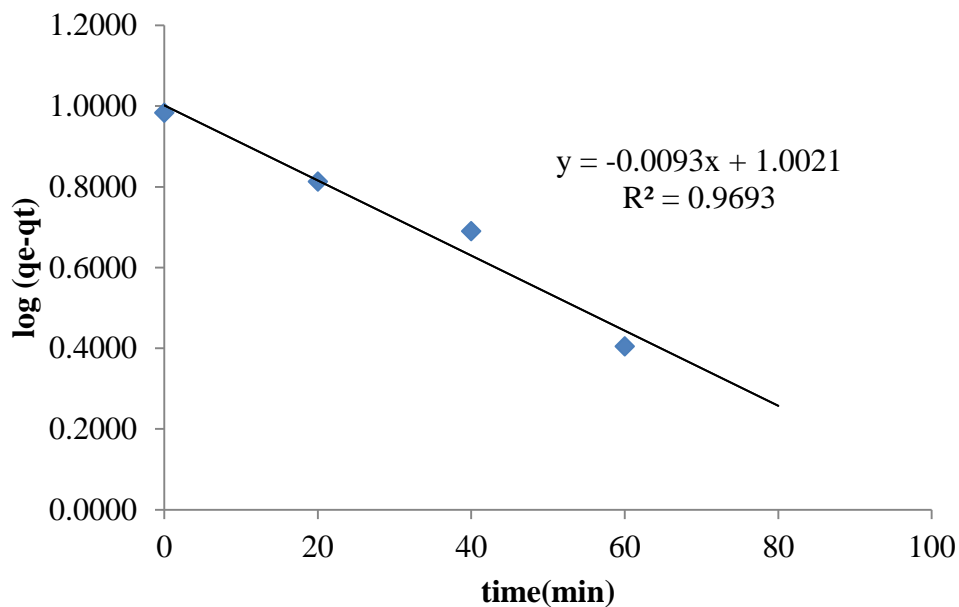
Appendix VIIa: Pseudo-first-order graphs for the adsorption of lead ions on ground water

hyacinth.

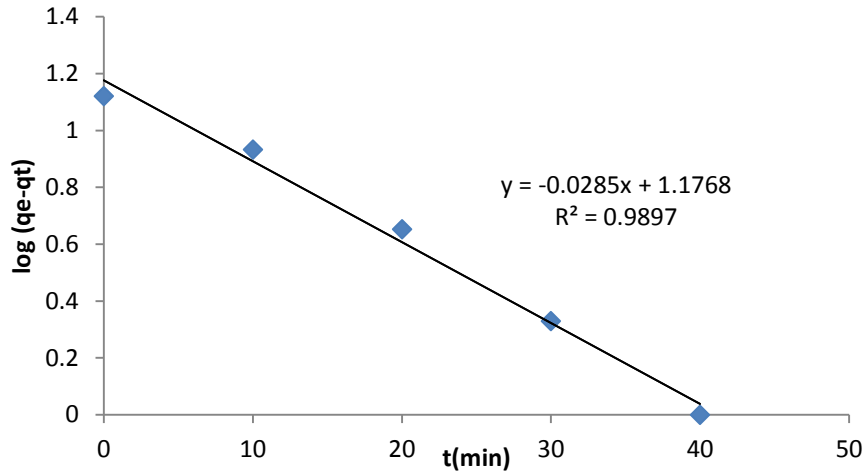


Appendix VIIb: Pseudo-first-order graphs for the adsorption of nickel ions on ground

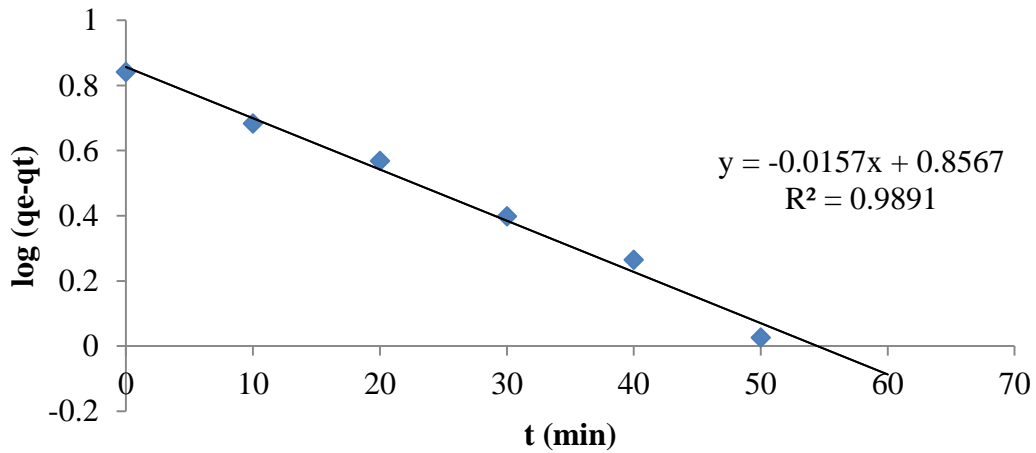
water hyacinth.



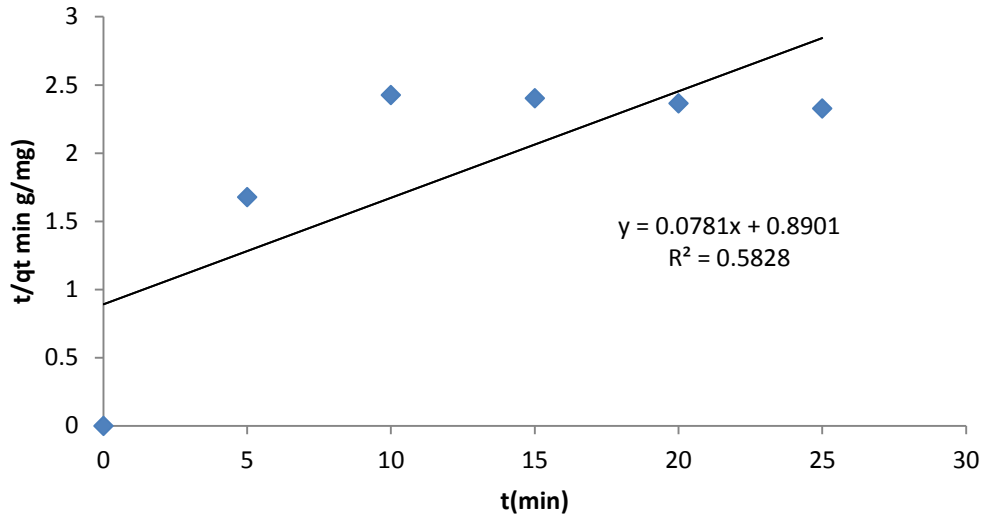
Appendix VIIc: Pseudo-first-order graphs for the adsorption of chromium ions on groundwater hyacinth.



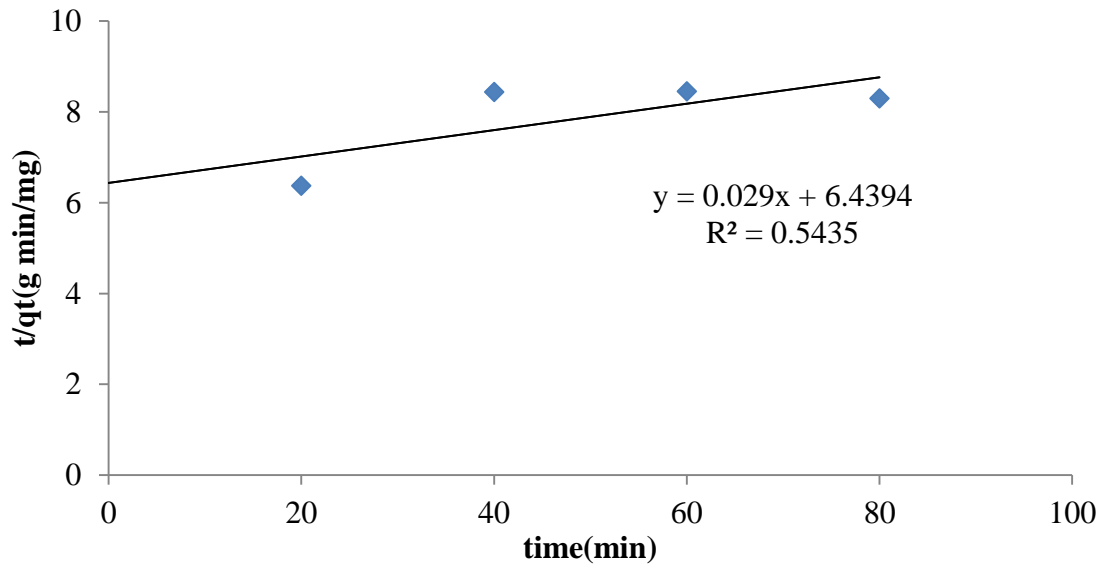
Appendix VIId: Pseudo-first-order graphs for the adsorption of cadmium ions on ground water hyacinth.



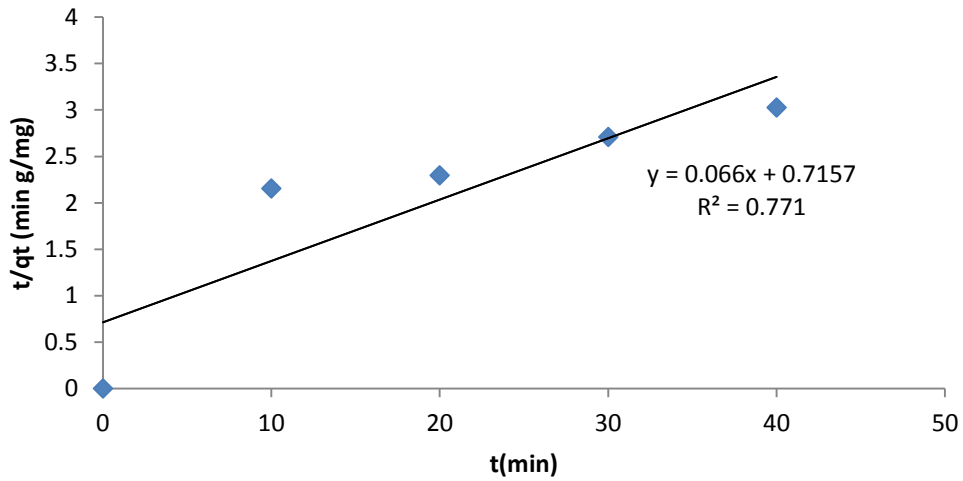
Appendix VIIe: Pseudo-second-order graphs for the adsorption of lead ions on ground water hyacinth.



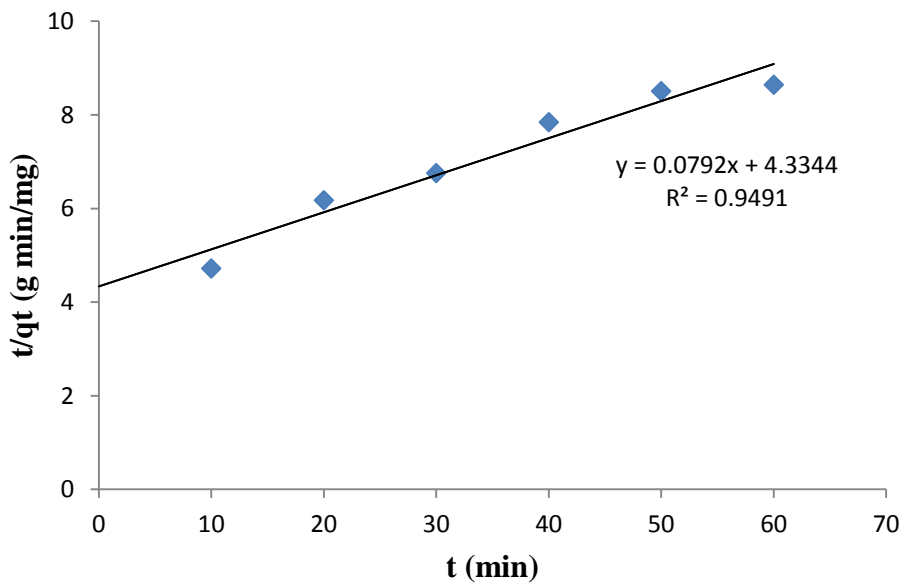
Appendix VIIIf: Pseudo-second-order graphs for the adsorption of nickel ions on ground water hyacinth.



Appendix VIIg: Pseudo-second-order graphs for the adsorption of chromium ions on ground water hyacinth.



Appendix VIIIh: Pseudo-second-order graphs for the adsorption of cadmium ions on ground water hyacinth.



Appendix VIIIk: Kinetic data for Kinetic graphs for Equilibrium data for Pb²⁺, Cd²⁺, Cr³⁺, Zn²⁺ and Ni²⁺.

Kinetic data for Cr³⁺ (87.6 ppm)									
Time	C _t	C _o	V	M	q _t	q _e	q _e -q _t	log (q _e -q _t)	t/q _t
0	87.6	87.6	0.1	0.5	0.0000	13.2200	13.2200	1.1212	Error
10	64.4	87.6	0.1	0.5	4.6400	13.2200	8.5800	0.9335	2.1552
20	44.0	87.6	0.1	0.5	8.7200	13.2200	4.5000	0.6532	2.2936
30	32.2	87.6	0.1	0.5	11.0800	13.2200	2.1400	0.3304	2.7076
40	21.5	87.6	0.1	0.5	13.2200	13.2200	0.0000	Error	3.0257
Kinetic data for Zn²⁺(95.5 ppm)									
time	C _t	C _o	V	M	q _t	q _e	q _e -q _t	log (q _e -q _t)	t/q _t
0	95.5	95.5	0.1	0.5	0.0000	15.6800	15.6800	1.1953	Error
10	64.1	95.5	0.1	0.5	6.2800	15.6800	9.4000	0.9731	1.5924
20	49.4	95.5	0.1	0.5	9.2200	15.6800	6.4600	0.8102	2.1692
30	42.2	95.5	0.1	0.5	10.6600	15.6800	5.0200	0.7007	2.8143
40	34	95.5	0.1	0.5	12.3000	15.6800	3.3800	0.5289	3.2520
50	21.9	95.5	0.1	0.5	14.7200	15.6800	0.9600	-0.0177	3.3967
60	17.1	95.5	0.1	0.5	15.6800	15.6800	0.0000	Error	3.8265
Kinetic data for Cd²⁺ (52.7 ppm)									
time	C _t	C _o	V	M	q _t	q _e	q _e -q _t	log (q _e -q _t)	t/q _t
0	52.7	52.7	0.1	0.5	0	5.88	5.88	0.7694	Error
10	42.1	52.7	0.1	0.5	2.12	5.88	3.76	0.5752	4.7170
20	36.5	52.7	0.1	0.5	3.24	5.88	2.64	0.4216	6.1728
30	30.5	52.7	0.1	0.5	4.44	5.88	1.44	0.1584	6.7566
40	27.2	52.7	0.1	0.5	5.10	5.88	0.78	-0.1079	7.8431
50	23.3	52.7	0.1	0.5	5.88	5.88	0.00	Error	8.5034
Kinetic data for Ni²⁺ (63.5 ppm)									
time	C _t	C _o	V	M	q _t	q _e	q _e -q _t	log (q _e -q _t)	t/q _t
0	63.5	63.5	0.1	0.5	0.0000	9.6400	9.6400	0.9841	Error

10	53.4	63.5	0.1	0.5	2.0400	9.6400	7.6000	0.8808	4.9020
20	47.9	63.5	0.1	0.5	3.1400	9.6400	6.5000	0.8129	6.3694
30	43.2	63.5	0.1	0.5	4.0800	9.6400	5.5600	0.7451	7.3529
40	39.9	63.5	0.1	0.5	4.7400	9.6400	4.9000	0.6902	8.4388
50	34.5	63.5	0.1	0.5	5.8200	9.6400	3.8200	0.5821	8.5911
60	28.1	63.5	0.1	0.5	7.1000	9.6400	2.5400	0.4048	8.4507
70	17.4	63.5	0.1	0.5	9.2400	9.6400	0.4000	-0.3979	7.5758
80	15.4	63.5	0.1	0.5	9.6400	9.6400	0.0000	Error	8.2988
Kinetic data for Pb²⁺ (75.3 PPM)									
time	C _t	C _o	V	M	q _t	q _e	q _e -q _t	log (q _e -q _t)	t/q _t
0	75.3	75.3	0.1	0.5	0	10.74	10.74	1.0310	Error
5	60.4	75.3	0.1	0.5	2.98	10.74	7.76	0.8899	1.6779
10	54.7	75.3	0.1	0.5	4.12	10.74	6.62	0.8209	2.4272
15	44.1	75.3	0.1	0.5	6.24	10.74	4.50	0.6532	2.4038
20	33	75.3	0.1	0.5	8.46	10.74	2.28	0.3579	2.3641
25	21.6	75.3	0.1	0.5	10.74	10.74	0.00	Error	2.3277

Example; the initial concentration of Pb²⁺ was 75.3 ppm while the final concentration was 21.6 ppm. Using the data in appendix VII and equation on figures in Appendix VIIb and VIIg.

Comparing $y = -0.0395x + 1.1197$ with equation 3.10

$q_e = 13.1735$, while $k_1 = -2.303 \times -0.0395 = 0.091$

Comparing $y = 0.0781x + 0.8901$ with equation 3.11

$q_e = 1/0.0781 = 12.8041$, $k_2 = 0.0069$.